



# Plastic railway sleepers

Creating a finite element model for  
hybrid plastic railway sleepers

A. H. Griemink

Technische Universiteit Delft

Cover image from <https://www.fxbricks.com/>, showing a custom LEGO® piece of train track.

# PLASTIC RAILWAY SLEEPERS

## CREATING A FINITE ELEMENT MODEL FOR HYBRID PLASTIC RAILWAY SLEEPERS

by

**A. H. Griemink**

in partial fulfilment of the requirements for the degree of

**Master of Science**

in Structural Engineering

at the Delft University of Technology,

to be defended publicly on 22 April 2021

Student number:	1504274	
Supervisor:	Dr. V.L. Markine	
Thesis committee:	Prof.dr.ir. R.P.B.J. Dollevoet	TU Delft, Railway Engineering
	Dr. V.L. Markine	TU Delft, Railway Engineering
	Dr.ir. F.P. van der Meer	TU Delft, Computational Mechanics
	A. van Belkom MSc	Lankhorst Engineered Products

An electronic version of this thesis is available at <http://repository.tudelft.nl/>.



# PREFACE

As a lot of people will know the Lego® company is being the largest tire producer in the world. And maybe not the first plastic sleeper producer, but certainly an early adopter. It easily could also be the largest plastic sleeper producer at the moment and therefore features on the cover.

This thesis marks the end of my master degree Civil Engineering. To say it has been quite a journey is perhaps an understatement. Certainly I visited some hilly terrain, but I am glad to present the end result. With regards to this thesis I would like to express my gratitude to my graduation committee. Their sharp but valid questions, their patience and support all aided in this final apotheosis. I hope that in the foreseeable future my contribution, how minor being, will have some influence on full integration of plastic sleepers.

My whole Delft University of Technology career has shaped me probably more than I even can imagine. I have met a lot of great people that made my years at this university unforgettable. Trying to mention everyone would leave some unnamed, so to everyone: thank you. Special thanks go to my colleagues at Moxio and Hylke in particular. First for allowing me to work on railway topics and thereby initiating my final graduation direction. Secondly by all the interest everyone showed in my research, the offered assistance and the freedom I got during my graduation.

Last but certainly not least, I want to thank my family, by allowing me to study in the first place, but also for your support on all possible levels. Finally there is one last person to thank, Lucie for her unconditional support and encouragement. I cannot, and do not want to, imagine how things would have went without you.

*A. H. Griemink  
Delft, April 2021*



# ABSTRACT

Railway sleepers form an important part of a classic track structure. Sleepers exist in their current form for a long time. The transition from wood to concrete sleeper has been made, but wood is still used and present in many track sections. As creosoted wooden sleepers are not allowed to be installed on the tracks anymore the search for durable and sustainable alternatives has started. One promising type is a hybrid sleeper constructed from recycled plastic (polyethylene) with steel reinforcement. The main part of this thesis is to create a finite element model that is capable of describing hybrid plastic sleepers. The ultimate goal is to be able to use this model to assist in sleeper acceptance. Current rules, regulations and high availability requirements make it difficult to test sleepers in the track under live loading conditions. Not many infrastructure managers are eager to install not already proven technology in their tracks.

The general parameters of the model were investigated and combined with some specific finite element modelling methods. Those formed the starting point of the design. Important design methods were the parametrisation of the model as much as possible to allow assessment of slightly different models. Secondly a mapped mesh was preferred above a free mesh to improve on accuracy. Also the amount of detail is kept high to be able to fully investigate the sleepers, e.g. to investigate the reinforcement bond.

The ANSYS APDL-language is used to program the FEM parametrically. This resulted in a comprehensive finite element model of one whole sleeper. Fully modelled with base plate (without detailed fastening), rail pad and rail section. Every part is constructed out of solids and meshed with a mapped mesh including the reinforcement. Two model methods, a general circular and a more element wise optimal octagonal model, were used to generate the reinforcement. All single sleeper models can be connected to form a piece of track with several possibilities in altering the foundation parameters per sleeper or allowing for different types of sleepers inside the track.

Concluding all generated finite element analysis (FEA) results could not impress enough to recommend the usage of FEA for sleeper acceptance. Especially with new, very non-linear behaving materials and a very dynamic loads, the effort involved in creating a validated finite element model (FEM) would be too great and the results not usable enough. For some parts a FEM can be beneficial, during design for example. Other simpler models than the one constructed here could be helpful if directly based on test results. But at least at this point in time, with relatively unknown materials, the direct testing of sleepers under loading conditions laboratory and in the track itself with close monitoring are regarded much more informative.



# CONTENTS

<b>Preface</b>	<b>iii</b>
<b>Abstract</b>	<b>v</b>
<b>List of abbreviations</b>	<b>ix</b>
<b>List of symbols</b>	<b>xi</b>
<b>1 Introduction</b>	<b>1</b>
1.1 Motivation	2
1.2 Problem definition	2
1.3 Research goal and research questions	3
1.4 Methodology	3
<b>2 Context</b>	<b>7</b>
2.1 Plastic sleepers	7
2.1.1 Producer	7
2.1.2 Considered sleeper types	8
2.2 Sleeper acceptance in general	8
2.3 Material properties	10
2.3.1 Used materials	10
2.3.2 Used material models	14
2.4 Conclusion	15
<b>3 Analytic Calculations</b>	<b>17</b>
3.1 Loading conditions	17
3.1.1 Maximum static loading	17
3.1.2 Quasi static loading	18
3.2 Characteristic length	18
3.2.1 Load distribution	19
3.3 Interface stresses	20
3.4 Beam on elastic foundation	21
3.5 Expected shear stresses	23
3.6 Conclusion	23
<b>4 Finite element model design</b>	<b>25</b>
4.1 Used terminology	25
4.2 Model composition	26
4.2.1 Determination of analysis and element type	26
4.3 Sleeper	27
4.3.1 Sleeper cross section	27
4.3.2 Circular reinforcement model	28
4.3.3 Octagonal reinforcement model	29
4.3.4 Base plate, rail pad and rail	31
4.3.5 Analysis settings	34
4.4 Multiple sleeper model	34
4.5 Code base	35
4.5.1 Features	35
4.5.2 Limitations	36
4.6 Summary	36

---

<b>5</b>	<b>Finite element results</b>	<b>39</b>
5.1	3-point bending results . . . . .	39
5.2	Multi-sleeper results . . . . .	42
5.3	General results and material limits . . . . .	42
5.3.1	201 sleeper . . . . .	42
5.3.2	202 sleeper . . . . .	43
5.3.3	Changing foundation stiffness . . . . .	43
5.4	Comparison with BOEF calculation . . . . .	48
5.5	Conclusion . . . . .	49
<b>6</b>	<b>Conclusions and recommendations</b>	<b>51</b>
<b>Appendices</b>		
<b>A</b>	<b>KLP sleepers</b>	<b>57</b>
<b>B</b>	<b>BOEF calculations</b>	<b>61</b>
<b>C</b>	<b>Rail profile</b>	<b>65</b>
<b>D</b>	<b>Finite element model accuracy</b>	<b>67</b>
<b>E</b>	<b>Bad foundation, influence of parameters</b>	<b>71</b>
<b>F</b>	<b>Gauge widening</b>	<b>75</b>
	<b>Bibliography</b>	<b>83</b>

# LIST OF ABBREVIATIONS

APDL	Ansys Parametric Design Language
BOEF	Beam On Elastic Foundation
DAF	Dynamic Amplification Factor
FEA	Finite Element Analysis
FEM	Finite Element Model
FFU	Fibre-reinforced Foamed Urethane
GUI	Graphical User Interface
HDPE	High Density PolyEthylene
KLP	Kunstof Lankhorst Product
PE	PolyEthylene
ProRail	Name of the Dutch infrastructure manager
RIVM	RijksInstituut voor Volksgezondheid en Milieu, Dutch national institute for public health and the environment
RST	Rolling Stock
TSI	Technical Specifications for Interoperability
UIC	Union Internationale des Chemins de fer, international Union of Railways



# LIST OF SYMBOLS

$A$	(-) Bad foundation modelling parameter: centre size multiplier
$C$	(-) Foundation modulus ( $\text{N}/\text{mm}^3$ ). Or Bad foundation modelling parameter centre magnitude multiplier
$\eta(x)$	(-) Eta-curve. Deflection curve of a Winkler foundation.
$G$	( $\text{N}/\text{mm}^2$ ) Shear modulus
$\gamma$	(rad) Conicity
$I_{zz}$	( $\text{mm}^4$ ) Second moment of area for bending around the y-axis
$k_d$	(m) foundation stiffness per sleeper
$\lambda$	(m) Wavelength
$L_c$	(m) Characteristic length
$Q$	(kN/m) Vertical wheel load
$Q_{\text{DAF}}$	(kN/m) Dynamic amplified vertical wheel load
$r$	(m) Radius
$s$	(m) spoorwijdte
$\sigma_{sb}$	( $\text{N}/\text{mm}^2$ ) Sleeper-ballast interface stress
$\tau$	( $\text{N}/\text{mm}^2$ ) Shear stress
$V$	(km/h) Speed of the track vehicles.
$Y$	(kN) Lateral wheel load
$E$	( $\text{N}/\text{mm}^2$ ) Young's modulus



# 1

## INTRODUCTION

The railways have a long history, dating back to the 18th century where it was first used in the mining industry. The track structure has not changed significantly since then. The most used type of railway track is the so-called ballasted track or also called standard track [1]. Ballasted track utilises crushed granite as ballast material to hold the railway sleepers in place and those sleepers on their turn hold the rails in place. To provide guidance for railway vehicles. The other important function of the track structure is to distribute the track loads. A traditional ballasted track is build up from a subgrade layer, a sub ballast layer and a thicker ballast layer. This ballast layer is the foundation for the railway sleepers or ties. The connection between the sleepers and the rail is made by a base plate attached to the sleeper and a fastening system that connects the rail to the base plate. Railpads are inserted between the rail and the base plate to improve the dynamic properties. In between and on the sides (the shoulders) of the sleepers more ballast is added to fully fixate the sleeper in the ballast bed [1]. In figure 1.1 a cross section of a classic ballasted track is shown.

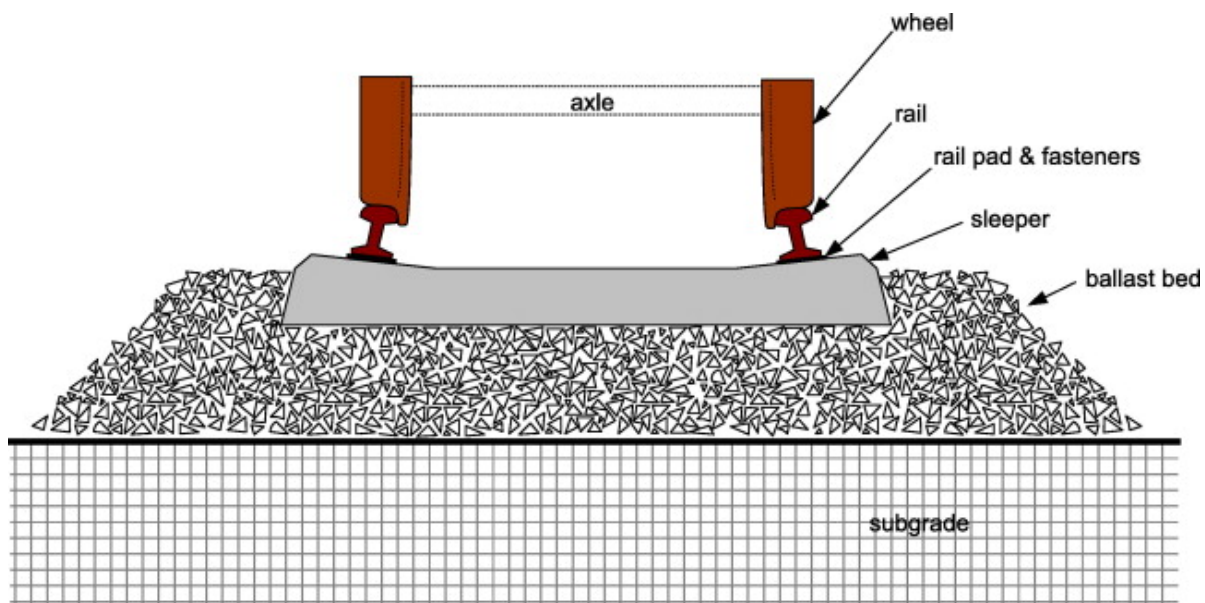


Figure 1.1: Cross section of normal ballasted track as assessed in this research [2].

Every component of the track has different functions, often more than one. As this research is based on the behaviour of sleepers, this will be the focal point. According to Esveld [1] the railway sleepers have the following functions:

- Holding gauge
- Distributing forces

- Transfer rail loads to ballast
- Insulate rails
- Dynamics, dampen impact forces
- Remain functional for the designed lifetime

In the early days of railway engineering, all sleepers were made out of wood. Wood was cheap, easy to obtain and easy to work with and it was strong enough. This does not mean that wood was or is the perfect material. It was at the time because of its abundant availability, but not per se out of a structural point of view. One of the big disadvantages of wood is its service life, it is susceptible to rot and decay due to organisms [3–5]. This short service life is the reason that all modern wooden sleepers were treated with creosote to protect against organic decay and to extend the service life.

After the Second World War wood became more and more scarce and the concrete technology had been improved. This led to the increased use of concrete sleepers, especially in Europe [1]. Steel sleepers also exist but are not used on a large scale, some reasons for this are their cost, possible corrosion issues and fatigue [6, 7]. Nowadays in the Netherlands all newly installed tracks section are constructed with concrete sleepers by default [8]. There are however some locations where concrete sleepers are not the most preferred type of sleeper to be used. As an example one can think of steel bridges without space for a ballast layer, where sleepers have to be fixed directly to the bridge. Concrete sleepers would degrade very quickly due to the dynamic contact forces between steel and concrete. A second example is the direct replacement for damaged wooden sleepers in a standard ballasted track. A replacement sleeper with different mass and stiffness would change the dynamic properties of the track and increase the contact forces in the wheel rail interface. These examples imply that concrete sleepers are not one hundred percent perfect so there is a part of the spectrum where there is room for improvement [9, 10].

## 1.1 MOTIVATION

The European Union banned the use of wood preserving creosotes in general as they have a negative impact on the environment. Wooden sleepers were treated with creosote, as preservative to improve their resistance to biological degradation. As creosote oil leaks into the soil over time, it pollutes the environment. The Dutch railway infra manager " ProRail " banned the use of creosote treated sleepers since 2006 [11]. Since then no new tracks with creosoted wooden sleepers are constructed. However still a lot of track sections with wooden sleepers exist and damaged sleepers need to be replaced. The ban on creosote means that any new wooden (replacement) sleepers have to be untreated and therefore will have an expected service life of 8-12 years. As this shorter service life increases the amount of wood needed in railway tracks and is not a sustainable practice, it opened the search for alternatives. The need for an environmental friendly, low elasticity and economically viable alternative, led to increased research into new materials [3, 12]. One of these researched materials is plastic and it is now used to construct a hybrid sleeper. These hybrid sleepers combine a recycled plastic base or matrix material with reinforcing steel. A recent report on sustainable sleeper alternatives by the Dutch National Institute for Public Health and the Environment ( RIVM ) mentioned the recycled plastic sleeper as a promising option on the ecological field [13]. Deciding that a specific material is a good alternative for existing sleepers is one thing, but the question arises how to determine if a newly designed sleeper based on a non conventional material is suited to be used in the railway track. To install a new type of sleeper, a significant basis has to be established, for wooden and concrete sleepers there exists Eurocodes that combine years of research, but not for plastic. A building code for plastic sleepers is being worked on, but for now one can only look to the wooden sleepers and concrete sleepers codes. The EN 13145:2001+A1:2011 [14], which covers wooden sleepers and bearers does not mention any structural properties that the chosen species of woods have to have, but focusses on geometric properties and visible defects and faults alone. Therefore it is not suitable to be used in this research. The recent standard on concrete 13230-6:2020 E [15] is much more based on structural properties and therefore will be used as basis despite being for a different material.

## 1.2 PROBLEM DEFINITION

To allow new sleepers to be placed in the tracks, there are regulations stated by the European Union, UIC and ProRail. As plastic sleepers are relatively new technology, not much is known about their behaviour. This

creates a circular chicken and egg situation as infrastructure managers are reluctant to integrate this new technology as it is not considered 'proven technology' but this does keep it from becoming proven technology. A lot of testing is done and a basic European standard has been introduced but there is still more to learn, for example on long term behaviour due to the time-dependend material properties. The vast amount of polymer types, each with different properties, makes that every research is not directly applicable to each and every use case. A lot of research is quite recently being done, so this topic could qualify as being a hot topic, other research involving the same sleepers are Koch [16], van Dam [17], Lojda et al. [18].

Plastic sleepers have advantages compared to conventional sleepers, but some weak points too. Ferdous et al. [10] lists some challenges on the use of plastic sleepers. Mentioned as points of attention are, the low stiffness of the plastic and the time dependant behaviour. Ferdous et al. [10] categories the considered Lankhorst sleeper as only suitable for light rail. This thesis takes a look at some properties of the sleepers and tries to determine if these sleepers are suitable to be used in heavy rail track. With the aid of a new finite element model ( FEM ) it is investigated if this route can aid the acceptation process of new sleepers and if successful provide more scientific backup to the sleepers background and documentation.

### 1.3 RESEARCH GOAL AND RESEARCH QUESTIONS

The difficulties experienced by introducing a new material for a sleeper design lead to the question if a finite element model can be used to provide a basis in analysing the track worthiness of a sleeper. To analyse the sleeper in terms of its capacity to withstand the bending stresses caused by the vertical rail seat loads, the sleeper support condition and its effect on the sleeper-ballast contact pressure must be quantified. The bending moment resulting from the vertical loads are heavily dependent on the ballast condition underneath the sleeper [19]. With a finite element model the behaviour of the hybrid plastic sleeper will be analysed. Internal stress distribution will be visible and by using a parametric design multiple analysis can be done on a lot of use cases, for example to allow a discrepancy in the sleepers ballast support condition.

The problem definition leads to the following research question:

*"Can a finite element model be used to improve railway sleeper acceptation?"*

To be able to answer this broad question, some other questions have to be answered first:

- What are the current acceptance practices?
- Which FEM data is useful in determining sleeper properties?
- Can the FEM provide the needed results in an accurate fashion?

The goal is to develop an finite element model that can be used to validate sleepers. As the question arouse from the limitations by the introduction of plastic sleepers, these form the use case on which the FEM is based. The scope of this research is limited to the structural properties and does not include thermal, environmental and creep effects.

### 1.4 METHODOLOGY

As mentioned, the basis of this research is the construction of a finite element model. The creation and solution process of the model is explained here, as well as the route that is taken to provide answers to the research questions. To get to the solution of the main research question the first step is to investigate the current practices. This is assessed in chapter 2 where the current codes on wood, concrete and plastic sleepers are examined. The information gathered from analysing the codes is used to determine a benchmark to compare the FEM results with and thus providing an answer to the first subquestion. Next to providing an answer to the first sub question, the chapter also provides some information about the examined sleeper types and information about the used materials in the model.

With the global boundary conditions determined some analytic calculations are done to create a better understanding of the to be constructed model. A beam on elastic foundation differential equation is solved to show the expected deformation. The interface stresses are determined as well as the expected load distribution over the sleepers when situated in a full track system. Chapter 3 does not directly solve any research questions, but does provide guidance on verification of the results.

In the next chapter, chapter 4, the construction of the finite element model is explained. The software package

that is used is Ansys and the model is constructed with 'Ansys parametric design language' ( APDL ) scripts that provide the code that let Ansys create and solve the model. In general a finite element model consists of several parts. These are the following:

- Geometry
- Mesh and elements
- Material models
- Analysis settings: type of analysis, time stepping, load cases

To be able to use the model for more than a single use case, a parametric model is set as design criterium. This allows minor changes to be made with ease but changes the way of assembling the finite element model. The geometry is fixed (rectangular) as the sleeper dimensions and properties are known in advance and are not subjected to change throughout this research. The choice has been made to start with a single sleeper model and extend that into a multiple sleeper model. This single sleeper model allows for easier verification and assessment of different models without having the increased calculation times of a large model. Next to the method of starting with a single sleeper, one other geometry variable is changed. Two slightly different versions are created, one with circular reinforcement and one with an octagonal reinforcement. The latter being able to be modelled easier and with less elements.

In general two meshing methods can be applied to mesh the geometry, a so called free mesh or a mapped mesh. The two methods are discussed in more detail in chapter 4, but a mapped mesh is in general more accurate than a free mesh [20]. Therefore the choice has been made to make this mapped mesh a key design principle and to mesh every part of the model this way. The downside of this method are the difficulties that arise when needing to mesh curved areas. It is however possible, as is explained in section 4.3.1 to model a round bar with a mapped mesh. To asses the influence of the mesh, the element size is decreased to see if the model behaves as it should and to find an optimal model that combines computational benefit and accuracy. This is done in appendix D.

The third important factor is the material model. The material model is the representation of the used materials in the finite element analysis. This is done by determining properties such as the Young modulus and Poisson's ratios for each material. The FEA results are compared to the laboratory 3-point bending tests done by van der Drift [21] so the experienced Young modulus of the plastic material is found. This is used as material stiffness for the other analysis.

Lastly the analysis settings can be set. The default analysis is set to be a static structural analysis. There is also an optional modal analysis setting, to provide insight in the dynamic behaviour of sleepers in the track. Any other time-dependent analysis types are not yet supported although can be implemented with relative ease. The mayor issue is the need to validate the more extensive material models. Therefore the static analysis is the only simulation of which the results are analysed. It is used to determine the stress and strain distribution in the sleeper and force distribution over several sleepers. The plastic material parameters and foundation properties are altered to provide insight on how both reinforcement models compare to each other and to see how the sleeper performs under non-optimal circumstances.

So summarising the following results are analysed and discussed:

- Comparison circular versus octagonal reinforcement modelling.
- Influence of element size on results
- Deformations of sleeper top and bottom
- Maximum stresses in the sleeper and foundation
- Maximum shear stress in reinforcement-plastic interface
- Gauge change due to bad foundation supports

All those results will assist in finding an answer to the main research question. If the FEM is able to assist in providing the needed parameters that follow from the current standards (discussed in chapter 2) and analytic analysis (discussed in chapter 3), then FEA can possibly be regarded as a tool in determining track worthiness

of new sleepers. Figure 1.2 shows the report structure graphically. Providing a visual overview of the chapters and how they assist in reaching the conclusions.

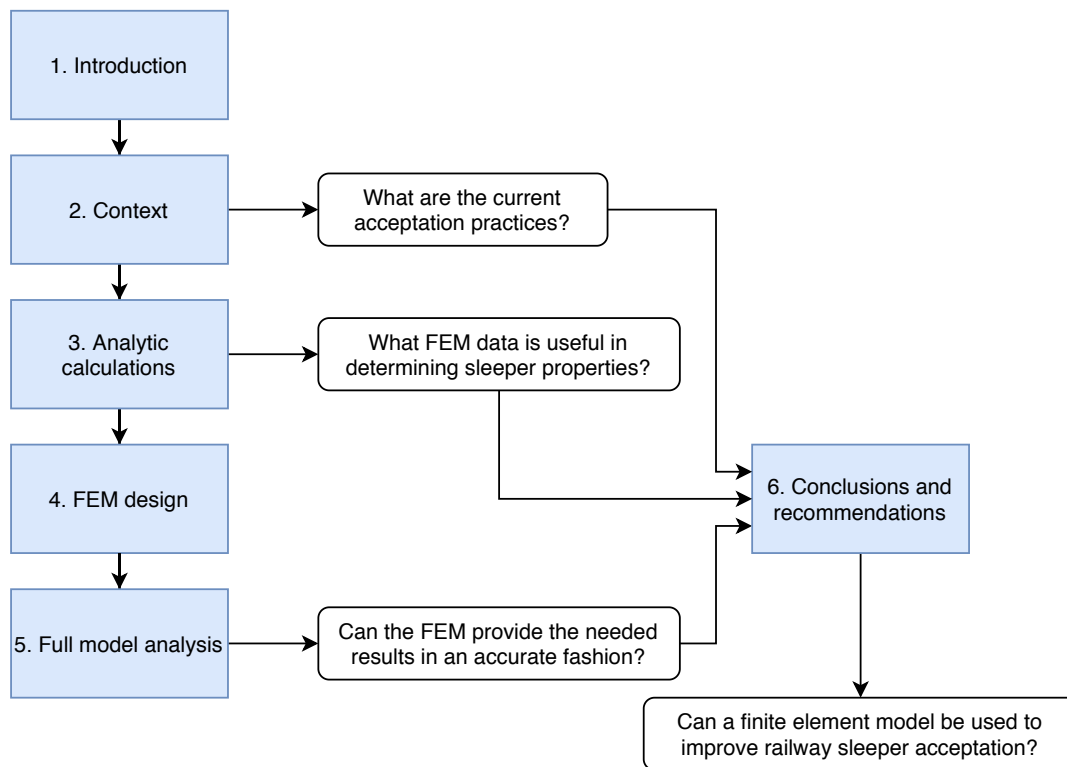


Figure 1.2: Graphic of the report structure including research questions.



# 2

## CONTEXT

This chapter provides some background information about the research and also answers the question about which requirements have to be fulfilled to be able to accept a new sleeper type. The first part is an overview of the regarded sleepers. This is followed by an extract of the current NEN-norms on sleeper design. The last section covers the general model properties including finite element model implementation. The main goal of this chapter is to provide a benchmark on structural values that (new) sleepers have to comply to. The only values considered will be stress and deformation based, thermal and environmental factors are excluded in this research. To clarify, the terms *plastic* and *polymer* both mean the total mixture that creates the sleepers base material including any enhancers. If plastic deformation or plasticity is considered, this is explicitly stated.

### 2.1 PLASTIC SLEEPERS

The introduction of plastic sleepers in the railway industry is a combination of the search for a replacement material for wood, and more recently, the look for durable and mostly more sustainable alternatives. Plastic sleepers do possess some interesting properties such as a high damping, and a long life span due to good chemical and biological resistance [22].

There are many different types of plastic sleepers. As polymers themselves are not stiff enough to be used as sleeper material on their own, a reinforcement material has to be added. This is done in the form of adding steel or glass fibres to the material, sometimes forming a full fibre reinforced polymer sleeper (glass fibre) [10]. Currently plastic sleepers are implemented into some railway tracks, however large scale implementation on heavy rail lines is still future. Many used sleepers are FFU (Fibre Foamed Urethane) sleepers, a fully glass fibre sleeper type [23]. A glass fibre type of sleeper is durable but not very sustainable. Once they are end of life they can't be recycled without downgrading [24]. This is where the sleepers from recycled plastic are coming into view. The sleepers researched in this thesis are made of polyethylene, being a thermoplastic material, reheating this kind of material melts it and it then can be remodelled into new products. The quality of this material is somewhat degraded but can be still reused in products [25].

#### 2.1.1 PRODUCER

The considered type of plastic sleeper is a hybrid sleeper made from recycled thermoplastic polymer reinforced with steel. The regarded sleepers are two types designed and produced by Lankhorst. Lankhorst is in this report short for Lankhorst Engineering Products / Lankhorst Rail, a specific branch of the company that focusses on products made from (recycled) plastic materials [26]. Lankhorst has a lot of experience with large recycled plastic products reinforced with steel. Their earlier constructed products using steel reinforced plastic is creating a tube stacking solution for pipes. The railway sleepers are however subjected to very different loading conditions and therefore create the need for a greater knowledge base. Along this research several other aspects of Lankhorst sleepers are researched, such as the research of Koch [16], van Dam [17], van der Drift [21] and Lojda et al. [18].

Table 2.1: Dimensions of the two sleeper types as considered in this report. Bending stiffness taken from Lojda et al. [18]

	KLP 201	KLP 202	Unit
Length	2600	2600	mm
Width	250	250	mm
Height	150	150	mm
Reinforcement diameter	16	25	mm
Reinforcement percentage	2.1	5.2	%
Bending stiffness	6655	12995	MPa

### 2.1.2 CONSIDERED SLEEPER TYPES

The researched plastic sleepers are called: 'KLP sleepers'. In appendix A all the sleeper details can be found. Table 2.1 summarises the basic parameters. This section describes the most important properties as well. The main goal of this type of sleeper is to provide an alternative to wooden sleepers. Secondary the aim is to provide a general type of sleeper that is more resilient than concrete sleepers and can be a good option in general heavy rail tracks. There are several types sleepers available:

- PE rectangular sleeper (201)
- HDPE rectangular sleeper (202)
- HDPE optimised sleeper

Figure 2.1 shows the rectangular and optimised sleeper types installed in a small piece of track at the university laboratory.

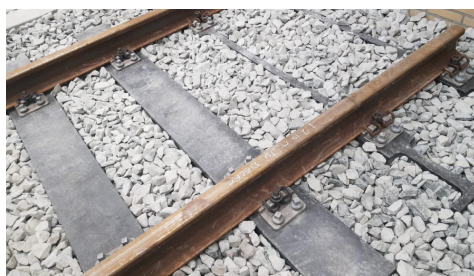


Figure 2.1: A set of two Lankhorst KLP-S sleeper types in a illustrative piece of track [17].

### SLEEPER GEOMETRY

The chosen types to investigate are the two rectangular sleepers. The optimised sleeper features a completely different design and uses the mass of the ballast to lock itself in place. As this complicates the analysis to a great extent, the choice is made to only use the rectangular sleepers. Both cross sections do not change over the length of the sleeper, with a small note that the reinforcement does not continue in the outer edges of the sleeper. To be easily interchangeable with wooden sleepers, the dimensions are set to:

$$2600 \times 150 \times 250 \text{ L, H, W [mm]} \quad (2.1)$$

The sleepers length is in practice variable, the standard length however is 2.6 meters. In general the HDPE-sleeper is considered, but as the FEM can be easily altered, the PE version is also taken into account. The sleeper dimensions are similar for both 201 and 202 types, the main difference is the size and location of the reinforcement which is not the same. The difference in reinforcement can be explained as follows: the 202-sleeper is made out of a stiffer material than the 201-sleeper and therefore needs more reinforcement to keep the general properties of the sleeper similar. The reason for this is, is that a stiffer material takes a greater load in any construction. So if more reinforcement would be used in a soft material, the steel bears take too much load and increase the sensitivity to fatigue damage .

## 2.2 SLEEPER ACCEPTATION IN GENERAL

When creating a new sleeper it has to be proven that a sleeper meets certain requirements. This section will describe which requirements have to be met in order to put a new sleeper type into service. In short, there

are no regulations for a sleeper constructed out of a new material. There exist three NEN-documents about sleeper design and requirements, these are based on the material that the sleepers are made of. Thus there exists a code for concrete, wood and plastic sleepers [14, 15, 27]. The latter being the one corresponding to the considered sleeper types in this thesis. However, the data on requirements in this code is only given as indicative values. The need for this code was the development of sleepers consisting of different materials and for a new material there will be an additional standard necessary, but any new standard will lack the detailed data as usage will increase the knowledge.

Basic requirements of railway sleeper should be material independent and provide a range where designed sleepers should comply to, something that is also endorsed by van Belkom [28]. The standard on wooden sleepers only covers acceptable wood species and acceptable and unacceptable defaults of sleepers. None of this is suitable for plastic sleepers, so this standard is not further regarded. The prestressed concrete sleeper norm features a new document that assess sleeper design, so this could provide some insight as well. The most informative should be the norm on plastic sleepers this is discussed first.

### NEN-ISO 12856-1, MATERIAL CHARACTERISTICS FOR PLASTIC RAILWAY SLEEPERS

The standard NEN-ISO 12856-1:2014(E) [27] is not specially tailored to hybrid sleepers, but the basic properties are provided with some design guidelines. Three types of sleepers are considered in this standard all with their specific use cases. The three types of sleepers that are considered:

1. tropical hardwood sleepers, track without ballast and special tracks, lines up to 20 t per axle for a speed of 130 km/h and 14 t per axle for a speed of 300 km/h.
2. wooden sleeper for UIC 5/6 track categories, lines up to 22.5 t per axle for a speed of 160 km/h
3. hardwood sleeper for heavy-haul track up to 35 t per axle for a speed of 80 km/h

The sleeper classification that is used in this research is the second type, which is equivalent to standard wooden sleepers. The standard requires the sleepers to have minimal dimensions similar to the wooden sleepers, something that is already the same as the regarded KLP sleepers. As this research focusses on the structural properties only, only those attributes are extracted from the standard. Table 2.2 shows the minimal required values that the sleeper material should possess according to the standard.

Table 2.2: Minimal physical characteristics for sleepers. Values taken from NEN-ISO 12856-1:2014(E) [27]

Type B	Required value	Unit
Bending strength	$\geq 18$	Mpa
Flexural modulus	$\geq 2500$	Mpa
Shear strength	$\geq 4.5$	Mpa
Longitudinal compression strength	$\geq 8$	Mpa
Lateral compression strength	$\geq 8$	Mpa

The prescribed method of determining the bending strength and flexural modulus is by testing a sample. This sample is not a full sleeper but a smaller sample, that makes it difficult for hybrid sleepers to be assessed as they heavily depend on the interaction with the steel. It is not clear if these properties may be determined by testing on full scale sleepers.

### NEN-EN 13230-6, DESIGN OF CONCRETE SLEEPERS AND BEARERS

In 13230-6:2020 E [15] the design of concrete sleepers is assessed. This standard is relatively new as the definitive edition was released in 2020. An easy method that can be applied is the empirical method. Permanent observation for at least 5 years is mandatory and the set should be large enough to give significant results. This method is easy from one side of the spectrum, on the other hand, one needs a test track and a frequent inspection interval.

The second method is the theoretical method, this method uses a standardized formula with several ' $k$ '-parameters that account for different track conditions. The default route is by determining the dynamic rail seat load  $P_k$  first. The rail seat load is then used as input for the bending moment calculations, centre maximum negative moment and rail seat positive moments. The formula for determining  $P_k$  is given by 2.2

and features four k-parameters. Please note that the parameter  $k_d$  has a different meaning here than as used in the rest of this research where it resembles the discrete foundation stiffness of a whole sleeper.

$$P_k = \frac{A_{\text{nom}}}{2} (1 + k_p \cdot k_v) \cdot k_d \cdot k_r \quad (2.2)$$

Where:

$k_p$  = Influence of rail pads, reduction of load  $0.78 \leq k_p \leq 1$

$k_v$  = Dynamic amplification factor

$k_d$  = Load bearing percentage of sleeper with respect to the axle load

$k_r$  = Variation in ballast support condition, recommended value = 1.35

The dynamic amplification factor (DAF)  $k_v$  is determined in equation 2.3 as given in NEN-EN 13230-6. A dynamic amplification is a multiplication factor that incorporates the increase in load due to dynamic impacts. Incorporating a DAF is quite common in railway track designs as it is an easy method to take dynamic impact loads into account [1]. Therefore this method is also used in the determination of the used loads for the FEM (section 3.1.2).

$$k_v = \begin{cases} 0.25 & \text{For } 0 \leq V \leq 60 \text{ km/h} \\ 0.25 + \frac{V-60}{280} & \text{For } 60 \text{ km/h} < V < 200 \text{ km/h} \\ 0.75 & \text{For } V \geq 200 \text{ km/h} \end{cases} \quad (2.3)$$

$$k_{v130} = 0.5 \quad (2.4)$$

The increased deformation that arises by flexible sleepers, such as plastic sleepers, is investigated by van Belkom [29]. NEN 13230 assumes a stiff sleeper, and therefore a uniform ballast distribution, which is fine as it considers concrete sleepers which are very stiff compared to wood and plastic sleepers [18]. Despite this the requirements for (concrete) sleepers are still included here.

Concluding the assessment of railway sleepers constructed out of a new material is not a trivial task. It is clear that the procedures are still being improved. The new concrete standard on design is aiding with providing general rules on sleeper design, but is still based on concrete sleepers. Plastic sleepers have their own standard that is not fully crystallized and therefore only provides some indicative values. For reference, the extracted requirements are given in table 2.2.

## 2.3 MATERIAL PROPERTIES

In this section the used materials are presented. First a short introduction about each type of material, followed by a summary of its properties. The last section is about the translation from material properties to a material model that can be used in finite element modelling. As the primary interest of the research is the polymer material, that particular section has a more elaborate explanation than the other materials.

Notice has to be taken, that not every aspect in this chapter is necessarily used in the final models. This is primarily the fact for the polymer parameters, as not all non-linear material properties can be used in static analysis. These extra properties are however included to feature a broader view of the possibilities or necessities, implementing such a material model.

### 2.3.1 USED MATERIALS

The used materials to construct the sleeper and the track system are the following:

- Ballast: crushed granite, 30/35 grade
- Sleeper
  - Reinforcement: Steel, S235
  - Base material: Polymer, being: HDPE or PE
- Fastening system

- Base plate: Steel
- Rail pad: Rubber
- Rail E541: Steel, R260Mn

Most of these materials are quite standard and commonly used in the railway industry [8]. The goal is to minimize the effect from outside sources so this validates the choice for common materials and therefore their origin is not further explained.

#### BALLAST

The material properties of the ballast are only an indirectly applied. As the ballast is modelled by spring-damper elements, (see chapter 4, which covers the full FEM model construction) and not by solid elements, the only parameter that is used to model the foundation is the spring stiffness  $k_d$ . The possible damping factor is not used as long as the FEA is a static analysis, if not the damping factor should also be considered. The spring stiffness that forms the input for the model is the whole stiffness that the track experiences. This means that the assumption is made that the sleeper is infinitive stiff. The determination of the foundation stiffness is hard as it depends on local circumstances such as the stiffness of the soil below the track. Therefore the used value here is an estimate. Esveld [1] provides upper and lower limits on the foundation modulus  $C$  which can be transformed to the sleeper foundation stiffness via:

$$k_d = C \cdot A \quad (2.5)$$

Where:

$$C = \text{Foundation modulus ballast} \quad (2.6)$$

$$A = \text{Sleeper contact area with ballast} = 2600 \cdot 250 = 650\,000 \text{ mm}^2 \quad (2.7)$$

The limit values given are  $0.02 \text{ N/mm}^3$  as lower limit for foundation in a bad state and  $0.2 \text{ N/mm}^3$  as upper limit for good track conditions. The standard on concrete sleeper design uses the value  $0.1 \text{ N/mm}^3$  as generic foundation modulus. Substituting all values in equation 2.5 results in the following possible values for  $k_d$  as summarised in table 2.3.

Table 2.3: Range of foundation moduli  $C$  and corresponding discrete foundation stiffness following from equation 2.5.  $A = 650\,000 \text{ mm}^2$ .

	Foundation modulus $C$ [ $\text{N/mm}^3$ ]	Discrete sleeper stiffness [ $\text{N/mm}$ ]
$k_{d_{\min}}$	0.02	13000
$k_{d_{\text{NEN standard}}}$	0.10	65000
$k_{d_{\text{Oregui et al. [30]}}}$	0.1385	90000
$k_{d_{\max}}$	0.20	130000

The value that is used as default foundation stiffness is the literature value of  $90 \text{ kN/mm}$  by Oregui et al. [30]. This is a value that is slightly higher than the standard value as stated by Esveld [1]. The value that is used in van Belkom [28] calculations is  $50 \text{ kN/m}$  where a lower value is preferred. If possible the foundation properties are changed to investigate its influence so this reduces the need for an exact value. It is just to declare a default and a relatively high default is chosen which increases the load on the sleepers. As some calculations use only a half sleeper, also half of the discrete sleeper stiffness is calculated:

$$k_d = 90.0 \text{ kN/m} \quad (2.8)$$

$$k_{d_{\text{half}}} = k_d / 2 = 45.0 \text{ kN/m} \quad (2.9)$$

#### RAIL AND BASE PLATE STEEL

The reinforcement is made of standard S235 structural steel. For the sake of simplicity, the reinforcement, the base plate and rail are all modelled out of the same material. There are differences between the steel used to construct rails and the standard B500 steel. Common railway steel has, in general a higher carbon content ( $\approx 0.70\%$ ) than general structural steel ( $0.22\%$ ) [31, 32]. Still both types of steel are generalised into

one material model. As yielding of anything other than the reinforcement is not of interest and secondly the Young modulus is the same for all considered steels, lastly the main analysis is static, where any material ultimate limits are not regarded. Concluding, any differences in ultimate strength are not a problem when used in a linear material model. The material model therefore is constructed with the following properties: The Young modulus of steel is set to 210 000 MPa, the Poisson's ratio is 0.3 [33].

#### CHOSEN RAIL PAD AND ITS PROPERTIES

The considered rail pad material is the FC9 type by Trackelast, a commonly used rail pad. The material properties are taken from a suppliers data sheet Trackelast [34], table 2.5 contains the density and Poisson's ratio values. The elastic properties that are provided, consist out of a static and a dynamic stiffness, these are given in kN/mm with a fixed force and area. The static stiffness is 480 kN/mm with a force of 58.8 kN and a pad with dimensions:  $140 \times 140 \times 4.5$  mm. The dynamic stiffness is given as 880 kN/mm for the same force and surface, for a loading frequency of 20 Hz.

To be able to insert the material properties into the model, the material properties have to be transferred to a general Young modulus independent of the material size. The following equations for the Young modulus, stress and strain are common in civil engineering and can be used to generate an expression for  $E$ .

$$E = \frac{\sigma}{\epsilon}, \sigma = \frac{F}{A}, \epsilon = \frac{\Delta l}{L} \quad (2.10)$$

$$F = u \cdot k \rightarrow \Delta l = u = \frac{F}{k} \quad (2.11)$$

Combining all equations from 2.10 into each other and with 2.11 results in the following expression for  $E$ :

$$E = \frac{\frac{F}{A}}{\frac{\frac{F}{k}}{L}} = \frac{k \cdot L}{A} \quad (2.12)$$

$$E_{\text{rail pad static}} = \frac{480 \cdot 10^3 \cdot 4.5}{140^2} = 110.2 \text{ N/mm}^2 = 110.2 \cdot 10^6 \text{ N/m}^2 \quad (2.13)$$

$$E_{\text{rail pad dynamic}} = \frac{880 \cdot 10^3 \cdot 4.5}{140^2} = 202.0 \text{ N/mm}^2 = 202.0 \cdot 10^6 \text{ N/m}^2 \quad (2.14)$$

Both Young moduli are possible, depended on a static or dynamic simulated case, but the choice is made to use the dynamic stiffness in all simulations as this is the most common and more demanding situation.

#### POLYMER MATERIAL PROPERTIES

The main matrix material is a HDPE (High Density PolyEthylene) polymer. It is difficult to determine precise material properties and that makes determining the precise material properties one of the largest unknowns of this research. Lankhorst uses two types of polyethylene for its two types of sleepers. The 201 sleeper is made from KLP - PE and the 202 sleeper is made from KLP -HS50. Both materials behave similar, so if not mentioned explicitly all properties hold for both types.

#### GENERIC PROPERTIES

Polyethylene is a thermoplastic polymer. Its thermoplastic behaviour makes it suitable for recycling purposes. The material can be melted and used for new products without minor degradation. This opposed to (glass) fibre reinforced materials that are difficult to separate and therefore can only be downgraded, at least at this moment in time [35].

Polyethylene possesses a non linear stress strain behaviour even for low stress loads. To illustrate this, the stress-strain graph of KLPHS50 is shown in figure 2.2. In table 2.5, the basic material properties are given for both materials used in the considered sleepers. Some properties are however less usable for this analysis as polyethylene is a visco-elastic material and the material properties do not only depend on the magnitude of the load, but do also depend on the rate of change. In other words, the loading frequency influences the material stiffness.

The tensile strength for plastics is relatively low and is in the range of 8.5 MPa to 18 MPa for PE and HDPE respectively [36, 37]. The strains experienced at this stress level are large and in the order of 20 %, where

standard steel breaks at around 3%. As this is currently the only available data, these values are used as ultimate limits to compare the FEA results with.

The next property that is also important is the bond strength between the steel and plastic materials. The shear stress ( $\tau$ ) limits are taken from push out tests [38]<sup>1</sup>. The said conservative limits that this internal specification presents are:

$$\tau_{PE} = 2.5 \text{ MPa} \quad (2.15)$$

$$\tau_{HDPE} = 2.5 \text{ MPa} \quad (2.16)$$

These values are the interface shear limits between the plastic and the reinforcement materials. The shear values of the FEA are compared to this limit values to be able to tell if the bonds should hold or if this is a probable point of failure.

#### VISCO-ELASTIC BEHAVIOUR

The following paragraphs are covering one important property of plastics, but one that is not yet incorporated into the FEM. The viscous-elastic behaviour is a time dependent property and is by definition not included in a static analysis. Some minor explanation is added here to address the possibilities and possibly necessity to incorporate such visco-elastic behaviour.

Visco-elastic behaviour is the delayed 'reaction' of a material on the loading conditions. If the material is subjected to a harmonic sinusoidal load (with loading frequency  $\omega$  and amplitude  $\sigma_0$ ), the shear stress ( $\sigma$ ) in the material lags behind. This phase angle ( $\delta$ ) is used to construct an in phase component and an anti-phase component of the shear stress [40, 41].

$$\sigma = \sigma_0 \sin(\omega t) \cos(\delta) + \sigma_0 \cos(\omega t) \sin(\delta) \quad (2.17)$$

This can be rewritten to make use of the shear modulus  $G$ . One modulus  $G'$ , is in phase with the shear strain and an other modulus  $G''$ , is out of phase with the shear strain. Both can be combined to create a complex shear modulus  $G^*$ :

$$G^* = G' + iG'' \quad (2.18)$$

This complex modulus is available from torsional tests done on the material and is the basis from which a material model is constructed that can be used in harmonic analysis. The material model properties are created by curve fitting and adjusting the parameters so the models curve follows the test results. As the choice is made to limit the analysis to static only for this research, curve fitting experimental data is done as example and test of the method, but it is not going to be used in this particular investigation.

The torsional test data is uploaded into Ansys where the curve fitting process takes place. The Prony curve is then fitted to match the experimental results. This is then subsequently set as a material parameter and can be used in harmonic analysis.

#### YOUNG'S MODULUS

Recent research on this topic has generated a comparison on the bending stiffness of several sleepers constructed out of different materials [18]. This forms the mayor input, accompanied by the individual material property-sheets provided by Lankhorst [36, 37]. As the whole sleeper is used to measure the stiffness, it is expected that the results behave better than the raw material data. The difficulty in determining the input data is clear as several options can be used. The material sheets provide a different value than the expected stiffness under loading conditions, with the reasoning that the plastic materials behave stiffer when the loading frequency is higher.

Table 2.4 shows the several Young's moduli, the first results from experiments by Lojda et al. [18] appended with the other possible values. What is clear from the experiments is that the high frequency does increase the experienced stiffness. More remarkable is the calculated material stiffness for the HDPE-plastic. In appendix A an expression for the cross sectional property " $EI$ " is given (equations A.12 and A.13). The used method combines the different Young moduli of steel and plastic and into an expression for the stiffness.

<sup>1</sup>This document is probably comparable with Prochazkova et al. [39] as referred to by others, but the author was not able to find this document, so the internal documentation is used.

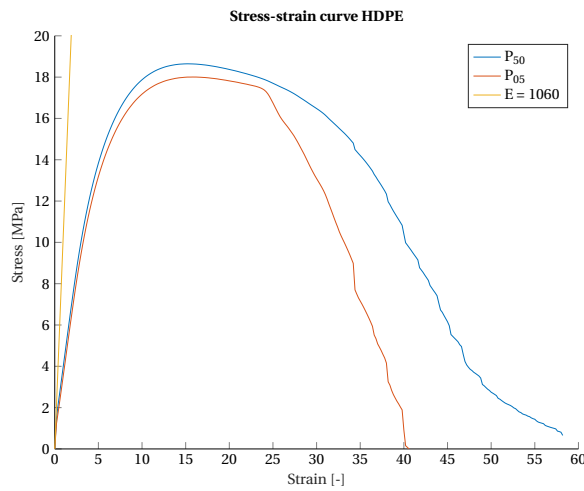


Figure 2.2: Stress strain curve of the 202 sleeper material with strain in percent. Data from Smid and van Belkom [37].

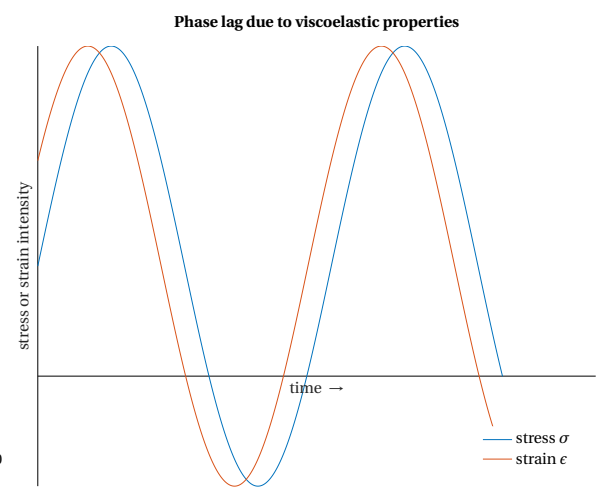


Figure 2.3: Graphical view of the phase lag between the stress and strain in a visco-elastic material under constant harmonic loading.

One important conclusion that can be drawn is the huge influence of the steel on the total stiffness of the sleepers, a minimal contribution of 90% is expected. Also a smeared Young modulus is calculated where the contribution of the steel is incorporated over the whole cross section. Substitution some approximate Young modulus for both materials ( $E_{p201} \approx 450$  and  $E_{p202} \approx 1000$  MPa) the following sleeper stiffnesses were found:

$$E_{\text{smeared}201} \approx 8000 \text{ MPa} \quad (2.19)$$

$$E_{\text{smeared}202} \approx 14700 \text{ MPa} \quad (2.20)$$

Also when incorporating the second moment of area of the sleeper:

$$I_{zz} = \frac{bh^3}{12} = \frac{250 \cdot 150^3}{12} = 70.3 \cdot 10^6 \text{ mm}^4 \quad (2.21)$$

Two approximate  $EI$ 's can be found:

$$EI_{\text{smeared}201} = E_{\text{smeared}201} \cdot I \approx 562 \cdot 10^9 \text{ Nmm}^2 \quad (2.22)$$

$$EI_{\text{smeared}202} = E_{\text{smeared}202} \cdot I \approx 1033 \cdot 10^9 \text{ Nmm}^2 \quad (2.23)$$

All stiffness values do not deviate a lot if the  $E_p$  is changed. Looking only at the smeared Youngs modulus, both sleepers also have an ultimate theoretical minimum where the stiffness of the plastic material is zero. These are 7566 MPa and 14700 MPa for the 201 and 202 sleepers respectively. Interesting is that the measured experimental values of from Lojda et al. [18] found stiffnesses below the the 202 sleeper threshold. This means that when inverting the calculations the stiffness of the HDPE becomes small or even negative, something that is certainly not true. Therefore this analytic calculation is not expected to be very accurate. The bending mechanics and / or the material bonding must have a large influence in the final stiffness.

### 2.3.2 USED MATERIAL MODELS

The material model that is used in FEA is relatively simple in linear elastic analysis. Such analysis, in principle, only require a stiffness and Poisson's ratio. For contact analysis the material model can be outfitted with a friction component etcetera. As the used polymers in general behave non-linear under loading, the Young's modulus can be imported as a stress-strain table that assumes linear behaviour between the input points. In this way, changing material stiffness could be added to the model. However, it is not equal to a full visco-elastic material behaviour.

The visco-elastic behaviour can be added by making use of the Prony Series, this method uses a summation of time depended terms to describe the [42]. This material behaviour could be added when conducting a transient analysis. It is however the question how detailed the material model needs to be in order to produce the wanted results. When looking at a larger scale such as a whole piece of track some properties could be

Table 2.4: Young's moduli for sleeper materials.

Material	Experimental values from Lojda et al. [18].			Material sheet	Estimated value Lankhorst
	Static [MPa]	5 Hz [MPa]	Increase [-]	[MPa]	[MPa]
Softwood (beech)	12900	13800	7%	–	–
Hardwood	20100	21700	8%	–	–
Concrete	37100	41900	13%	–	–
PE (whole sleeper)	5500	7900	43%	–	–
PE-only	–	341	–%	240	330
HDPE (whole sleeper)	11500	13900	21%	–	–
HDPE-only	–	170	–%	760	880

Table 2.5: Properties of all used materials when used in FEA. Values from Lojda et al. [18], European union agency for railways [33], Trackelast [34], Smid and van Belkom [36, 37].

Material	Steel	Railpad (dynamic)	HDPE	PE
Name	S235	FC9	HS50	PS
Density (kg/m <sup>3</sup> )	7850	1150	870	880
Young's modulus (MPa)	210 000	202	1060	330
Young's modulus by Lojda et al. [18] (MPa)	–	–	8653	341
Poisson's ratio (-)	0.3	≈ 0.4	≈ 0.4	≈ 0.4
Tensile strength (MPa)	235	–	18.6	9
Compression strength [20%] (MPa)	–	–	26.4	14

unnecessary time consuming. In general it is good practice to first use a simplified model and then look at which properties are needed if the results do not agree with the real life case. In table 2.5 all the used material models with their parameters are listed for reference.

## 2.4 CONCLUSION

This chapter consists of several and diverse sections. The investigated sleepers are shown and the used material models were explained. However, the most important section is about current regulations and sleeper acceptance. As answer to the first subquestion, "what are the current acceptance practices?", the current regulations on wooden, concrete and plastic sleepers where all examined. The standard about concrete sleeper design 13230-6:2020 E [15] provides the most background information about sleeper design, but focusses on concrete and is therefore less useful. Every requirement has to be weighted if it is applicable to hybrid or plastic sleepers. The standard about plastic railway sleepers NEN-ISO 12856-1:2014(E) [27] does only provide indicative values as this standard is still in development. This makes it not easy to provide a definite answer to what defines a capable sleeper, but the standard does provide minimal required resistance values for bending strength, flexural modulus and shear strength (see table 2.2). Those can already be compared to the material parameters as found in this chapter. With the properties from table 2.5 placed next to the values of table 2.2, all material properties meet the required values set by the standard. So for this 'analysis' the most important values where obtained by laboratory testing on whole sleeper combined with factory test of individual material components. All of this can already be done without any finite element calculation.



# 3

## ANALYTIC CALCULATIONS

This chapter contains the analytic basis on which the finite model is based. The main goal of these calculations is to get an idea what is to be expected from the FEA. The most extensive calculation considers a beam on elastic foundation calculation. The BOEF differential equation is solved and the deformations are later used for several other analysis. Other calculations that are done are more back of the envelope type calculations. This is acceptable as some input parameters are assumptions as well, so it is not going to be fully accurate anyway, but provides insight in the order of magnitudes and the general expected behaviour. The calculations that done are the following:

- The determination of the characteristic length to determine the maximum load on a single sleeper
- The maximum shear stress in the plastic-reinforcement interface
- BOEF calculations
- Expected ultimate stresses in other interfaces

### 3.1 LOADING CONDITIONS

As general constraint in railway track construction, the maximum axle loads and maximum allowed speed are the two main input parameters. The maximum speed has a great influence on the loading as it amplifies the impact forces when a train encounters a weld for example. The maximum loading on the track is determined by the traffic load. The allowed axle loads are limited by load classes. In NEN-EN 15528 [43] the different railway track classifications are given. In the Netherlands all the railway tracks are required be of class C2 and all mayor freight corridors are of class D4 [44]. This means that the maximum axle load on the Dutch tracks is 22 tons for the C2 class and 22.5 tons for the D4 class. Two possible values for loads are be established, one maximum static load and one maximum quasi-dynamic load. The latter incorporates dynamic effects to be used in static analysis, hence the naming. The allowed speed that is used will be 130 km/h as this is the common limit speed for passenger trains. Some parts are allowed to have higher top speeds, but 130 km/h is regarded a reasonable value. This is also due to the fact that passenger trains generally have much lower axle loads than freight trains and the speed limit on freight trains is lower than for passenger trains [1].

#### 3.1.1 MAXIMUM STATIC LOADING

The static load on the track purely depends on the axle loads. The basic input is a single axle load  $Q$ . The forces are applied on a single rail, so the axle load is split into two wheel loads. Derived from the D4 class load, the resulting static value for one wheel that is used in this thesis is 110 kN, based on a maximum axle load of 22.5 tons.

$$Q_{\text{static}} = \frac{M_{\text{axle}} \cdot g}{2} = \frac{22.5 \cdot 9.81}{2} = 110.4 \approx 110 \text{ kN} \quad (3.1)$$

Where:

$Q_{static}$  = static load, representing a loaded single wheel.

$M_{axle}$  = class D4 max axle load =  $22.5 \cdot 10^3$  kg

$g$  = gravitational constant =  $9.81$  m/s<sup>2</sup>

There are other factors that contribute to the vertical forces on the rails, such as wind loading and cant in curves. Their contribution is neglected as the maximum allowed loading is assumed. In the case of narrow margins these loads should be regarded as well.

The lateral, or sideways, loading  $Y$  on the rail is based on the Prud'homme formula (equation 3.2). Prud'homme gives a value for the lateral resistance a track should have [1]. In this model it is used to get a maximum lateral load without having to assume cant and wind factors, influencing the lateral loading conditions.

The maximum value for lateral loading is therefore the following:

$$H_{tr} > 10 + \frac{P}{3} \quad (3.2)$$

$$Y_{static} = 10 + \frac{Q_{static}}{3} = 10 + \frac{110}{3} \approx 47 \text{ kN} \quad (3.3)$$

Where:

$H_{tr}$  = lateral track resistance

$P$  = axle load in kN

$Y_{static}$  = lateral track loading

### 3.1.2 QUASI STATIC LOADING

As the dynamic effects have a high effect on the total load on the track system, several speed related coefficients were developed. A commonly used method that is used in this research is an empirical method developed by Eisenman [1]. This method uses a DAF to artificially increase the static load to account for dynamic effects.

$$DAF = 1 + t\phi \quad \text{if } V < 60 \text{ km/h} \quad (3.4)$$

$$DAF = 1 + t\phi \left( 1 + \frac{V - 60}{140} \right) \quad \text{if } 60 \leq V \leq 200 \text{ km/h} \quad (3.5)$$

Where:

$t$  = multiplication factor of standard deviation. Probability:  $t = 1$  (68.3%),  $t = 2$  (95.4%),  $t = 3$  (99.7%).

$\phi$  = factor depending on track quality. Very good = 0.1, good = 0.2, bad 0.3

$V$  = train speed [km/h]

With  $t = 3$  and  $\phi = 0.2$ , equation 3.5 gives a DAF of 1.69 for  $V = 80$  km/h and 1.90 for  $V = 130$  km/h.

This DAF is the multiplier of the static load from equation 3.1, and results in a quasi static load. Applying this new value as  $Q_{DAF}$  on the Prud'homme formula 3.2, the following value for  $Y_{DAF}$  is found:

$$Q_{DAF} = DAF \cdot Q_{static} = 1.90 \cdot 110 = 209 \text{ kN} \quad (3.6)$$

$$Y_{DAF} = 10 + \frac{Q_{DAF}}{3} = 10 + \frac{209}{3} \approx 80 \text{ kN} \quad (3.7)$$

## 3.2 CHARACTERISTIC LENGTH

An important track parameter that gives information about the track condition is the so-called characteristic length ( $L_c$ ). The characteristic length is a parameter that can be used to identify the quality of the track.

Table 3.1: Overview of the typical values for the characteristic length  $L$  [1, p. 79].

Track condition	$L_c$ [m]
good	0.70
research case	$0.7156 \approx 0.72$ (equation: 3.9)
poor	1.30

The characteristic length depends on the resistance of the rail profile and on the foundation stiffness. The characteristic length is determined as follows [1]:

$$L_c = \sqrt[4]{\frac{4 \cdot EI}{k}} = \sqrt[4]{\frac{4 \cdot EI_{54E1} \cdot a}{k_d}} \quad (3.8)$$

Table 3.1 shows some typical values of the characteristic length. The order of magnitude is around 1 meter, with a value of 0.7 meters for good conditions track (a higher foundation stiffness decreases the characteristic length) and 1.3 for poor track conditions. Given the values deduced previously for the spring constant  $k$  in 2.8 and 2.9, the characteristic length can be calculated. The values used in this equation are for a single rail, so the used discrete spring constant  $k_d$ , has to be the spring constant for half a sleeper. The resulting value is about 0.7 meter (equation 3.9). This value is on the better side of the 0.7-1.3 meter range and can therefore be considered as a good track. The reason this value is close to the lower bound as stated in the literature is due to the assumed, relatively stiff foundation and not using the stiffest rail profile. This short characteristic length means that the sleeper loads are relatively high, as the load is not distributed along many sleepers.

$$L = \sqrt[4]{\frac{4 \cdot EI_{54E1} \cdot a}{k_d}} = \sqrt[4]{\frac{4 \cdot 210 \cdot 10^3 \cdot 2346 \cdot 10^4 \cdot 600}{45.0 \cdot 10^3}} = 716.0 \text{ [mm]} \approx 0.72 \text{ m} \quad (3.9)$$

### 3.2.1 LOAD DISTRIBUTION

As a railway is loaded by a train, the load transfers through the rail and sleepers to the ballast. Every component has influence on the distribution of the loads in each component. Below the load distribution over multiple sleepers and the expected stresses in each (internal) interface are addressed.

#### LOAD BEARING PERCENTAGE

The distribution of forces on adjacent sleepers is can be calculated by using the deflection graph  $\eta(x)$  (further addressed as 'eta-curve')[1]. The deflection depends on the characteristic length  $L$ , as shown in equation 3.8 and on the distance  $x$  from the loading.

$$\eta(x) = e^{-x/L} \left[ \cos \frac{x}{L} + \sin \frac{x}{L} \right] x \geq 0 \quad (3.10)$$

This curve is also visualised in figure 3.1, the eta curve represents a shape curve for the elastic deformation line of the rail. The percentage of the load on each sleeper depends on  $\eta(x)$  and therefore on the characteristic length. The characteristic length is a function of the foundation stiffness and the bending stiffness of the rail. A stiffer foundation or smaller rail profile gives a higher load on the centre sleepers. The characteristic length has an order of magnitude of 1 metre. The characteristic length use in this research has been calculated in equation 3.8 which gave a value of 0.72 m. This value is close to the reference value of 0.7 m that corresponds to good track conditions.

With the aid of the eta-curve the deflections can be calculated at each sleeper location. This approach uses a discretized eta-curve where the deflections at each sleeper position are expected to be the value of the non-discrete eta-curve. In this calculation the elastic deformation of the sleeper material is not taken into account. If taken into account, the foundation stiffness should have been adjusted for each different sleeper materials which complicates the calculation heavily and as the general foundation stiffness is an estimate, it does not increase the accuracy. As can be seen in table 3.2, the maximum loading of the middle sleeper is between 23 and 50%. The discretization of the foundation and not incorporating the elastic material properties, make

these percentages approximations, but they still provide a reasonable value for a single wheel load. This due to the reasoning that these loads are a maximum load and is a relatively arbitrarily chosen value as well. The 41.6% value corresponds to the characteristic length of 0.72 m, which followed from previous calculations, so this value is used in general throughout this thesis. The design code on concrete sleepers lets the designer assume a load bearing factor of 0.5 (50%) as table 3.2 shows this suggested value is indeed on the safe side.

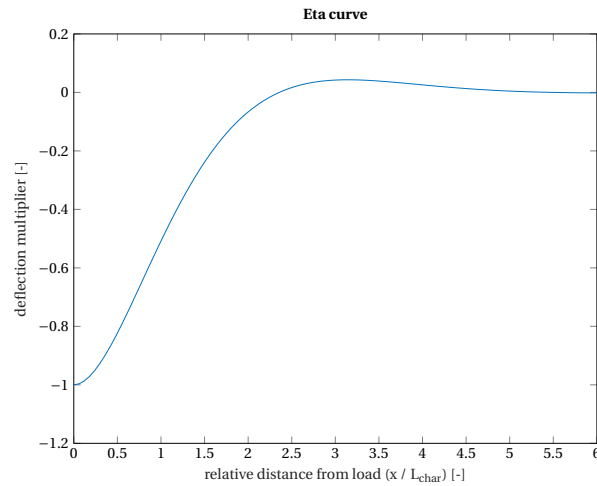


Figure 3.1: Eta-curve according to equation 3.10.

Table 3.2: Load distribution over sleepers for a point load, for several characteristic lengths. For reference a characteristic length of 0.7 m is considered good track and 1.3 m is considered bad track [1].

Sleeper #	0	1	2	3	4	5	6	7	8	9	10
L = 0.60 m	49.7%	25.3%	3.3%	-2.1%	-1.3%	-0.2%	-0.1%	0.1%	0.0%	0.0%	0.0%
L = 0.70 m	42.7%	25.6%	6.5%	-1.0%	-1.7%	-0.8%	-0.1%	0.1%	0.1%	0.0%	0.0%
<b>L = 0.72 m</b>	<b>41.6%</b>	<b>25.5%</b>	<b>7.1%</b>	<b>-0.7%</b>	<b>-1.7%</b>	<b>-0.9%</b>	<b>-0.2%</b>	<b>0.1%</b>	<b>0.1%</b>	<b>0.0%</b>	<b>0.0%</b>
L = 0.80 m	37.4%	25.0%	8.9%	0.6%	-1.6%	-1.2%	-0.5%	-0.1%	0.1%	0.1%	0.0%
L = 1.00 m	30.0%	22.9%	11.7%	3.7%	-0.2%	-1.3%	-1.1%	-0.6%	-0.2%	0.0%	0.1%
L = 1.20 m	25.0%	20.6%	12.7%	6.0%	1.7%	-0.4%	-1.1%	-1.0%	-0.6%	-0.3%	-0.1%
L = 1.30 m	23.1%	19.5%	12.8%	6.7%	2.5%	0.2%	-0.8%	-1.0%	-0.8%	-0.5%	-0.2%

### LOAD INFLUENCE AREA

As the eta-curve declines, there is a point where the applied force has a negligible influence on a individual sleeper. The point at which this is assumption is valid, is generally taken as the distance is more than  $2\pi L$  [1]. In the case of the calculated characteristic length of 720 mm this becomes:

$$L_{\text{influence}} = 2\pi \cdot 720 = 4524 \text{ mm} \quad (3.11)$$

With a sleeper to sleeper distance ( $a$ ) of 600 mm this encompasses 8 sleepers. For a symmetric model as is used in this research this becomes:

$$N_{\text{sleepers}} = 2 \cdot (L_{\text{influence}} / a) + 1 = 2 \cdot (4524 / 600) + 1 = 17 \quad (3.12)$$

17 sleepers is therefore the minimum amount of sleeper that the multi-sleeper model should have so the boundary effects are negligible. For less stiff foundations the characteristic length increases so the amount of sleepers, something that should be kept in mind.

### 3.3 INTERFACE STRESSES

With the known loading percentage of a sleeper and the known dimensions of the sleeper and fastening system, the average stresses in each component can be calculated. One of the main functions of the track structure is to spread out the load over a larger area. Every component distributes the load over a greater area of

the structure, therewith reducing the stresses. This simplified calculation assumes an evenly distribution of the force over the area so  $\sigma = F/A_{\text{interface total}}$  holds for all interfaces. The average expected stresses in each interface are shown in table 3.3. As example force, an easy load to work with load of 100 kN is used. If loaded on a single sleeper this is an exceptional load where one sleeper carries  $\approx 50\%$  of the whole  $Q_{\text{DAF}}$  (as determined in equation 3.6). But as the calculation is just linear, any other wheel load is just easy to calculate. E.g. a 55 kN wheel load results in an average sleeper-ballast stress of  $0.31 \cdot 0.55 = 0.17 \text{ N/mm}^2$ .

Table 3.3: Expected average stresses in track structure elements for a 100 kN wheel load. Half of the sleeper is used as one wheel load is regarded.

Interface	Area description	Area [mm <sup>2</sup> ]	$\sigma$ [N/mm <sup>2</sup> ]
Wheel - Rail	'thumbnail sized'	$\approx 100$	1000.00
Rail - Rail pad	Rail width x base plate width = $140 \times 170$	23800	4.20
Base plate - sleeper	base plate size = $360 \times 170$	61200	1.63
sleeper - ballast	1/2 sleeper footprint = $1300 \times 250$	325000	0.31

If the sleeper is supported by the ballast for only a fraction of the total area e.g. only directly below the base plates, the stresses increase. When an internal slope of 1:1 is assumed the affected area becomes equal to the base plate width plus 2 times the height of the sleeper:

$$A_{\text{interface reduced}} = W_{\text{sleeper}} \cdot (W_{\text{base plate}} + 2 \cdot H_{\text{sleeper}}) \quad (3.13)$$

$$A_{\text{interface reduced}} = 250 \cdot (360 + 2 \cdot 150) = 165\,000 \text{ mm}^2 \quad (3.14)$$

The resulting area is about half of the full area (0.51%). As the behaviour between the force and area is linear, the value for the sleeper-ballast interface stress  $\sigma_{sb}$  then becomes twice as large:

$$\sigma_{sb} = \frac{F}{A} = 100000/165000 = 0.61 \text{ N/mm}^2 \quad (3.15)$$

Esveld [1] provides an upper limit for the ballast contact pressure of  $0.5 \text{ N/mm}^2$ . This value is not exceeded when taking into account the whole sleeper, but is exceeded when only a fraction of the bearing area is used. As the loading value is an ultimate value and not an mean value this is not expected to be any problem. Secondly the dimensions of this sleeper are equal to a wooden sleeper, so the calculated interface stresses are not different to common sleepers.

### 3.4 BEAM ON ELASTIC FOUNDATION

Common usage for calculating of a railway track deflections is making use of a beam on elastic foundation model. This is generally done for the whole track in lengthwise direction [1], however the same methodology can be applied to the sleeper itself. For a BOEF calculation where the sleeper is considered as the beam element, the ballast is regarded as a series of parallel springs. Only the ballast is taken into account and the rail pad and subgrade are disregarded for this calculation. Their influence in the experienced stiffness will be implicitly incorporated in the foundation stiffness. But as the loads and foundation properties are estimations it is not considered worth the effort. The general differential equation for a BOEF is the following:

$$EI \cdot \frac{d^4 w}{dx^4} + k \cdot w = q \quad (3.16)$$

The homogeneous solution of this differential equation is given by:

$$w(x) = e^{\lambda x} (C_1 \sin \lambda x + C_2 \cos \lambda x) + e^{-\lambda x} (C_3 \sin \lambda x + C_4 \cos \lambda x) \quad (3.17)$$

Where:

$$\lambda = \sqrt[4]{\frac{k}{4EI}}$$

The particular solution depends on the loading conditions. The method of choice is to subject the beam to distributed loads at the location of the base plates. The in depth explanation about the calculations can be found in appendix B. In short, Matlab is used to calculate the integration constants and to solve the differential equation. The sleeper dimensions are fixed as determined in section 2.1.2. Only the 202 sleeper results are shown here, the material stiffness modulus is somewhat variable, but the choice is made to use a Young modulus of  $900 \text{ N/mm}^2$  for the plastic material. As the sensitivity analysis (see appendix B.1 for details) shows: the Young modulus does not affect the results in large manner. The load is 41% (load bearing percentage) from 209 kN (ultimate single wheel load), thus 85.69 kN per sleeper half. This load is spread over the base plates length of 360 mm as a distributed load. The foundation stiffness of  $k_{d_{\text{half}}} = 45 \text{ kN/m}$  follows from equation 2.8, as the sleeper is symmetric only one half of the sleeper has to be modelled.

The results are shown in the form of the deformation and moment line. Figure 3.2a shows the deformation of the sleeper, the maximum deformation occurs directly below the load, as expected and is in the order of 2 mm with a maximum of 2.2 mm. The difference between the centre and the rail seat is 0.8 mm. This value are to be expected as if the beam had been infinitely stiff the displacement would have been:

$$w = \frac{F}{k_{d_{\text{half}}}} = \frac{85.69}{45} = 1.9 \text{ mm} \quad (3.18)$$

Figure 3.2b shows the experienced moment of the sleeper. As the rotation is the first derivative of the moment line it is not hard to imagine the behaviour of the rotation as well. The points on the moment line which are a local minimum or maximum are the points with no rotation. Reading the figure, the extreme moments that the sleeper experiences under a a 85.69 kN wheel load are:

$$M_{\text{railseat}} = +6.7 \text{ kNm} \quad (3.19)$$

$$M_{\text{centre}} = -5.3 \text{ kNm} \quad (3.20)$$

Both similar in magnitude.

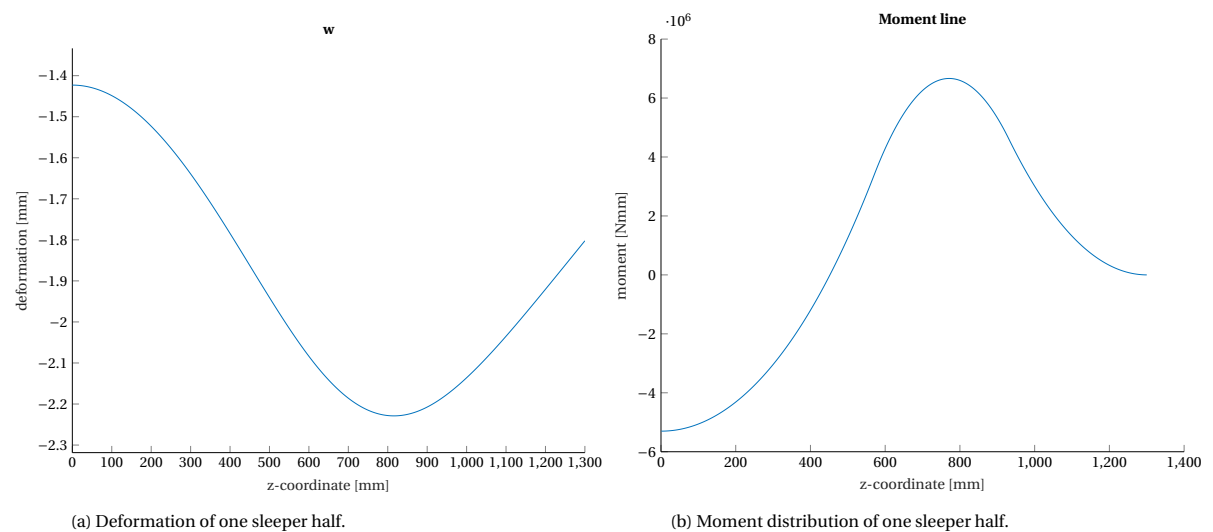


Figure 3.2: Deformation and moment values for a BOEF representing a symmetric half 202 HDPE sleeper. The sleeper is loaded by a wheel load of 85.69 kN (41% of  $Q_{\text{DAF}}$ ).

### 3.5 EXPECTED SHEAR STRESSES

Another secondary parameter aside of the gauge change, is the stress between the reinforcement of the sleeper and the plastic base material. The bond between the steel and the plastic is an important part of the strength. The maximal shear stress  $\tau_{\max}$  is present at the centre of the cross section and zero at the top and the bottom of a beam, or sleeper in this case. The formula to determine the maximum shear stress for a rectangular beam is as follows [45]:

$$\tau_{\max} = \frac{3V}{2A} \quad (3.21)$$

Where:

$V$  = shear force

$A$  = cross sectional area

In for the sleepers considered here, the maximal shear force is experienced at the locations where the base plate ends. Figure 3.4 shows the shear force distribution that followed from the BOEF simulations. The maximum experienced shear stress value is 32.7 kN. The area of the sleeper cross section is 37500 mm<sup>2</sup> and this results in the maximum shear stress being:

$$\tau_{\max} = \frac{3 \cdot 32.7 \cdot 10^3}{2 \cdot 37500} = 1.3 \text{ N/mm}^2 \quad (3.22)$$

Figure 3.3 shows the vertical distribution over the height of the sleeper. Next to the calculated maximum, also the value at the reinforcement is indicated. This is equal to 1.581 N/mm<sup>2</sup> and is supposed to be the highest shear value experienced by the plastic-steel interface. For the interfaces stresses at the height of the reinforcement the simplification is made to smear the Young modulus across the cross section. So the calculated second moment of area, including the reinforcement, is used as general second moment of area. Thus the contribution of the reinforcement is 'spread' over the whole cross section. Comparing this value with the found maximum stresses from equation 2.15 and 2.16 show that this expected value is below the range of 2.5 N/mm<sup>2</sup>.

### 3.6 CONCLUSION

This chapter tried to provide an answer to the subquestion which FEM data is useful in determining sleeper properties. The answer depends a lot on the previous chapter and specifically section 2.2 that covered the sleeper acceptance. The main required parameters are the maximum experienced stresses, mainly inside the sleeper to verify that the ultimate stresses are within the material range. Secondly the other, to investigate, variables are the:

- Vertical deformations, to compare to the BOEF-deformation.
- Rotations and horizontal deformations to investigate the gauge widening.
- Internal shear stresses to investigate the reinforcement-plastic interface.

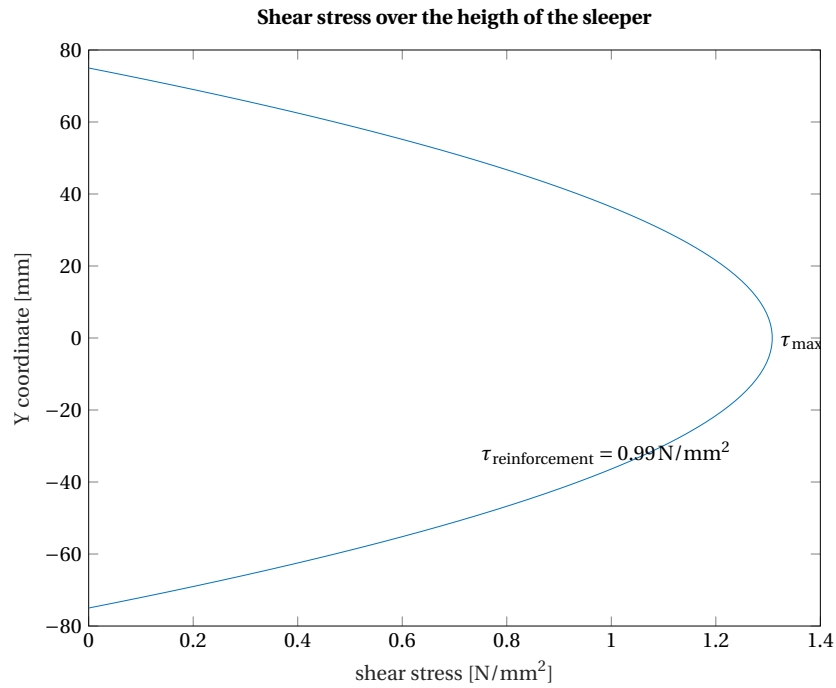


Figure 3.3: Shear stress distribution over the height of the sleeper at the maximum shear force value from figure 3.4. Indicated are the maximum value and the value just below the reinforcement.

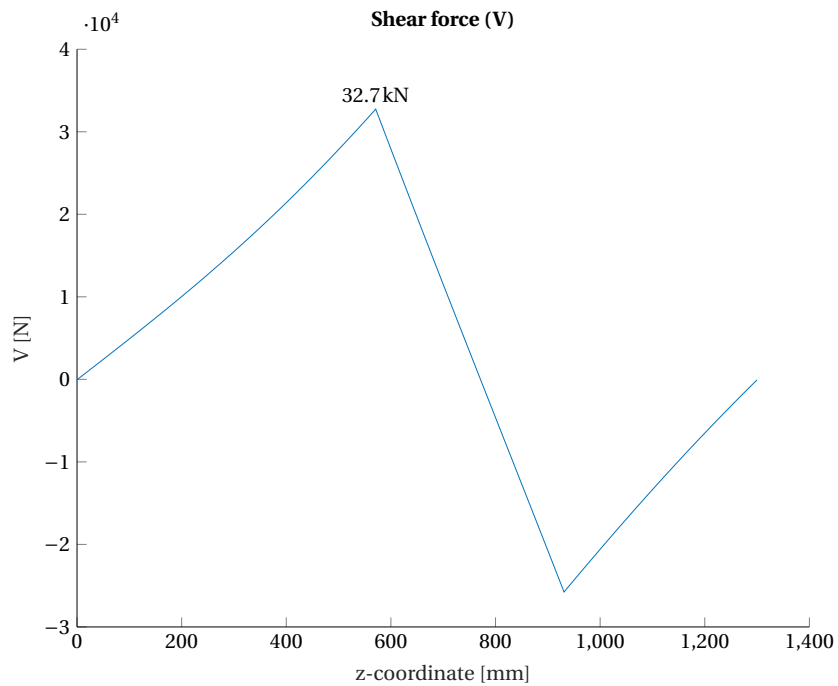


Figure 3.4: Shear force on one sleeper half loaded with a wheel load of 85.69 kN (41% sleeper load of a 209 kN axle load).

# 4

## FINITE ELEMENT MODEL DESIGN

This chapter focusses on the design steps followed to create the final FEM. After this chapter the full model can be used in several simulations to verify its results and to start validating the results. As the geometry of the sleeper is fixed by choosing a particular sleeper, the other elements have to be created as well.

First the determination of the models coordinate system and some terminology is presented. The following explanation of the models design starts with explaining the types of analysis that are used. Also the used elements are determined as the rest of the models construction depends on that decision. Then the step-by-step creation of the model is explained in detail. It starts with explaining the modelling of the sleepers cross section, followed by the cross sections of the secondary parts (base plate and rail). To finalize the single sleeper model: the boundary conditions, including the modelling of the foundations are included. With the single sleeper model in place, the extension to a multiple sleeper model is easy.

### 4.1 USED TERMINOLOGY

It is hard to fully grasp every aspect of the created model. This section tries to create a clear understanding about the used coordinate system and used terms throughout this thesis. The sleepers or track axis, are defined as *vertical*, *lateral* and *longitudinal*, just as is shown in figure 4.1. Also the *left* and *right* rail or side of the sleeper are defined, something that is not of mayor importance and is just there to take away any ambiguity. Note that this definition does not follow direction of the axis, but the viewing direction instead. The defined axis are also shown, as is used in the finite element model as well. One point of attention is that the lateral force is denoted by a capital 'Y', but does not act along the y-axis. Instead it acts along the z-axis as shown in figure 4.1.

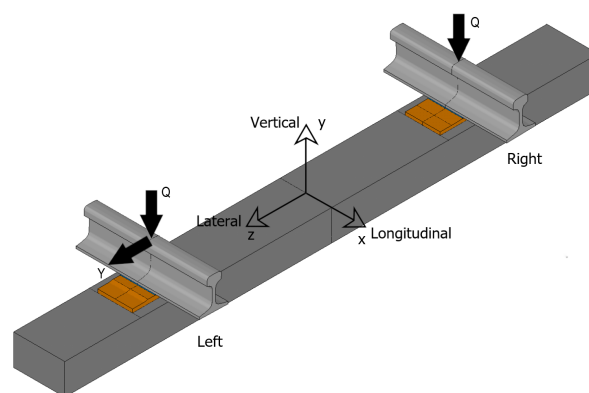


Figure 4.1: Graphical overview of the used axis and their used names, including the considered left and right side of the track and sleeper. The thick arrows indicate the forces.

## 4.2 MODEL COMPOSITION

This section explains how the FEM is constructed. There are some design decisions made that make it possible to construct separate models, but all originate from one sleeper type so one model is an extension of the other. The basic model consists of a single sleeper completely modelled together with base plates and a section of rail. Every component is modelled as a volume, including the reinforcement. Two types of reinforcement modelling are considered which split the basic model into two types. The last major difference is the full track section model where single sleeper models are combined to form one large model.

In general the FEM constraints are based on beam on elastic foundation theory, something that is quite common and allowed in the code as calculation practice [15, 29]. This results in the sleeper being supported vertically by a series of elastic springs so the sleeper becomes a beam on elastic foundation. In the lateral direction the sleeper is also supported elastically, springs at the one end of the sleeper form the lateral support.

The rail is modelled as a volume as well and provides support in the longitudinal direction. With this model a second model is created that is composed of several of single sleepers connected by an extended rail. The sleepers stay individually supported and only connected to each other by the rail.

### 4.2.1 DETERMINATION OF ANALYSIS AND ELEMENT TYPE

In short the two types of analysis that are implemented, are the following:

- Static structural
- Modal analysis

The to be used static and modal analysis are discussed below, but this means that a transient or harmonic analysis is not part of this research. There are several reasons why these methods are not used. First, the transient analysis focusses on the application of loading, including inertia effects and therefore time. The points of interest lie in the reaction of the structure directly after and during load application. Railroad loading conditions are very dynamic and therefore it looks like this kind of analysis is necessary. However, as the information that is looked for is the deformation after the load and any possible increase of deformations due to repeated loading. This does introduce the need for an material model that accurately describes the viso-elastic material properties. And as is explained further on in section 2.3, this is not yet the case. Therefore the choice is made to not use the transient analysis albeit the interesting results that can be expected.

The harmonic analysis is also expected not to grant enough information to justify the increase in work. The phase shift can be interesting, but the absolute deformations are not different, so when the lowest Young modulus is used, or the modulus that is around the experienced loading frequency, the deformation values from a static analysis should be appropriate.

Returning to the analysis that are used. The static structural analysis is probably the most common used in FEM. It is also relatively simple as not the most basic type of analysis. It provides material stresses, strains and displacements of the model. The linear material properties have to be checked on stress level, to verify that the materials stresses are still within elastic limits. The structural analysis is in this thesis by far the most important one and forms the spine of the research.

Secondary, a modal analysis can be used to get the eigenvalues of the most important eigenmodes. Those eigenvalues represent possible resonance frequencies and should not be close to general train related frequencies. Ideally they are close to frequencies experienced at current sleepers (concrete or more probable wood).

#### ELEMENT TYPE

The specific general element type chosen in this model is a 8-Node structural solid (SOLID185) element. This element type is capable of all the necessary non-linearities that are possible with regards to any material properties. There also is the option to use a higher order (quadratic) element with mid-side nodes. That type of element is capable of following curved edges in a better way than linear elements, but as the sleeper section only contains curved volumes in the reinforcement region, and the whole model only contains curves in non critical locations (e.g. the rail head and rail foot), a linear element is chosen.

It is expected to be sufficiently accurate to discretize the circular element by individual elements with straight edges. The chosen element is used for every solid that the model contains. The only incentive to use a differ-

ent kind of element is to reduce the calculation difficulty, which is possible, but should be tailored to specific regions and is not regarded worth the needed time investment. If in the future a different element is needed it should be easy to replace the current with an other type of element.

There are also some secondary elements present in the model. These are the contact and foundation elements. The contact elements are contact pairs that consists of two individual element types: 'CONTA174' as 3-D 8-Node surface-to-surface contact element and the 'TARGE170' a 3-D target segment. Both elements are overlaid upon the solid elements and provide the contact interaction by predetermined element parameters. The details of the contact are discussed below in section 4.3.4. That leaves the foundation elements to be discussed. The foundation elements are modelled with COMBIN14 spring-damper elements. There is also an element possible that has sliding and gap capabilities (COMBIN40), but for simplicity only the spring-damper element is used. It has to be noted that, as the current analysis are all static, the damper elements do no have any function. They do when time dependent analysis are used. The detailed modelling of the foundation is covered in section 4.3.4.

So to summarize, the used elements are the following:

- General elements: SOLID185, 8-Node structural solid
- Contact elements: CONTA174 and TARGE170 contact pair.
- Foundation elements: COMBIN14, spring-damper

## 4.3 SLEEPER

The model creation starts with construction a cross section of a sleeper. This can then be extruded into one 3-D sleeper. To recall, the following principles are used during the model construction:

- Model the reinforcement as volume
- Utilisation of a mapped mesh
- Parametrization of the cross section

The mesh and used finite elements are one of several design choices that influence the final model. The sleeper mesh of the polymeric elements depends on the reinforcement meshing, as this are the smallest elements. The meshing of the reinforcement is explained further on. As a design choice it is chosen to construct the whole model out of solid 3D elements. In finite element modelling, there exists several types of other elements such as shell elements, plane stress and plane strain elements. All having its own pros and cons (increased calculation time for example), but the ease and flexibility of solid elements provides a good starting point.

### 4.3.1 SLEEPER CROSS SECTION

All parts are created by code in Ansys files. This ensures that almost everything is adjustable, but this method requires a bottom up method:

keypoints → lines → areas → volumes

Opposed to an also possible top down method where you start by construction volumes and add or remove other volumes to create a specific geometry. In the end a parametric model creates the room to experiment a lot, as a different material model is easy to implement and for example, the reinforcement location can be altered if wanted and many other geometric properties can be altered with ease.

#### REINFORCEMENT

The choice is made to model the reinforcement as separate solids within the sleeper elements. This is different opposed to some prestressed or reinforced concrete models where the reinforcement is integrated into the element stiffness. The two main reasons for using solid elements are: the behaviour of the steel-plastic interface is not so well known as, for example, the influence that steel reinforcement has on concrete. Secondly, fully modelling the steel section adds the possibility to investigate the stresses in and around the steel. So construction the model with solids should result in more information about the interface stresses and gives also the (not yet used) option to change the behaviour of the steel-plastic interface.

The type of mesh greatly influences every part of the modelling process. There are two meshing methods possible. The first is a so called free mesh. This type of mesh is constructed with triangles (2D) or tetrahedral elements (3D). The advantage of this mapping method is the ability to mesh complex geometries. The disadvantages are the amount of elements needed and the reduced accuracy [20]. The reinforcement is fully modelled inside the cross section. This removes the ability to easily mesh with a mapped mesh. It is however possible to model a circular reinforcement in the cross section so a mapped mesh can be applied. As this has been a major part of the model preparation the choice is made to explicate the modelling, therefore the full mapped mesh generation is shown. This is done for two types of reinforcement a circular 'real' representation and a schematized or simplified octagonal reinforcement bar. The latter having a lot less elements to improve solution time.

This leaves the integration with the sleeper as only remaining point to be discussed. The reinforcement is in this model embedded in the parent material by using one mesh for the whole cross section of the sleeper. The element type is kept the same, the only parameter that is changed is the material type. This implies a fully bonded interface between the steel of the reinforcement and the plastic (matrix) material, this is of course a simplification, one which is fully internal and could have a significant influence on the behaviour of the model. This is one of the aspects where more attention and research is needed to allow for a more realistic connection, or to be sure that this effect is neglectable. There is some research done on the steel-polymer interface [39], but as the researched case is quite different and the increased difficulty in modelling an elastic interface, the choice is made to create a fully fixed reinforcement. Knowing that this is an approximation. The interface stresses however is something to investigate, so the stress range is known.

Figure 4.2 shows the full mesh of the right top quarter for different mesh sizes. The circular reinforcement bar is recognisable from the mesh. As is clear from the figures, it is still possible to have quadrilateral elements and a circular element (the reinforcement in that case). Two modelling techniques are used, one is a circular cross section which uses a meshing technique to allow for a mapped mesh. The other reduces the circular cross section to an octagon. The modelling is done in 2d, but al everything applies to the 3D-case as well, as it is just an extrusion of the cross section.

#### 4.3.2 CIRCULAR REINFORCEMENT MODEL

A circular element to model the reinforcement is the most accurate in terms of physical resemblance. However, due to the fact that the reinforcement, or any other part, is always built up from a (finite) elements, the result is not a perfect circle. In other words, due to the individual elements having straight edges, a circular mesh with a small amount of elements loses accuracy as well. When modelling the reinforcement as a circular bar, a mapped mesh with hexahedral elements is not trivial anymore. To allow for a mapped mesh some extra lines need to be defined. The solution is explained by Štigler [46]. In short the application is as follows: start with a square and within that square a circle is drawn, the reinforcement. The area in the square but outside this circle is the sleeper material. Inside the circle an inner square is constructed, with curved sides. This 'square' allows the centre to be mapped easily. Secondly from each of the corner points of this inner square, diagonal lines are drawn to the outside. This creates quadrilateral sections, one quadrilateral inside the circle and outside of the inner block and one outside of the circle. The resulting mesh is shown in figure 4.2.

The only problem with this solution is that a small amount of reinforcement divisions create large elements on the edge of the considered sleeper section. And the other way around, a large amount of reinforcement divisions, meaning more elements create small sleeper elements. Figure 4.2 figure show several versions for an increasing amount of reinforcement elements so the dependency on divisions is visible.

### 4.3.3 OCTAGONAL REINFORCEMENT MODEL

The meshing of a circular cross section is somewhat cumbersome and gives rise to small elements in the cross section. To allow for easier meshing and larger elements an octagonal reinforcement cross section is considered. There are differences in cross sectional area and the area moment of inertia ( $I_{zz}$ ) between a circle and an octagon. In the model, the area moment of inertia between the two is set equal to each other. This means that the 'radius'  $r_{\text{polygon}}$  of the circumscribed circle of the octagon is changed, so the resulting inscribed octagon matches the area moment of inertia of the reinforcement.

The area moment of inertia of a circle is expected to be common knowledge, the area moment of inertia of a polygon is a bit different and calculated by its coordinates [47]. By dividing the polygon in triangles and summing every component, the area moment of inertia can be calculated. Due to the symmetry of an octagon, only 2 contributions have to be determined.

$$I_{zz\text{circle}} = \frac{\pi}{4} R_{\text{circle}}^4 \quad (4.1)$$

$$\begin{aligned} I_{zz\text{simple polygon}} &= \frac{1}{12} \sum_{i=1}^{n-1} (y_i^2 + y_i \cdot y_{i+1} + y_{i+1}^2) (x_i \cdot y_{i+1} - x_{i+1} \cdot y_i) \\ &= \frac{1}{12} \cdot \left[ 4 \left( \frac{R_{\text{polygon}}^4}{4} \sqrt{2} \right) + 4 \left( \frac{R_{\text{polygon}}^4}{4} \cdot (3\sqrt{2} + 2) \right) \right] \\ &= \frac{R_{\text{polygon}}^4}{6} \cdot (2\sqrt{2} + 1) \end{aligned} \quad (4.2)$$

Where

$n$  = amount of corner points of the polygon

$R_{\text{circle}}$  = radius of the reinforcement

$R_{\text{polygon}}$  = radius of the circumscribed circle.

(4.3)

Setting both area moments of inertia, from 4.1 and 4.2 equal to each other a new  $R_{\text{compensated}}$  is found. It is replacing the  $R_{\text{polygon}}$ , the resulting difference in radius is about 5%:

$$\begin{aligned} R_{\text{compensated}} &= R_{\text{polygon}} \\ R_{\text{compensated}} &= \sqrt[4]{\frac{6 \cdot \frac{\pi}{4} R_{\text{circle}}^4}{2\sqrt{2} + 1}} = 1.05331 \cdot R_{\text{circle}} \end{aligned} \quad (4.4)$$

This compensated radius  $R_{\text{compensated}}$  does give a minor error between both areas, the cross section of the octagonal reinforcement is somewhat larger than the circular, however the difference between both cross sectional areas is only 0.30%.

### OCTAGONAL REINFORCEMENT MESH

It easy to mesh an octagon with a mapped mesh, with four elements the whole octagon can be meshed and when smaller elements are needed, each rectangular element can be divided into four smaller elements. This allows for great adaptability of the element size. In figure 4.3 the meshes are given for the first four possible division possibilities.

### EFFECT OF REINFORCEMENT MODELLING ON 3D ELEMENT SIZE

Both reinforcement modelling techniques are possibilities. The differences are quite clear; the octagonal mesh trades accuracy for speed. Speed as the computational difficulty increases with the amount of elements in a cross section of the sleeper. Table 4.1 shows the differences in element count of the reinforcement cross section versus the total amount of elements of a single sleeper. As mentioned in section 4.3.2 the elements on the inside and outside of the described block have a large influence on each other. Larger element sizes of the sleeper elements make the inner reinforcement elements small. This is not a problem when looking in

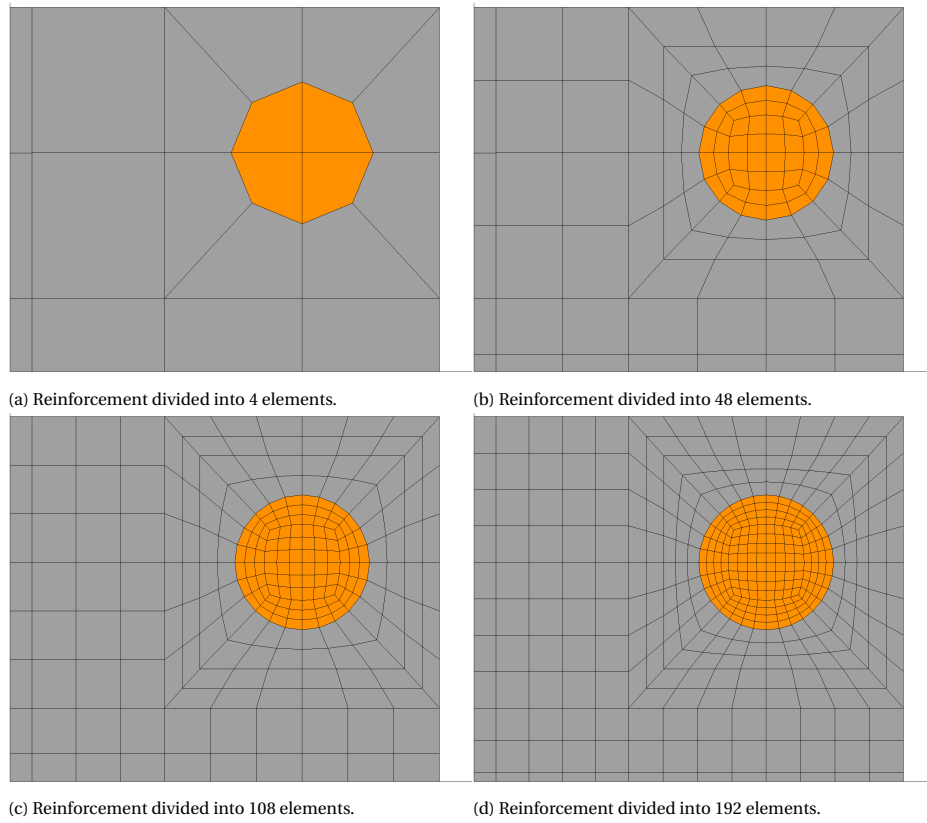


Figure 4.2: Different element sizes for an octagonal representation of the circular reinforcement rods. Visible is the still rectangular (mapped) mesh of the reinforcement without compromising on the circular reinforcement.

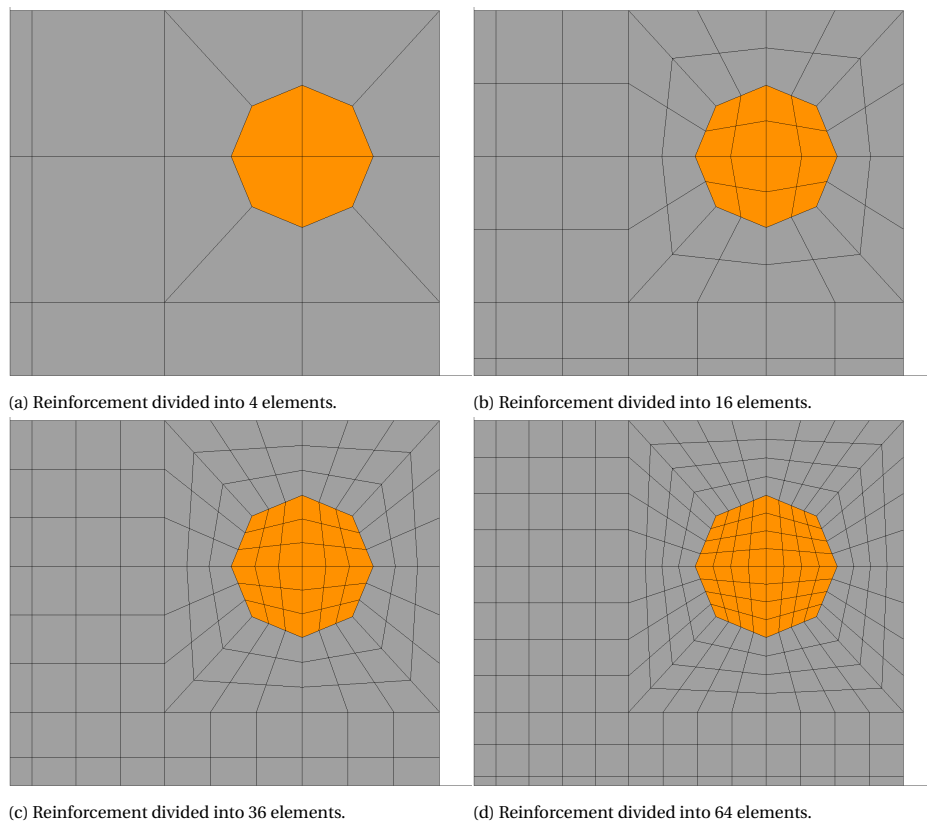


Figure 4.3: Different element sizes for an octagonal representation of the circular reinforcement rods.

Table 4.1: Amount of elements for each used reinforcement model, per reinforcement bar and per cross section.

	Cross sectional elements		Full sleeper element count	
	Circular	Octagonal	Circular	Octagonal
1 Division	4	4	1956	1956
2 Divisions	48	16	156448	30960
3 Divisions	108	36	743478	150642
4 Divisions	192	64	2313544	483144

2D, but becomes a problem in 3D. The problem that arises is that elements solutions become inaccurate if elements are too slender. So to keep the elements as square as possible the element length has to be limited.

To limit the stretch of the elements, the maximum element size has to be small compared to the sleepers length. This requirement results in a lot of elements in the sleeper as a whole. As can be seen from the cross sections (4.2, 4.3) the elements become increasingly smaller, especially for the circular model this is creates a lot of elements when extended in 3D. And as a hexahedral (mapped) mesh cannot be reduced in terms of its number of elements over along its cross section, there is no possibility to mitigate this dependence. The small elements influence even the parts of the sleeper where there is no need for small elements, such as the sleepers ends. For a single sleeper this is manageable, but when using a model with multiple sleepers, it is better to use the octagonal reinforcement, at least on the outer sleepers of the model.

There are possible ways to change the element size over the sleepers length. It can be done by creating two meshes and 'gluing' them together by using fully fixed contact elements. This requires a lot of extra modelling steps and therefore this method is not used in this research.

#### 4.3.4 BASE PLATE, RAIL PAD AND RAIL

The system of secondary components is formed by the base plate, rail pad and the rail. This subsystem has two structural functions, first the transfer of the loading from a point load to a dispersed stress over the area of the base plate. Secondly the rail provides the connection between multiple sleepers when multiple sleepers are used, which is sort of equivalent to dispersing the load. The rail pad could be considered to have another function, namely reduce the vibrations and impact of forces on the sleepers and ballast bed due to dampening. As the considered analysis for the time being only static and therefore time independent, this is not further addressed. Of course it is possible to use the dampening of the pad in dynamic analysis if needed.

For the modelling of all components there are minor adaptations made to improve the modelling. Some curved edges are straightened and extremities are not always modelled. As these parts fulfil a secondary role in the whole system, this is accepted although the changes remain minor. The modelling of the rail and the resulting mesh is shown in appendix C as the rail itself is bit more complicated as it has very few straight section in its cross section.

The base plate provides a slanted surface, as in the real world, so the rail is inclined by a 1:40 slope. Some sharp corners that exist in the base plate as well as the clamps for the fastening system are omitted. The sharp corners are smoothed, but still exist in on the edges of the base plate. Something that introduces peak stresses, no matter what.

#### INTERFACES

An important part in the modelling of the base plate and rail to the track structure, is the connection between them and the sleeper. In real life the base plate is bolted to the sleeper and the rail in its turn is connected by a fastening system. To simplify the model, both connections are included in a different way. Two types are used, both having the same effect on the structure namely creating a fully fixed bond. To limit the difficulty of verifying and calculating the connections, all connections are fully fixed: rail - rail pad, rail pad - base plate, base plate - sleeper.

The rail - rail pad interface is created by a conformal mesh and without any contact elements. This is established by extruding the rail pad from the rail foot mesh so they always match each others mesh. The next interface is modelled with contact elements that have the 'fully fixed' option set to them. This is the rail pad - base plate interface. Here the meshes do not line up due to the rotation of the rail and rail pad. The last con-

nection is also made by contact elements and provides the bond between sleeper and base plate. For the two contact pairs, the properties can be altered if wanted to change the type of contact possibly with the addition of some springs to model the fastening system.

#### ELASTIC FOUNDATION MODELLING

In the model the sleeper is founded on an elastic foundation. Every bottom node of the sleeper is connected to a spring-damper (COMBIN14) element, which in their turn is connected to a fixed node. The longitudinal spring-damper element is a uniaxial tension-compression element and no bending or torsion is considered [48]. COMBIN14 elements act only in the direction their placed in, so vertical for the foundation nodes. The used element has a symmetric spring constant, the stiffness in tension is equal to the stiffness in compression, that means that tension is possible in the current ballast representation. Something that is of course not applicable to ballast, but the amount of tension is expected to be low and negligible [49]. If wanted the more comprehensive COMBIN40 elements should be used, with the gap ability.

For simplicity, the foundation is modelled as a series of parallel springs, which means that their individual spring constants may be added together. The difference between this summation and a new calculation based on elastic beam theory is not likely to be of great influence, especially because the input values are mostly based on key figures. This means that the resulting spring constant for each individual spring is equal to the total sleeper spring constant  $k_d$  (as derived in 2.8), divided by the amount of nodes  $N$ . As the time-dependent analysis are not within the scope, the damping component of the elements is not of interest and therefore omitted.

$$k_{\text{element}} = k_d / N_{\text{bottom nodes}} \quad (4.5)$$

The bottom nodes are not perfectly spread over the total width of the sleeper, however the difference in element size is less than 1 mm, see figure 4.4 for the actual positioning. Also due to the extrusion of the sleeper cross section there are some minor size differences along the sleepers length as well. Next to this general foundation model, a second option is implemented to be able to investigate different stiffnesses below certain areas. This is explained in detail in F, but in short: the area is divided in a centre and two outer sections and both inner and outer parts can have a different stiffness and size. This allows for various support conditions and more options to investigate the sleeper behaviour and for now mainly to examine gauge widening.

The lateral restraint is modelled in a similar manner. The connection is made by the same COMBIN14 spring damper elements. As the element layout of the cross section is not very uniform with the inclusion of the reinforcement bars. Dividing the spring stiffness over every node creates stiffer areas. Therefore only the centre portion of the cross section is supported laterally by the springs. Also only one side of the sleeper is restrained by this foundation, as this represents the reality a bit better, where ballast cannot take up any tension forces.

The way the foundation is modelled has some flaws where the reality and model do not match. One important one are the lateral restraints. In reality the bottom and sides of the sleeper also provide lateral resistance as there exist friction between the sleeper and ballast. In this model those contributions are not taken into account, however they are included in the total stiffness. So the shoulder stiffness at the sleeper end is larger than it is in reality, as it corrects for the missing lateral friction. The second not included attribute is the ballast-ballast interaction, in real life situations, the ballast stones interacts with each other. With the use of individual springs this effect is. It is expected not to influence the results too much, as the definition of the foundation stiffness is relatively arbitrary so minor changes in the foundation should not change the outcome.

#### MAXIMUM LOAD PERCENTAGE

The distribution of forces on adjacent sleepers is an important parameter as it defines the amount of loading on a single sleeper. As the rails provide vertical stiffness to the track, they spread the load. The vertical displacement curve is an heavily damped wave Esveld [1]. The frequency of this wave is dependent on the previously calculated characteristic length (equation 3.9). In section 3.2.1 the determination of the load distribution is explained. In short, the deformations are discretized into individual sleeper contributions and the resulting load percentage on the middle sleeper is expected to be between 23 and 50% of the full wheel load, these values reasonably correspond to the found values by Lankhorst where values 28-37% are found [50]. The values 33% and 50% are therefore taken as standard percentages for the load per sleeper and as governing loads. One important remark is the current linear behaviour of the model. As the whole model acts

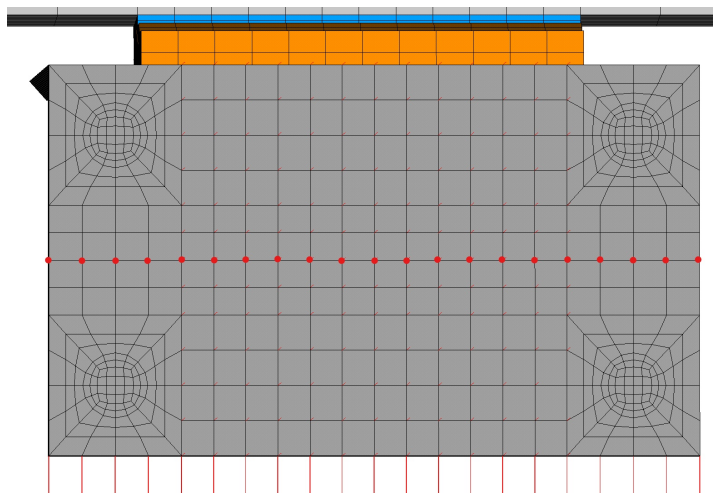


Figure 4.4: View of the vertical and lateral foundation elements. The elements are shown in red. Visible are the vertical springs at the bottom and the lateral springs in the middle section of the cross section.

linear the experienced deformation is linear with respect to the loading, so a 100% load increase also doubles the deformation. This does change when non linearities are introduced, so this the load determination stays an important part and therefore several load cases are determined.

#### CONSTRAINTS

The last part that has to be assessed are the constraints. The three directions all have to be constraint in some manner to prevent rigid body movement. The most obvious constraint is already covered. This is the vertical constraint and consists of the foundation springs. And more specifically the fixed nodes at the bottom end of the spring elements. The nodes are fixed in all directions, but due to the nature of the COMBIN14 elements and they way they are implemented. The elements only act in the vertical direction. That leaves the lateral and longitudinal directions to be constraint. The lateral direction is also constraint by spring elements. A single row at the middle of the sleeper edge provides the resistance in this direction and similar with the vertical foundation, the springs only act in the lateral direction. Lastly the longitudinal direction. The rails are the only constraints of the model in longitudinal direction. In practice the sleepers in combination with the ballast also provide resistance, but this contribution is omitted albeit being significant. The longitudinal direction generally has not active force component so the reaction forces in this direction should be near to zero. The restraint acts only in the longitudinal direction and only on the outer edges of the rail, every other direction the rail is not constraint. If all edge nodes are constrained, the constraint acts as a clamped condition, to counteract this, only the centre nodes of the rail are fixed so only a rotation is allowed around the z-axis. For a single sleeper which has only a short piece of rail modelled, this rotational freedom is more than in practice is experienced, but this setting is thought to fit better than a clamped constrained, which is overly stiff.

#### LOAD CASES

The loads calculated in combination with the (expected) distribution of the load over multiple sleeper, form the basis for the load cases that are used in the FEM. To make it easy to compare analytic calculations with FEM results, these load cases are also used in the analytic calculations. The cases feature an increasing load and later addition of lateral force on one rail. The latter being most representative with forces experienced in a curve. In table 4.2 all the used cases are shown. The most representable cases are the second case for a one single sleeper analysis, the sixth and seventh load cases are more representative for a multiple sleeper model. All these load cases are not expected to be perfect representations, more detailed analysis should be done to create a better understanding of the loading conditions if needed. One advantage of the static linear model is the scalability, as there are no non-linearities the deflections and stresses all behave linearly. This means that an increase of Q with, say 50%, also has the same effect on the stresses and deformations, they too increase by the same 50%. This is later used to provide results exactly to the needed loading conditions.

The loading is applied in the local coordinate system of the rail. As the rail is slanted in the model as is in reality, the loads act not fully vertical in the global coordinate system, in other words; they do not align with

Table 4.2: Overview of the load cases used in the FEM. The lateral load is only present on one single rail.  $Q$  follows from 3.1,  $Q_{DAF}$  from 3.6.

Load case	vertical load $Q$ [kN]	lateral load $Y$ [kN]	scenario
1	0	0	Gravity alone
2	15	0	50% of 3-Point bending test load.
3	30	0	3-Point bending test load.
4	60	0	intermediate value roughly 50% of $Q$ .
5	110	0	Full load $Q$
6	110	$Y = 47$	Full load $Q$ and lateral load equal to $Y$
7	$Q_{DAF} = 209$	$Y_{DAF} = 80$	Full load $Q$ and $Y$ , both with a DAF

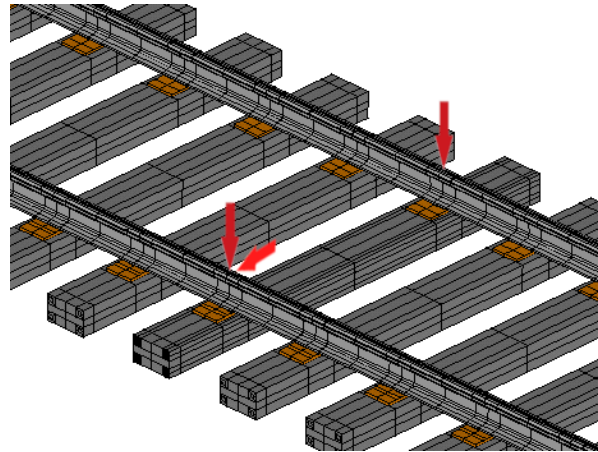


Figure 4.5: Graphical view of the applied forces (not to scale). The lateral force is not present in every load case.

the sleeper orientation. The rails are slanted by the standard 1:40 angle which comes down to 1.43 degrees. Figure 4.5 shows the loading directions with respect to the local coordinate system of each rail.

#### 4.3.5 ANALYSIS SETTINGS

This section provides a brief overview over the used FEM analysis settings in the static and modal analysis. The models that have been designed are built in Ansys. The load cases are determined and this section describes which type of analysis are used for the analysis. Considering the static structural analysis, the settings are relatively simply implemented. As the material stiffnesses are implemented with a basic linear material model with only a single stiffness property, the sub steps are chosen by the software, 'automated time stepping'. If any non-linear material properties are implemented this part needs some more attention, as introducing more steps between the load increments to capture any changes in material stiffnesses and its consequences. However it is expected that is just a sanity check a the software automatically uses more steps.

### 4.4 MULTIPLE SLEEPER MODEL

The multi-sleeper model is used to remove the influence of the boundary conditions. This also spreads the loading over the sleepers so this behaviour has not to be mimicked as is in a single sleeper model. The amount of differences between the single sleeper and whole model is practically non-existent as general model sleepers are just copied further onto the track. So every aspect covered in the single sleeper sections applies for the multiple sleeper model as well. As the amount of nodes expands very rapidly for increasing reinforcement element size, a full model of several sleepers needs simplification to keep the model solvable. The determination which sleepers to use is a choice between accuracy and calculation power. The amount of sleepers that is needed, so the influence of the boundaries is negligible is calculated in equation 3.12. The resulting amount of sleepers found is 17, as the amount of needed sleepers increases when the foundation stiffness is reduced this is increased in the current analysis to be safe.

The middle sleeper, and in this research the only sleeper that is loaded, always has circular reinforcement.

Table 4.3: Tabular representation of the multi-sleeper model. The whole model is mirrored about the centre sleeper and features 19 sleepers in total.

Sleeper nr.	1 (middle)	2	3	4	5	6	7	8	9	10
Reinforcement type:	circular					octagonal				
Reinforcement divisions:	2	3	2	1	1	1	1	1	1	1
# Elements	156448	150642	30960	1956	1956	1956	1956	1956	1956	1956

With results from verification analysis which is explained in appendix D it became clear that octagonal sleeper reinforcement is a valid method so moving away from the centre sleeper, the other sleepers are modelled in this way. As the model became too large, the outer sleepers are not as accurate as the middle ones, but it is expected to be enough as the middle sleeper is of most interest and the provided stiffness should still be similar to the other models. The resulting model configuration, so the model stays solvable within reasonable time, is shown in table 4.3

As the model with no extra divisions has the least nodes, this is be used at the outer 10 sleepers. The second and third sleepers have more elements and therefore a higher accuracy. For now this setup is expected to yield reasonable results as the influence of the loading reduces fast. The mayor difference with the single sleeper model is the amount of simulations. Only two simulations are done, one with the 201 sleeper type and thus PE material and one with 202 type sleepers out of HDPE.

## 4.5 CODE BASE

The whole FEM is generated with the use of 'Ansys parametric design language' ( APDL ) files. Adapting analysis files and changing some folder pointers is all that is needed. Other files can be altered to change some defaults or change the loading conditions. To start the whole analysis, only the specific index file has to be started from within Ansys and the analysis starts. If finished it also provides some automated post processing such as generating images and csv-files with stress and deformation data. With this output, Matlab is then used the further post process the results. This includes creating graphs and combining data. The model is available on <https://github.com/agriemink/AnsysSleeperModel> under the MIT license. It still has some flaws though and a lot of room for improvement. Some flaws originate from the use of Fortran based code, some parameters have length limitations for example.

### 4.5.1 FEATURES

The basic concept of the code is somewhat explained between the lines in the geometry parts of this chapter. The most special features that the model is capable of handling are briefly explained. The parametric design was a key point set at the beginning. This feature allows every geometry variable to be altered to taste, reinforcement size and centre can be adjusted. The only remark is that at way of generating the reinforcement is not changed, so the blocks with reinforcement (as can be seen in figure 4.2) only change in size and this can create too distorted elements. If a different or more reinforcement lay-out is needed, a new sleeper geometry can be added and used instead. The next example of parametrisation is the determination of material models. Each material has its own file with its properties. Within the individual files for each analysis the materials per sleeper element can be defined: sleeper, reinforcement, base plate and rail.

The next feature is the multi sleeper model as mentioned before. Actually any model is a 'multiple' sleeper model just coincidentally consisting of one sleeper. Any combination can be implemented, the only remark is that the final lay-out is expected to be symmetrical. With each sleeper the properties of the foundation can be altered as well. In the current research the foundation stiffness is kept constant per sleeper. Only the stiffness distribution below each sleeper is changed (see appendix E for a more detailed explanation about this feature). All foundation properties are adjustable per sleeper so hanging sleepers can be implemented if wanted. Finally there is a feature option to create the model with the use of symmetry. So not creating every sleeper on both sides, but using symmetry boundary conditions. This feature is not thoroughly tested and should be considered a pre alpha version.

Lastly the post processing should be mentioned. Post processing is time consuming and especially with many models and analysis, it becomes a lot very fast. To be able to create concrete data from all analysis a post

processing script is added as well. Its main goal is to create images from the model, deformation images for example and extract solution values such as equivalent stress levels. The non-graphical data is transferred to '.csv'-files some directly usable, some need more treatment. As the Ansys environment is not regarded as user friendly as should be by the author, another part of post processing is done with the aid of Matlab to combine multiple files and output graphs of the data.

#### 4.5.2 LIMITATIONS

Next to the implemented features there are some wanted features and also known flaws. Some limitation are Ansys based and not necessarily an introduced problem, it could be however that limited knowledge of the APLD language has had a negative influence on the final code. However a lot of effort is put in adapting the programming language and there was not much room for the 'extra mile'. Back to the model itself, in general the whole model should be considered as alpha version. Leaning towards a beta if the current analysis are used and no changes are made. This list with limitations is therefore not expected to be complete.

- The code lack functions and methods to group code. The implementation of functions is however not standard, but probably can be done by using Fortran, C or C++. The lack of functions results in many global parameters that make it difficult to keep track of them. Such an implementation or upgrade would be time-consuming and is therefore only recommended if it is clear that the model is certainly going to be used.
- Adding new items, geometries for example, is difficult. It is expected to be error prone as everything has to match perfectly.
- Debugging the code requires a lot of knowledge about the model or a lot of reading and debug time.
- Post processing code can be improved and extended. The current implementation focusses a lot on gauge change change and more items can be added on the processing of stresses on specific locations. Extracting data remains difficult and requires external software (Matlab) to aid in the post processing, which not perfect as well. The extra problem that arises is the amount of information that can be generated by allowing parametric input and solving multiple models in consecutive order. Every post processing run generates a lot of images and those still have to be investigated and processed.
- Modal analysis and post processing, improve the modal results by fixating some nodes to make it easier to extract the bending nodes in a particular direction. In the current model; if two found frequencies between two models are close to each other, the corresponding modes can be different. In other words the n'th mode is not always the same over multiple models, which makes the post processing more tedious and error prone.
- The problem with creating geometries in Ansys is the lack of tracking possibilities of: keypoints, lines, areas and volumes. Keeping track of them with id's, which they all have, is very hard and requires a lot of searching by coordinates. Again something that is tedious and prone to errors.

#### RECOMMENDATIONS

To conclude the harsh list of 'problems' some recommendations are done. First anyone that wants to alter this model, or wants to build upon should consider Ansys Workbench software as core program. It is still bases on the same program, but features a nice GUI. It can work in a parametric way, although the effect on the mapped mesh is not sure. It does however still supports APDL code so there is room to implement own solutions. Combined with the steep learning curve required to understand the current code base. It is however recommend that anyone interested in this model does try to get to know the current methods used.

#### 4.6 SUMMARY

Concluding, the most drastic design choices are the type of elements used, the mesh and the methods used to model the several interfaces. Therefore those are summarised in table 4.4. The modelling of these interfaces could be upgraded to allow for some internal displacements to be somewhat more realistic. Further the model does represent the whole sleeper in detail and the mapped mesh should yield more accurate results than an ordinary meshing method with tetrahedral elements. This is verified in appendix D. Based on the results on accuracy and computational difficulty, a 19 sleeper multiple sleeper model is constructed. A larger model will reduce the influence of boundary conditions and will automatically distribute the applied loads over more sleepers.

Table 4.4: Overview of the interface modelling and the used elements to establish connections.

	Interface description	Ansys Element type
rail to railpad	fixed, conformal mesh	-
railpad to base plate	fixed with contact elements	CONTA174, TARGE170
base plate to sleeper	fixed with contact elements	CONTA174, TARGE170
sleeper to reinforcement	fixed, conformal mesh	-
sleeper to ballast	linear elastic springs	COMBIN14

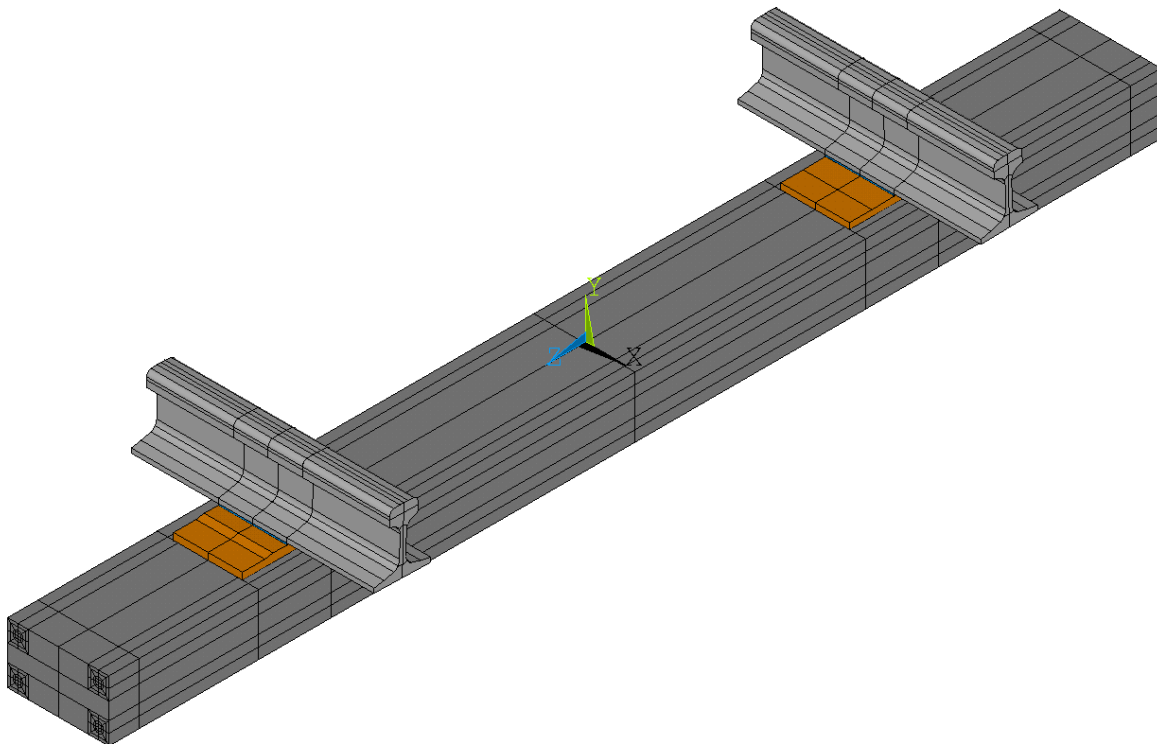


Figure 4.6: Overview of the full Ansys model as used in all calculations.



# 5

## FINITE ELEMENT RESULTS

Several analysis are executed to be able to investigate and validate the FEM-results. The setup of the model makes it easy to run several analysis with different values and also makes it possible to model a 3-point bending tests so a comparison between laboratory tests and the FEA is possible. Next to the validation, two other topics are addressed in this chapter. First, the check if the resulting deformations and stresses are within the composed limits. Secondly the comparison of FEA results with analytic calculated values, to investigate the added value of the FEM. Both sleeper types, the 201 and 202 (stiffer version), are reviewed. Whenever there is only one sleeper type considered, this is the 202 type that was used as default.

In more detail, the following list shows the chapters structure:

- 3-point bending tests; validation  
Provides insight in the behaviour and quality of the model. An analysis with changing Youngs modulus is performed and compared with the laboratory results. Compared are the maximal deformation and reinforcement strains. The analysis shows which Youngs modulus fits the tests results.
- Multi sleeper load distribution; comparison with analytic method  
A multi-sleeper model is used to investigate if the calculated load percentage is corresponding with the FEM. This resulting percentage is used throughout the other results.
- Single sleeper results compared to sleeper limits  
The next section compares the individual sleeper models with the material limits and deformation limits as composed earlier in this report. After the first analysis the foundation properties are also changed to investigate the influence on the stresses and deformations.
- Remaining analytic calculations compared to the FEM results  
This covers the BOEF calculation and the shear force calculations. If the values are comparable, the added value of a FEA is reduced. If the values are different, it has to be investigated where the differences occur. Is the analytic calculation less accurate or is the FEM flawed?

### 5.1 3-POINT BENDING RESULTS

The FEM is compared with laboratory testing on the considered sleepers, van der Drift [21] has performed 3 and 4-point bending tests on the 201 and 202 sleepers. Only the 3-point bending tests are used to verify if the FEM behaves properly. The 3-point bending setup can be fully modelled with the model, something that is not possible with the 4-point bending tests. The 3-point bending setup can be created by supporting the sleeper only in the middle with a very stiff foundation. The FEM capability to adjust the foundation parameters is therefore used to alter the stiffness locally, without creating a whole new model. Figure 5.1 shows the setup of the final model. The dimensions of the supports are equal to the dimensions of the loading plate as used in the laboratory tests.

Two types of laboratory test where executed, a 5 Hz dynamic test and a 4 hour static test, both with a loading of 30 kN. Each test provides a maximal deformation value of the sleeper and the measured strain of the bottom

Table 5.1: Overview of the 3-point bending test results for a 201 and 202 sleeper [21]. The reinforcement strain is measured at bottom of the reinforcement bar, which is at the highest expected strain location. All deformations are for a load of 30 kN.

Type of test	Unit	201		202	
		Dynamic 5 Hz	Static 4 hour	Dynamic 5 Hz	Static 4 hour
Deflection	[mm]	7.270	11.824	3.480	5.768
Reinforcement strain @centre	[ $\mu$ -strain]	1339.342	2261.448	773.236	1017.975

reinforcement. These values are compared with single sleeper FEM models with different plastic Young's moduli as the only changing variable. All tests results are summarized in table 5.1 per sleeper type and in figures 5.2 and 5.3 the FEM results are drawn. The 201 sleeper data is on the left and the 202 sleeper data is shown in the right figures. One other piece of available data is present in the form of static test by Hoffmann and Freudenstein [51]. These tests have been executed only on the 201 sleeper and only for a short static tests. The found deformation values for the 30 kN load where  $7.3 \pm 0.4$  mm. This seems to be in line with the long static sets.

Starting with some general remarks that apply to both types. All static tests deformations are not reached by any of the FEA. The time dependent effects have such a big influence on the experienced Young modulus that a heavy reduction is necessary to mimic the behaviour. Therefore the static results cannot be analysed and the validation has to focus on the dynamic case alone. This is not a mayor problem as this is the main loading case after all. But which not means that the high static strains should not be a point of interest.

Continuing with the 201 sleeper, that is on the left of both figures, it is clear that there are some differences between the FEA and tests. Looking at the deformation and strain graphs (figures 5.2a and 5.3a) the intersection for the FEM-results with the dynamic deformation value are not the same for both parameters. Figure 5.2a shows almost perfect correspondence with the  $400 \text{ N/mm}^2$  FEA. The strain graph in figure 5.3a however has the best agreement with the  $650 \text{ N/mm}^2$  Young modulus. This means that there is some discrepancy between the model and the tests. Possibly this is due to the simplifications in the model interfaces and the used linear material model. The choice is made to use both found Young moduli as lower and upper limit and review all stresses, strains and deformations for both models.

There is a better agreement between the 202 bending test results and the FEM. Figures 5.2b and 5.3b show that both the deformation and strain curves intersect around a Young modulus for the plastic of approximately  $1000 \text{ N/mm}^2$ . This means that for this material the FEM and tests correspond very well with each other and this increases the confidence about the results greatly. As the FEA are already executed, the same approach as with the other sleeper type is used and both 900 and  $1080 \text{ N/mm}^2$  are used as lower and upper limit respectively.

Concluding, for both sleeper types the to be used Young's moduli are established. The stiffer sleeper (202) showed almost perfect agreement and the less stiffer (201) sleeper did not match the test results quite well, but reasonable and should therefore be used with more care when interpreting the results.

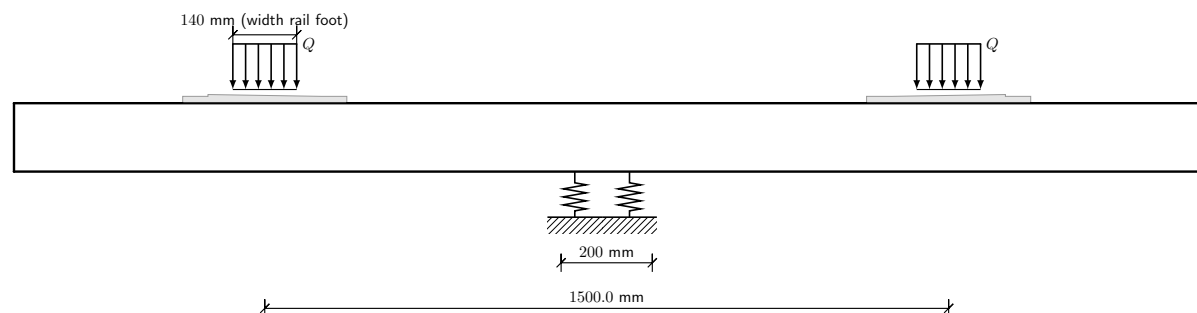
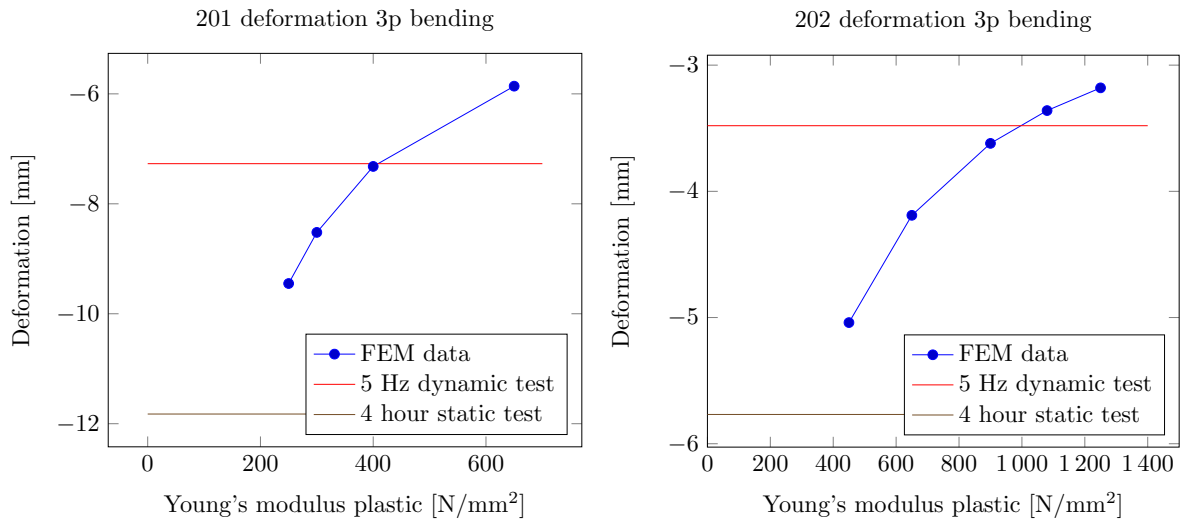


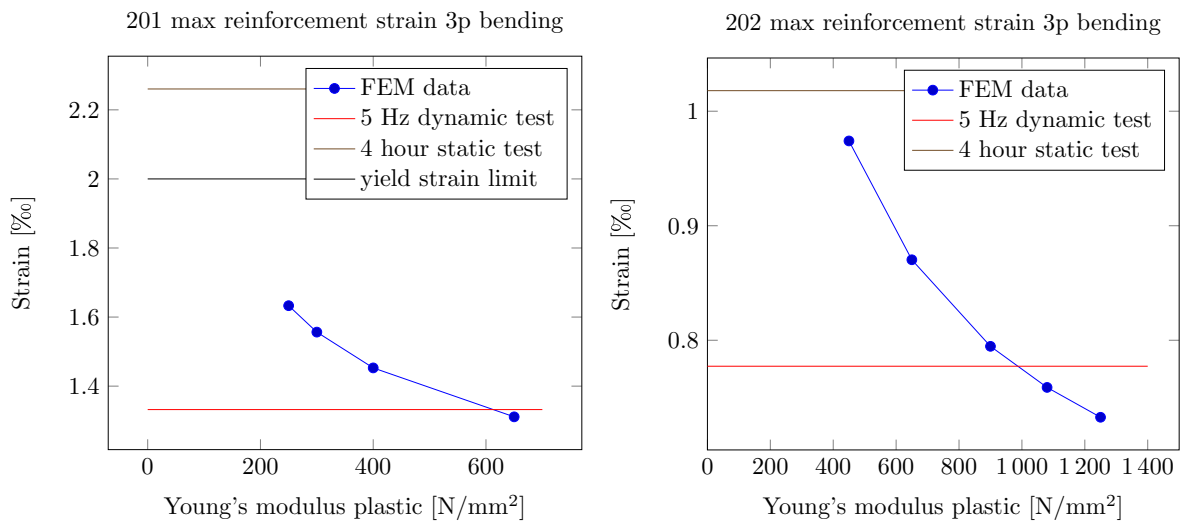
Figure 5.1: Setup of 3-point bending test as FEM.



(a) Maximal deformations 201 sleeper.

(b) Maximal deformations 202 sleeper.

Figure 5.2: Deformation measurements of 3-point bending experiments and FEM results under a 30 kN wheel load.



(a) Maximal reinforcement strain in 201 sleeper.

(b) Maximal reinforcement strain in 202 sleeper.

Figure 5.3: Reinforcement strain measurements of 3-point bending experiments and FEM results under a 30 kN wheel load.

## 5.2 MULTI-SLEEPER RESULTS

The multi sleepers analysis main purpose is to remove the influence of any boundaries that exist. As the single sleeper model is much more easier to solve the best result would be a comparable result between the single and multi-sleeper model so that the single sleeper model can be used for all analysis and is known to produce the same results. The main result from this analysis is the load distribution over the sleepers.

Table 5.2 shows the results from the FEA for both sleeper types combined with the analytic value for the previously determined characteristic length of 0.7160 m (see equation 3.9). Also a second analytic curve has been added that matches the FEA-results the best. As can be seen from table 5.2 the load percentage of the centre sleeper is about 41% and really close to the expected value of 42% when rounded. The value of 41% is used in further analysis, but the analytic calculation proves that it can provide good values as well. This means that the FEA does not has to be used to get a good insight in how the load is distributed.

Table 5.2: Load percentages of both multi-sleeper models, matching analytic eta-curve ( $L = 0.7160$  m) and best match eta-curve ( $L = 0.7275$  m).

Sleeper nr.	Eta-curve		FEM	
	$L = 0.7160$ m	$L = 0.7275$ m	201	202
1 (centre)	41.8%	41.1%	41.1%	41.2%
2	25.5%	25.5%	24.8%	24.9%
3	7.0%	7.3%	7.5%	7.4%
4	-0.8%	-0.6%	-0.2%	-0.2%
5	-1.7%	-1.7%	-1.6%	-1.6%
6	-0.9%	-0.9%	-1.0%	-0.9%
7	-0.2%	-0.2%	-0.3%	-0.3%
8	0.1%	0.0%	0.0%	0.0%
9	0.1%	0.1%	0.1%	0.1%
10	0.0%	0.0%	0.0%	0.0%

## 5.3 GENERAL RESULTS AND MATERIAL LIMITS

As the previous section showed which analysis are the most comparable to the real life experiments, the two best fitting FEM analysis of both plastic materials are analysed. In appendix B.1 the sensitivity of the Young modulus and the foundation stiffness was investigated. According to these results the foundation stiffness has a much bigger influence on the maximum deformation than the same relative change in the Young modulus. The general results are however only analysed for one fixed foundation modulus. To investigate the influence of the foundation on the FEA, the results of the 202-sleeper are extended with a ‘changed foundation modulus’-analysis in section 5.3.3.

As the material properties are linear and the type of analysis is static, the results follow a linear path as well. This means that any intermediate point can be found by interpolating between the other measurement points, without significant accuracy loss. A multi-sleeper analysis provides input on the load bearing percentage of the centre sleeper. The found load percentage of the multi-sleeper experiment is 41% of the wheel load  $Q$  (see table 5.2).

### 5.3.1 201 SLEEPER

First the results of the 201 sleeper are investigated. It has to be noted that the 3-point bending test results do not correspond very well to the FEA, but the two outer Young’s modulus that had the best agreement with the test are analysed here. So the  $E_{\text{plastic}=400}$  and  $E_{\text{plastic}=650}$  are compared with the limits determined in earlier chapters.

As table 5.3 shows, there are some parameters that exceed the expected limit values. This includes the deformation limit, plastic material strength for the  $Q_{\text{DAF}}$  and the reinforcement-plastic shear stress for both load cases. First the deformation limit of the sleeper. The value is exceeded for expected very infrequent loads and as the 2 mm limit is not a fixed value as well, there is some room to allow this higher deformation under extreme loads.

Secondly the exceedance of the material strength should be investigated further. Some local yielding however, could be allowed as the maximal stresses are occurring at the connection with the base plate. Especially when this only occurs for sporadic loads.

The shear values however are above the limit for both load cases. Which implies that the interface between the reinforcement and the plastic should be investigated further. The current shear stress values are well above the expected material limit, so this is a part of interest. Secondly, the values found are a lot higher than the calculated values in section 3.5, but this can be explained by the fact that the analytic calculation only uses the height of the sleeper and not the total sleeper-baseplate-rail system, which increases the height of the system and therefore the shear stresses. The shear stress distribution is further discussed in the section about foundation stiffness tests, section 5.3.3.

Also some parameters that are within the allowed range, are on the edge of that range. In combination with simplifications, assumptions that have been made or when including safety factors, these values could become problematic in real life cases. The foundation loading is close to its limit for extreme loads, something which can be accepted to happen occasionally. The material strength and reinforcement material strength are however close to their limits as well. High steel stresses could lead to fatigue failures as the type of loading is almost always dynamic. That makes that this typical sleeper, when subjected to the worst case scenario, performs really at its limits as it seems from this research. All should not be a problem as tight performance is the goal of most, designs. No excess of material is unused and thereby wasted. It does make it hard to provide hard conclusions about the sleeper. As the used simplification in the material model could influence the behaviour of the sleeper and without any remaining strength, this could mean that this type will underperform under working conditions.

Concluding, the bond strength and behaviour of steel-plastic interface bond should be a point of further investigation. Secondly the fatigue conditions of plastic and steel should be observed to make sure a long enough life span is possible.

### 5.3.2 202 SLEEPER

The 3-point bending test showed good agreement to the test results and a FEM with a Young's modulus just below 1000 MPa (see section 5.1). Therefore only the two values 900 and 1080 MPa are examined. The most valuable results are summarised in table 5.4. As can be seen, almost all values are below the established threshold. Only the shear stress value is exceeded, something that also occurs for the 201 type. Shear stress is therefore certainly a point of interest and further needed research. Also the maximal deformation is exceeded in the case of the dynamic amplified wheel load. For this value the same arguments hold as for the 201 sleeper. This 2 mm is not a fixed value and an indicative value and in combination with a exceptional load that should not occur frequently this is probably not a problem. It is however a possible property to check in a real track how the sleepers deformation behaviour is and if this needs adjustments.

With the interface stress calculations, an average stress for the ballast-sleeper interface has been calculated. As table 5.3 and 5.4 show, the experienced values are between 0.19 and 0.24 when  $Q = 45.1$  kN. The analytic results from section 3.3 provide two stress values. One based on a fully supported sleeper and one based on a semi-supported sleeper (around 50%). When corrected for the load (45.1 kN instead of 100 kN) the following stresses are to be expected:

$$\sigma_{sb_{full}} = \frac{45.1}{100} \cdot 0.31 = 0.14 \text{ N/mm}^2 \quad (5.1)$$

$$\sigma_{sb_{partial}} = \frac{45.1}{100} \cdot 0.61 = 0.28 \text{ N/mm}^2 \quad (5.2)$$

As equation 5.2 shows, the analytic calculation is relatively accurate. The distribution is subject to change if a stiffer or less stiff sleeper is used, but in general this method provides a reasonable value for the stresses.

### 5.3.3 CHANGING FOUNDATION STIFFNESS

Next to the general results, one analysis is investigated where the foundation stiffness is changed to be able to see the influence on the same parameters as in the previous section. The main reason for this analysis is that the changes in foundation stiffness are expected to be the most influencing as followed from the BOEF sensitivity analysis (section B.1). The foundation modulus is changed from 0.02 to 0.2 N/mm<sup>3</sup> the whole range covered in table 2.3. The  $k_d$  for the whole sleeper is therefore between 13 and 130 kN/mm, a broad range

Table 5.3: Overview of the FEM-results of the **201** sleeper type. Values are interpolated to match the correct load.

	Material limit	41% of Q (110 kN) = 45.1 kN		41% of $Q_{DAF}$ (209 kN) = 85.7 kN	
		$E_{plastic} = 400$ MPa	$E_{plastic} = 650$ MPa	$E_{plastic} = 400$ MPa	$E_{plastic} = 650$ MPa
Maximal deformation [mm]	$\approx -2$	-1.78	-1.61	-3.35	-3.04
Reinforcement strain [‰]	$\approx 1.1$	0.4224	0.4032	0.7991	0.7629
Reinforcement stress [N/mm <sup>2</sup> ]	235	88.3	84.5	167.1	159.8
Reinforcement shear stress [N/mm <sup>2</sup> ]	2.5	4.66	3.26	8.82	6.17
Von Mises stress plastic [N/mm <sup>2</sup> ]	9	4.83	5.42	9.13	10.25
Foundation vertical stress [N/mm <sup>2</sup> ]	-0.5	-0.24	-0.22	-0.46	-0.41

Table 5.4: Overview of the FEM-results of the **202** sleeper type. Values are interpolated to match the correct load.

	Material limit	41% of Q (110 kN) = 45.2 kN		41% of $Q_{DAF}$ (209 kN) = 85.7 kN	
		$E_{plastic} = 900$ MPa	$E_{plastic} = 1080$ MPa	$E_{plastic} = 900$ MPa	$E_{plastic} = 1080$ MPa
Maximal deformation [mm]	$\approx -2$	-1.42	-1.38	-2.67	-2.61
Reinforcement strain [‰]	$\approx 1.1$	0.2896	0.2757	0.5478	0.5217
Reinforcement stress [N/mm <sup>2</sup> ]	235	60.4	57.6	114.3	108.9
Reinforcement shear stress [N/mm <sup>2</sup> ]	2.5	3.21	3.07	6.09	5.82
Von Mises stress plastic [N/mm <sup>2</sup> ]	18.6 – 26.4	4.43	4.67	8.38	8.83
Foundation vertical stress [N/mm <sup>2</sup> ]	-0.5	-0.19	-0.19	-0.37	-0.36

that covers general occurring foundation stiffnesses [29]. This analysis is done with the assumption that the load distribution does not change for different foundation moduli, something that does happen in reality. A stiffer foundation modulus increases the loading percentage on sleepers close to the load and a less stiff foundation disperses the loading more over each sleeper. Therefore the results of the less stiff foundations can be considered to be strict, as the experienced loading will be lower in those circumstances.

Figure 5.4 shows the displacement of the middle nodes of the sleeper for all analysis. The showed deformation is for a 104.5 kN load, so the values are really on the high side of the spectrum. The non-linear sensitivity is however clearly visible in the figure. This means that the found values are very close to each other for low values of  $C$  and all values increasingly grow. To recall, the standard used foundation stiffness had a  $k_d$  of 90 kN/m which is equal to a  $C$ -value of 0.1385 N/mm<sup>3</sup>. The same parameters are gathered in tables 5.5 and 5.6 one for 41% of the wheel load  $Q$  and one for the same percentage of the DAF amplified value.

Looking at the table for a normal wheel load  $Q$  (table 5.5), the values do not differ significantly for increasing foundation stiffness. The exception is the maximal deformation that occurs, this vertical is discussed later. For all other parameters, the same arguments hold as for the general analysis, nothing is significantly different compared to the previously found data for the default foundation modulus. Most results can be considered on the safe side and within margins.

Then the one parameter that does change significantly. Considering the vertical deformation of the sleeper, when the foundation modulus reduces to 0.1 N/mm<sup>3</sup>, the deformation values start to exceed the set threshold of 2 mm. Figure 5.4 is a graphical representation of the the experienced deformations and also shows how the deformations do not follow a linear path. The conclusion that can be drawn considering these results is, that any foundation stiffness below 0.1 N/mm<sup>3</sup> will have a too large vertical displacement. This is even under normal loading conditions, and without incorporating any dynamic effects. The only mitigating factor is a reduction of the total load if more sleepers contribute to load bearing, which happens when the foundation stiffness is decreased.

Looking at the values that occur for dynamic amplified loads, which are summarised in table 5.6, the conclusions are again not different compared to previous results from section 5.3.2. The vertical deformations become large even for the standard analysis foundation stiffness of 90 kN/mm. Something that only worsens when the foundation stiffness is decreased. The conclusion therefore stays the same, this is a important area to investigate.

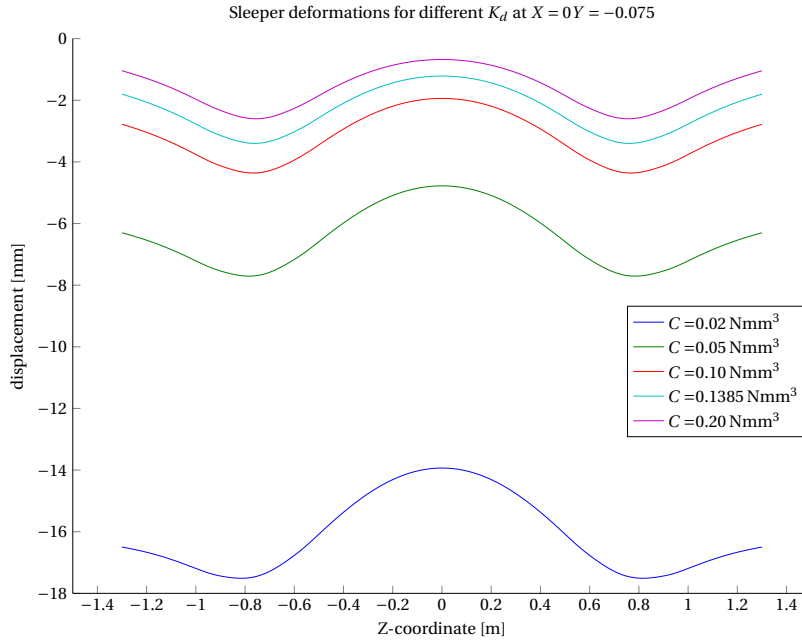


Figure 5.4: Centre line displacements of a 202 sleeper FEM for different foundation moduli and thus a changing  $k_d$ . Wheel load is 104.5 kN.

### SHEAR FORCE

The lateral shear stress ( $\tau$ ) calculation is done to assess the reinforcement-plastic interface and is based on calculating the maximal shear stress that occurs in the middle of the cross section:

$$\tau_{\max} = \frac{3V}{2A}$$

The resulting maximum expected value of the shear stress as calculated in equation 3.22 was  $1.3 \text{ N/mm}^2$ . This is based on a maximal shear stress value from the BOEF analysis. The maximum shear force value found was 32.7 kN for a 85.7 kN load.

The FEA results however, showed that the occurring shear stresses within the plastic-steel interface were much higher than the expected values. Regarding only one load case of 85.7 kN, the following values were found at the steel-plastic interface in the FEM:

$$\tau_{\max_{201}} = 4.66 \text{ to } 3.36 \text{ N/mm}^2 \quad (5.3)$$

$$\tau_{\max_{202}} = 3.07 \text{ to } 3.21 \text{ N/mm}^2 \quad (5.4)$$

The two values correspond to different used Young's moduli, but the increase with the calculated  $1.3 \text{ N/mm}^2$  is significant and not really comparable with the analytic values. The increased height of the 'beam' due to the fixated base plate and rail is likely a large contributor to the difference.

To provide more insight into the shear stress distribution, the shear stress values are summarized in two figures. Figure 5.5 shows the shear stress distribution for three lines. The minimal and the maximum shear stress at each z-coordinate and thirdly the single fibre that has the highest shear stress value. It is clear that the peak is below the load application point, which is not a surprise. The increased height due to the fixated rail and base plate could influence the stress distribution. So fully understanding the behaviour requires a specific look at the reinforcement interface and the base plate interface as well.

The other figure 5.6 shows the maximal shear stress values for different foundation moduli. It clearly shows that the shear stress does not depend much on the foundation stiffness. A minor increase can be seen for less stiff foundations, but the maximum does not change.

Table 5.5: Ultimate values of the 202 sleeper for different foundation moduli loaded with a single wheel load so:  $Q = 110 * 41\% = 45.1$  kN.

	C [N/mm <sup>3</sup> ] =	0.02	0.05	0.10	0.1385	0.20
	Material limit					
Maximal deformation [mm]	$\approx -2$	-7.39	-3.23	-1.81	-1.41	-1.07
Reinforcement strain [%]	1.1	0.3076	0.3075	0.2981	0.2896	0.2764
Reinforcement stress [N/mm <sup>2</sup> ]	235	64.1	64.1	62.2	60.4	57.6
Reinforcement shear stress [N/mm <sup>2</sup> ]	2.5	3.10	3.13	3.18	3.21	3.26
Von Mises stress plastic [N/mm <sup>2</sup> ]	18-26	5.12	4.93	4.63	4.43	4.14
Foundation vertical stress [N/mm <sup>2</sup> ]	-0.5	-0.15	-0.16	-0.18	-0.20	-0.21

Table 5.6: Ultimate values of the 202 sleeper for different foundation moduli loaded with a single wheel load amplified by a DAF so:  $Q_{DAF} = 209 * 41\% = 85.7$  kN.

	C [N/mm <sup>3</sup> ] =	0.02	0.05	0.10	0.1385	0.20
	Material limit					
Maximal deformation [mm]	$\approx -2$	-14.18	-6.20	-3.48	-2.70	-2.04
Reinforcement strain [%]	1.1	0.5818	0.5817	0.5640	0.5478	0.5229
Reinforcement stress [N/mm <sup>2</sup> ]	235	121.3	121.3	117.6	114.3	109.1
Reinforcement shear stress [N/mm <sup>2</sup> ]	2.5	5.87	5.93	6.02	6.09	6.18
Von Mises stress plastic [N/mm <sup>2</sup> ]	18-26	9.68	9.33	8.77	8.38	7.84
Foundation vertical stress [N/mm <sup>2</sup> ]	-0.5	-0.28	-0.31	-0.35	-0.37	-0.41

The shear force seems one of the critical parameters. The maximal values occur on the edge beneath the load application point or the base plate the magnitude is around  $3 \text{ N/mm}^2$ . As mentioned before, this is above the expected  $2.5 \text{ N/mm}^2$  that the steel-plastic interface can withstand. The length of the area that has a too high stress value is around 15 cm. The conclusion therefore is that the shear force distribution should be investigated for all load cases. Appended with the remark that shear force is not dependent on the foundation properties in a significant manner.

#### GAUGE CHANGE

Gauge change is also one possible weakness of these sleepers. Preliminary results showed that the gauge did not change for vertical loads under standard foundation circumstances. To be able to see under which circumstances the gauge does change too much, the foundation was further adapted. This is done to introduce a degraded foundation that features centre sleeper loading and introduces more bending of the sleepers.

A stiffer centre is introduced to show the behaviour when the sleeper is mainly supported by the centre. The size of the centre section and the stiffness difference between the outer and centre can be altered to investigate different foundation settings. The total  $k_d$  is kept the same so only the distribution changes. All details can be found in appendix F, but the main conclusion that can be drawn is the following. In highly degraded track sections with centre supported sleepers and extreme loading conditions, the gauge easily exceeds the allowed maintenance state, but remains within the ultimate safety values. As the deformations are mostly elastic it hard to say something about the gauge after some amount of time. Therefore the main conclusion is that a proper foundation and a regular inspection interval is needed. This ensures a proper starting behaviour and track any degradation of the foundation to be able to intervene if necessary.

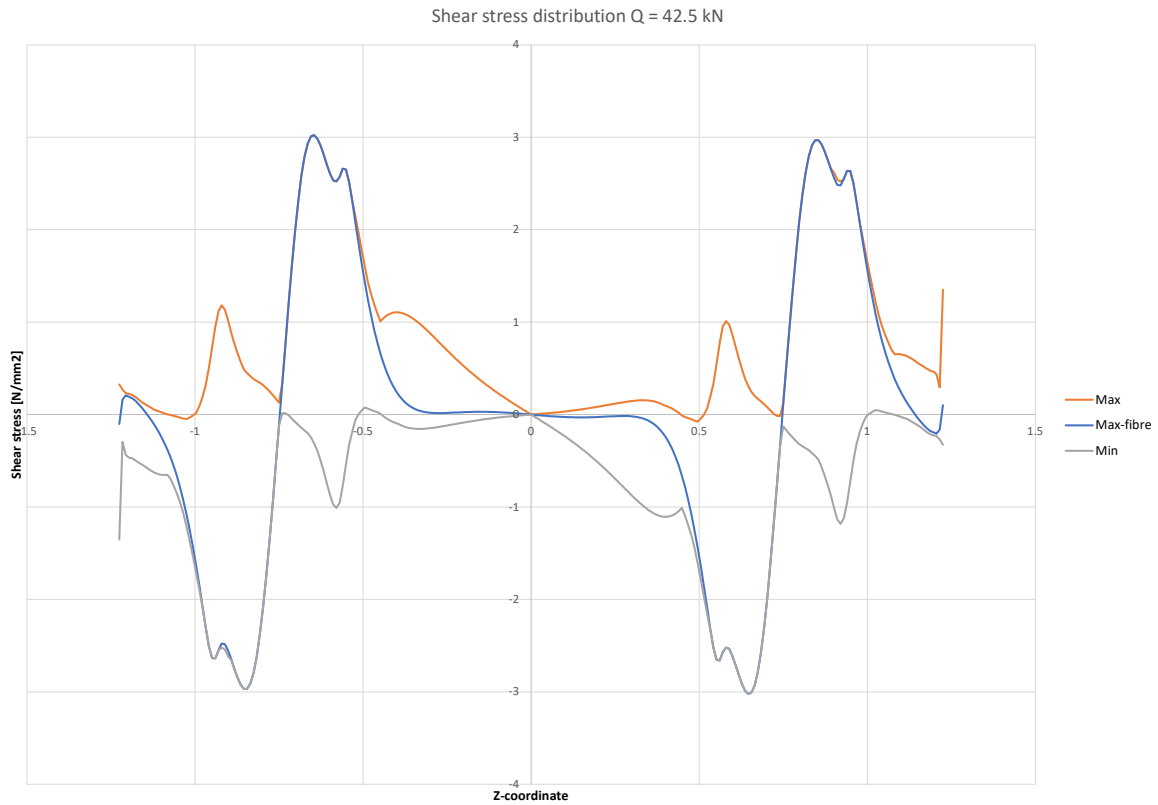


Figure 5.5: Maximal shear stress of a 202 sleeper with standard foundation modulus of 90 kN/mm. Wheel load is 42.5 kN and plastic material Young's modulus is 900 N/mm<sup>2</sup>. Non-symmetry of the graph is due to the fact that the shear stress changes sign at Z = 0. Thus the other part of the graph is mirrored and negative on the other side.

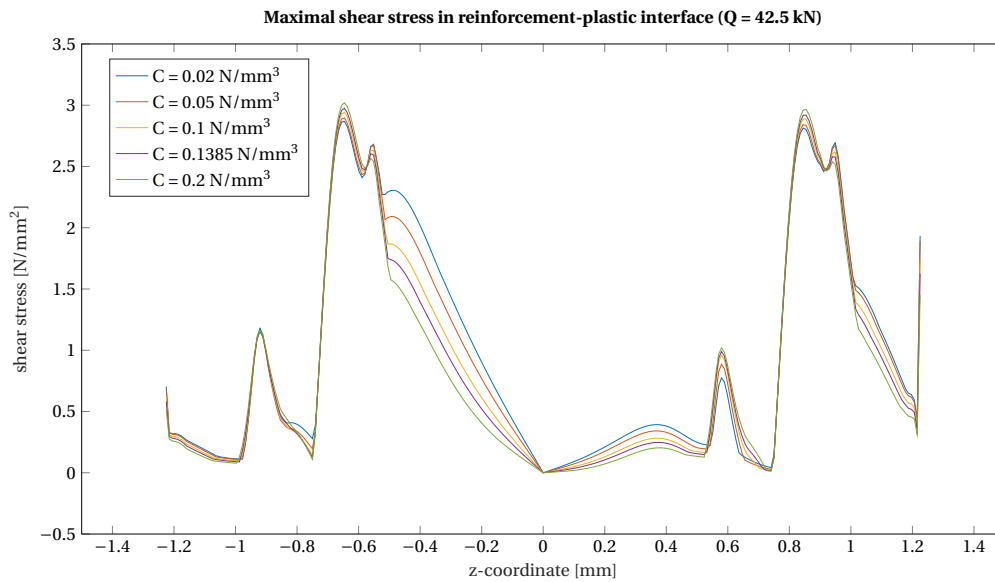


Figure 5.6: Maximal shear stress of a 202 sleeper with different foundation moduli and thus a increasing  $k_d$ . Wheel load is 42.5 kN. Non-symmetry of the graph is due to the fact that the shear stress changes sign at Z = 0. Thus the other part of the graph is mirrored and negative on the other side. Max-fibre is the stress along the one fibre that experiences the maximal stress value.

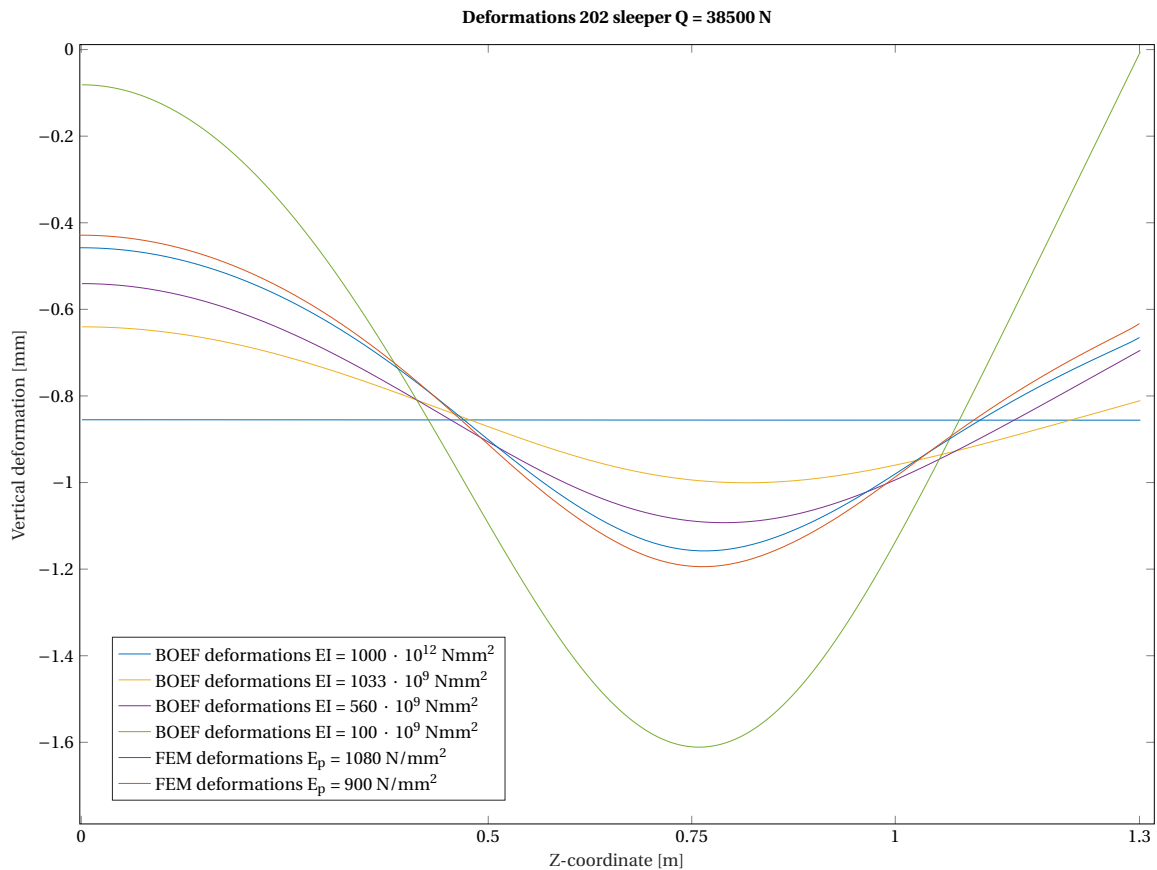


Figure 5.7: Deformation curves of the FEM and BOEF calculations.  $EI = 1033 \cdot 10^9 \text{ Nmm}^2$  is the BOEF-deformation for the theoretical 202 sleeper stiffness (value from equation 2.23).

## 5.4 COMPARISON WITH BOEF CALCULATION

The BOEF calculations in section 3.4 are an important part of the analytic calculations, as they are also the basis for the shear distribution calculation. The calculations all consider a half sleeper and make use of symmetry. To verify the analytic calculation that is made by solving the BOEF differential equation, a comparison is made between the two 202 sleeper models ( $E_p = 900 \text{ N/mm}^2$  and  $E_p = 1080 \text{ N/mm}^2$ ) and several BOEF-deflection curves for varying values of the stiffness ( $EI$ ). The BOEF  $EI$ -values cover a broad range from  $1000 \cdot 10^8$  to  $1000 \cdot 10^{12} \text{ Nmm}^2$ , with the latter representing a more or less infinitely stiff sleeper. Two intermediate values of  $533$  and  $1033 \cdot 10^9 \text{ Nmm}^2$  are also used and represent the approximate theoretical sleeper stiffnesses of the 201 and 202 type respectively.

In an ideal case, the theoretical BOEF-curve of  $1033 \cdot 10^9 \text{ Nmm}^2$  perfectly matches the FEM-results, unfortunately there is quite some difference between both deflection graphs. Figure 5.7 shows the six deflection lines together, the FEM-result lines are close together and assumed being one. As is easily visible, the FEM behaves less stiff than is expected. The deflection curve of the 202 results shows more correspondence with the theoretical 201 stiffness value. So the difference is significant and the question arises how this difference can be explained. Both are models and are therefore a schematisation of reality. The difference in load application, full evenly distributed load over the base plate versus a point load distributed by the rail and base plate has some influence, but not enough to explain the difference. The same holds for the discretization of the elements. In appendix D is shown that the deformation does not change for more elements, so this cannot be the source either. The mismatch between both results at least means that some more investigation is needed to let the BOEF be really functional as measurement tool instead of being a design tool. In other words, to use the BOEF for more than a quick investigation or replacement for the FEM more research is necessary, but this is only encouraged if this will be used with great certainty.

Table 5.7: Utilization factors of all parameters  $\eta = \frac{\text{load}}{\text{resistance}} \leq 1$ . Values taken from tables 5.3 and 5.4.

Sleeper type	Q = 45.1 kN		Q = 85.7 kN	
	201	202	201	202
Sleeper deformation	0.89	0.71	1.68	1.33
plastic material stresses	0.54	0.26	1.01	0.49
reinforcement stress and strain	0.38	0.26	0.71	0.49
plastic-reinforcement interface shear stress	2.17	1.28	3.53	2.44
foundation stresses	0.48	0.38	0.92	0.74

## 5.5 CONCLUSION

To conclude, all topics are shortly summarised. The main results were analysed and provided promising results. First the FEM had to be compared with 3-point bending tests results to validate its usage. This was executed for both sleeper types the 201 and the stiffer 202 type. The reinforcement strain and the maximum deflection were the two parameters used to compare both results. And with a running Young modulus, the agreement between both parameters was investigated to see which Young modulus provided the best match. The 201 sleeper showed quite some difference and the weaker material apparently has a lot of influence considering time dependent deformation factors. The 202 sleeper however showed almost perfect agreement with the 3-point bending results.

With a set of Young moduli determined by the validation, both sleeper types FEA were checked on their individual strength. A series of parameters were checked to see if they were below the in previous chapters established thresholds. This included the items:

- sleeper deformation
- plastic material stresses
- reinforcement stress and strain
- plastic-reinforcement interface shear stress
- foundation stresses

Looking at the normal load case where the wheel load  $Q = 45.1$  kN, table 5.7 shows the utilization factors of all parameters for both sleeper types. Please keep in mind that no safety factors are incorporated in the results, so that will have some influence as well. From the five parameters one parameter has an factor  $\eta \geq 1$  and therefore is considered critical for both sleeper types. This is the shear stress between steel and reinforcement. All other values are within range, with the deformation being the next critical value. As the design of the model with fully fixed interfaces could have a lot of influence on the shear distribution, this is designated as one of the primary subjects for further research. A last property to mention is the steel stress. The maximal values are not close to the limit stress, but one remark has to be made. The dynamic nature of the track loads could induce high fatigue damage to the reinforcement. And reinforcement fatigue should be a property to pay attention to.

Also an exceptionally high wheel load was investigated. For the load case with an DAF-increased value of  $Q_{\text{DAF}} = 85.7$  kN, two parameters become critical and two parameters are just on the boundary. Table 5.7 shows that the deformation started to exceed the allowed value, but as this is or should be a sporadically event a temporarily exceedance could be allowed with enough investigation and risk analysis. The two new values that are (close to being) exceeded are the material stress and foundation stress. Both parameters are only exceeded for the weaker 201 sleeper and not for the 202 type. For the foundation stress the same argumentation can be used as for the deformation and possibly allow some exceedance for extreme loads. The PE material stress could be more challenging and should be investigated further. Especially as time dependant effects and environmental effects are not yet taken into account and could have a great influence, at least after some time.

Next to the default foundation stiffness, the full range of stiffnesses from  $0.02$  to  $0.2$  N/mm<sup>3</sup> is investigated. The mayor conclusions do not differ from the general analysis, all values are even fairly consistent considering the broad range. The biggest change is the deformation of the sleeper that becomes too high (larger than 3 mm) for stiffness values below  $0.10$  N/mm<sup>3</sup> when loaded by the 45.1 kN load.

As the shear force had been a probable problem, it was also taken into account when analysing the foundation stiffness models. The resulting figures showed high peak stresses below the loading around the base plate width. Outside of this area the shear stress values show a better agreement with the analytic results from chapter 3. This could still mean that the way of modelling the base plate-sleeper interface has a large influence on the distribution. Concluding, the deformation and shear stresses are the two mayor problems that are likely to occur under high loads.

So is the sleeper usable in the track? Laboratory testing seemed to give proper results and the simulated analysis did include a lot of worst case assumptions. Therefore the conclusion can be drawn that it is reasonably to believe that the sleeper functions properly under real live basic cases. It is however not certain that under live conditions the sleepers keep behaving properly after some time of usage. To limit the difficulty of creating assumptions and simplifications it is therefore advised to do more physical tests in the laboratory and in tracks if possible and observe the sleepers behaviour over time and under real loads. This could also provide an answer to the influence of the shear stresses that are above the limits. Are the limits too strict, and is stress redistribution happening? And how much is the integrity affected by spurious high loads? Also the extending of the model has to be considered. Is it feasible to extend the model and which parts should be improved? Several options come to mind, such as: making the material model time dependent and improving the interfaces.

Lastly and somewhat secondary item to investigate was the behaviour of the analytic methods. If the analytic calculations provide the same results as the FEM, no FEA is needed. The four analytic calculations that were done are:

- Load distribution over sleepers
- Foundation interface stress
- BOEF deformations
- Maximal shear stress

The load distribution provided perfect results. The foundation interface stress calculations provided good results, when taking into account that they were not corrected for any internal sleeper properties. The expected deformations of the BOEF-calculation are compared with the FEM-deformations. The main conclusion is that for yet unknown reasons the FEM behaves less stiff than was anticipated. Therefore the BOEF presents a lower deformation than in the model. And as the shear stress value also depended on the BOEF-calculation this value was not of much use either. So this leaves room for a FEA to be beneficial, but also reduces its necessity somewhat. Combined with the current limits of the model, without any non-linearities in place, there is still a lot to investigate.

# 6

## CONCLUSIONS AND RECOMMENDATIONS

The objective of this research was to provide a finite element model (FEM) to assist in determining if a newly designed sleeper is suited to be used in the track. With the aid of a newly designed and constructed FEM, the behaviour of two hybrid (plastic-steel) Lankhorst sleepers were examined. The research questions formulated for this thesis is the following: "*Can a finite element model be used to improve railway sleeper acceptance?*". This is substantiated by finding an answer to the subquestions which are addressed one by one to finish by answering the main question.

### CURRENT ACCEPTATION PRACTICES

The current assessment of new sleeper is very material type based. Creating a new sleeper from a new material is therefore not a trivial task. The standard on plastic sleepers NEN-EN 12856 is relatively new and created after new sleeper types were introduced. The in April 2020 added part 6 of the concrete sleeper standard, creates a good basis for design but still has a specific material in mind. It is easy to follow tests protocols for sleepers, but the standards could be more abstract in their basis. As it is difficult to interpret multiple standards to figure out what works best for a new material. The choice for specific material influences the need for some material specific test, but the most basic requirements should be fixed values. E.g. specifying limit values for deformations instead of maximum moment values in a sleeper. The search to new materials is not at an end, so a more easier way in validating a viable sleeper design should be possible. Of course it is difficult as many infrastructure managers can have different requirements.

### NEEDED FEM OUTPUT

The needed FEM output is defined by the values required in the standard and complemented with some other stresses that are of special interest, regarding the type of sleepers investigated. The latter introducing the need for shear stress calculations so the reinforcement-plastic interface can be analysed. Considering the stress analysis, as the used material models are linear and without stiffness changes, it has to be investigated to what extend the materials are within the elastic portion of their stress-strain curve. It is clear that the plastic materials will not behave as such, but the probable impact can be analysed. Secondly it was found that the foundation properties have a larger influence on the behaviour than the material stiffness.

### THE POSSIBILITIES OF THE FEM

After analysing the FEM results, the solutions in general look promising. To improve on a simple beam model, the reinforcement is modelled with solid elements. Next to creating more data this introduces also uncertainties that still exists after this research about the interaction between the steel and plastic. The validation step was executed by comparing the model with 3-point bending tests and comparing the test values to the FEA, the investigated values were the deformation and reinforcement strain. The stiffer 202-type provided good agreement with the real life test, the more flexible 201 sleeper had some disagreement but within reasonable margins.

With the determined Young moduli, all relevant material and sleeper parameters were compared to the established limit values. The solved models included only linear properties and static analysis, so no nonlinearities were investigated yet. The used load was a relatively high load to simulate harsh conditions. The found results

showed that one property seems to exceed the limit values in all cases. This happened to be the steel-plastic interface shear stress. The limit value of 2.5 MPa was exceeded in all cases in the area directly under the load. This should be further analysed and possibly improved in the model by implementing a more realistic sleeper-base plate interface and sleeper-reinforcement interface. And real life sleepers should be examined if any problems occurred in this interface.

All other values were within the acceptable range for normal to high loads. Under exceptional loads of for deteriorating foundations the deflection and reinforcement fatigue are the first things that become critical. The deflection is easily measurable, but frequent inspection is needed. And as the reinforcement stresses were relatively high compared to the maximum allowed stress and with the dynamic loading conditions of the railways, this could lead to fast degradation of the steel and fatigue problems. Therefore it is advised to keep paying attention to those parameters and their behaviour under live loads. Secondly as the non-linear properties were not incorporated this is still an open point and will require more investigation and also additional material model verification. The time dependent behaviour of the plastic material, such as creep and changing material stiffnesses are still properties to be added to the model. To be independent of real life tests, an improved material model should be put into place, which is not trivial. Lastly as the foundation properties have a lot of influence on the stresses and deformations. Any further investigation should use a range of foundation moduli, as is done in this research, or really use a measured foundation modulus from a specific location.

#### FINAL CONCLUSION

Combining all previous information and results, the following conclusions can be drawn:

- It is, at least the moment, not beneficial to use finite element analysis (FEA) as tool in assessing a new sleeper that is constructed from very non-linear behaving materials. Analytic calculations seem to provide good results in linear cases, so only when incorporating non-linearities the FEA can be beneficial but then it will need additional validation.
- Laboratory test are more valuable than FEA. Mainly due to the fact that individual material models need validation and secondly that the whole model needs to be validated as well. Both steps require actual tests results, so test have to be performed in any case.
- Extending the previous point; creating sleepers and putting them to real life test is a great method of testing. Mass products that are used under dynamic loading especially with non-linear materials, have large costs modelling and creating FEM, as such a model also needs validation. Therefore it is expected to be easier to do more real life (laboratory) tests on sleepers in varying situations and loading conditions. This opposed to buildings where there are one, or very few instances constructed and where the used materials are generally standard building materials.

Next to the more negative conclusions, there are some positive conclusions as well although less applicable to the main question. The model does exist, so is ready to be used and may be freely adapted. It is available on <https://github.com/agriemink/AnsysSleeperModel> under the MIT license. For sleeper design or track system analysis the model can still be used. Therefore a list is presented with the properties of the model as implemented:

- Basic analysis types are possible. Currently static and modal analysis are supported, others can be easily implemented, only lacking automated post processing
- Two types of reinforcement can be modelled, more accurate versus less elements (octagonal simplification)
- Adjustable foundation parameters, symmetric portions be modelled with different stiffnesses
- Single sleeper models are easily chained to create a multiple sleeper model
- In a multiple sleeper model each sleeper can have different properties
- Basic automated and semi-automated (Matlab) post processing
- The possibility of running several analysis and models after each other without manual interaction

'Concluding' the conclusions, the new sleepers are a gain to the sleeper spectrum and hopefully the results from some in field testing are promising, so that in 20 years these sleeper in one form or another are fully integrated in the railway industry.

## RECOMMENDATIONS

Extending on the conclusions, some recommendations are done. Most are suggestions that should improve the research on this kind of topic, so it may be possible to use FEA to a greater extend. The finite element model does exists and is capable of producing lots of data. So with some effort on validating, improving the post processing and eventually incorporating time dependent analysis it could become a useful. Only the amount of invested time does not seem to balance with the produced results. Some more recommendations with regards to the model:

- Before starting the creation process of a new model make sure it is as simple as can be. Versatility is nice, but also very complicating. As well as in design, validation and post processing.
- If detailed finite element models are wanted for (new) visco-elastic material compositions, a large investment has to be made, to be able to create and validate individual material models. Each new material needs validation. If then the usage of this finite element model is not guaranteed, then this 'not validated' model, invalidates the finite element results. So FEA is less economical in such cases an effort should be made to create a validation pipe-line for material models.
- Tackling this kind of problems is better done by broad field of engineer as the problem is multifaceted. Ranging from programming, material science to highly non-linear FEA, all covering a civil engineering topic.
- When heavily using or extending the model, section 4.5 contains the detailed recommendations, but in short: Using the model is possible if not much changes are needed and they are only parametric. Any additions to the code are expected to be hard to implement. Trying to improve the code does require a steep learning curve for programmers at least.
- Utilize ANSYS Workbench an its GUI and limit the amount of programming with APDL as much as possible. The APDL programming language has more drawbacks than that it provides usefulness, it could be that there are methods to work around some of these. Its just not recommended to try, unless one knows what to do or has the time.



# **Appendices**



# A

## KLP SLEEPERS

The incentive for this research is the newly developed sleeper by Lankhorst. This appendix gives the geometric properties of the considered sleeper and provides an expression for the whole sleepers Young's modulus as a function of the plastic modulus.

The addressed sleeper types are the the 201 and 202 type. Both sleepers have a rectangular cross section over their full length and contain four reinforcement bars. The mayor difference is in the used plastic material and a minor difference are the reinforcement dimensions. To be able to use plastic sleepers as substitute for wooden sleepers, using the same dimensions is almost mandatory. Therefore both used types have the following dimensions:

$$2600 \times 150 \times 250 \text{ L, H, W} \quad (\text{A.1})$$

Which is the same as wooden sleepers [11]. Figure A.1 shows some details about the sleeper composition and how it fits in a track situation.



Figure A.1: Overview of two Lankhorst KLP-S @sleeper [28].

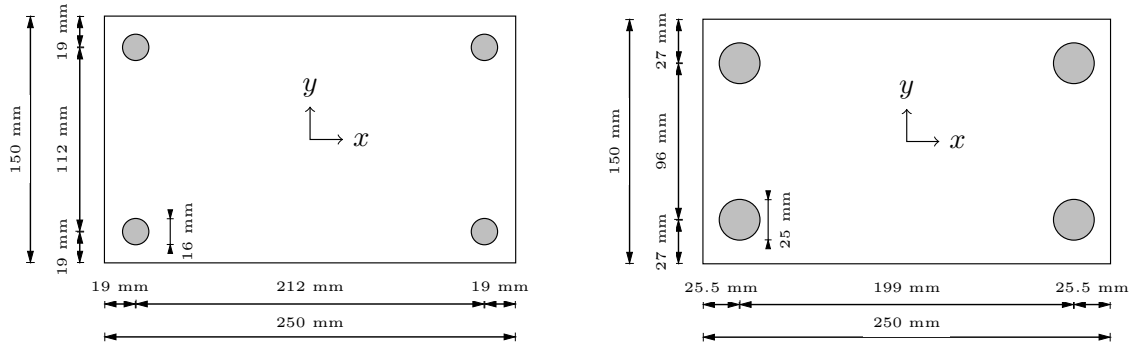
### A.1 GEOMETRIC PROPERTIES

Both sleeper types are in general the same. The main difference is the used material, the 202-sleeper is made out of a stiffer material than the 201-sleeper and therefore has more reinforcement to keep the general properties of the sleeper similar. The reason for this is quite trivial, a stiffer material takes a greater load in a construction. So more reinforcement in a soft material is going to load the steel too much.

The sleepers length is in practice variable, the standard length however is 2.6 meters. The cross sections of both types are similar in shape. The main difference is the size and location of the reinforcement that differs slightly. In figure A.2a and A.2b the cross sections are shown. Both cross sections do not change over the length of the sleeper, with a small note that the reinforcement does not continue in the outer edges of the sleeper. This can be seen in figure A.3 where a longitudinal cross section is shown. The dimensions of both sleeper types are summarised in table A.1.

Table A.1: Dimensions of the two sleeper types as considered in this report. Bending stiffness taken from Lojda et al. [18]

	KLP 201	KLP 202	Unit
Length ( $L$ )	2600	2600	mm
Width ( $b$ )	250	250	mm
Height ( $h$ )	150	150	mm
Reinforcement diameter	16	25	mm
Reinforcement coverage (vertical)	11	14.5	mm
Reinforcement coverage (horizontal)	11	13	mm
Reinforcement length	2450	2450	mm
Bending stiffness	6655	12995	MPa
Second moment of area ( $\frac{bh^3}{12}$ )	$70.3 \cdot 10^6$	$\text{mm}^4$	



(a) Cross-section of the 201-type sleeper. Base material is of the type PE, reinforced with steel.

(b) Cross-section of the 202-type sleeper. Base material is of the type HDPE, reinforced with steel.

Figure A.2: Cross-section of both covered sleeper types.

### A.1.1 BENDING STIFFNESS

As the material properties are not constant in a cross section, the contributions of each material to the bending stiffness have to be incorporated. The bending stiffness consist of the Young modulus ( $E$ ) and the second moment of area ( $I_{zz}$ ). The bending stiffness is in general different for each bending direction, therefore the bending axes are given as subscript. Young's modulus is constant and stays therefore without subscript, the second moment of area gets an subscript  $x$  for bending around the  $x$ -axis. The standard formula for calculating the second moment area is taking the integral over the area multiplied with the distance to the origin:

$$I_x = \int \int y^2 dx dy \quad (\text{A.2})$$

For a filled rectangular square around its horizontal axis is, the value becomes:

$$I_{x_{\text{rectangle}}} = \frac{bh^3}{12} \quad (\text{A.3})$$

And for a filled circular shape the value is equal to:

$$I_{x_{\text{circle}}} = \frac{\pi}{4} r^4 \quad (\text{A.4})$$

Where  $b$ ,  $h$ ,  $r$  are the width, height and radius of the shapes respectively.

To incorporate the contribution of the reinforcement to the bending stiffness of the cross section the Steiner's theorem is used. This method is a way to sum multiple contributions. The general rule to compute the contribution of an arbitrary shape with respect to a given point is given by equation A.5.

$$I_x = I_{x_{\text{shape}}} + Ay^2 \quad (\text{A.5})$$

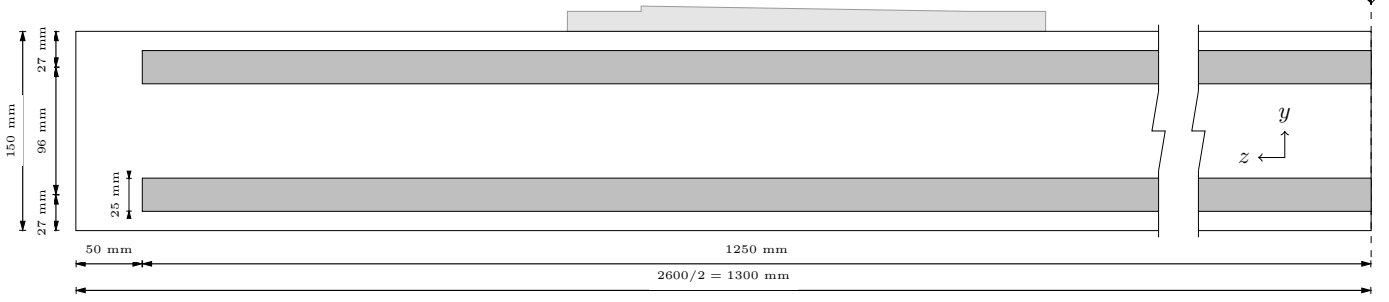


Figure A.3: Longitudinal cross-section of the 202-type sleeper with base plate.

Where:

$I_{x_{\text{shape}}}$  = the second moment of inertia of the shape itself, with respect to its own centroid.

$A$  = the area of the cross section.

$y$  = the vertical distance between the centre of the shape and the origin.

As second moment of inertias can be superposed the total is the summation of the individual components. As the elements that make up the cross section differ in stiffness, the contributions are multiplied by  $E$  to get the full bending stiffness of the cross section.

$$\begin{aligned} EI_x &= E_{\text{plastic}} \cdot I_{x_{\text{sleeper}}} + E_{\text{steel}} \cdot I_{x_{\text{reinforcement}}} - E_{\text{plastic}} \cdot I_{x_{\text{sleeper material overlapping with reinforcement}}} \\ &= E_{\text{plastic}} \cdot (I_{x_{\text{sleeper}}} - I_{x_{\text{sleeper material overlapping with reinforcement}}}) + E_{\text{steel}} \cdot I_{x_{\text{reinforcement}}} \end{aligned} \quad (\text{A.6})$$

The  $I_{x_{\text{reinforcement}}}$  has to be calculated with Steiner's theorem. The contribution of the circular reinforcement is given by A.8 substituting A.4 into A.5. Where the value of  $y_{\text{reinforcement}}^2$  is the vertical distance from the sleepers centre of mass to the reinforcement centre of mass.

$$I_{x_{\text{reinforcement single bar}}} = \frac{\pi}{4} r^4 + \pi r^2 \cdot y_{\text{reinforcement}}^2 \quad (\text{A.7})$$

$$I_{x_{\text{reinforcement}}} = 4 \cdot I_{x_{\text{reinforcement single bar}}} = 4 \cdot \left( \frac{\pi}{4} r^4 + \pi r^2 \cdot y_{\text{reinforcement}}^2 \right) \quad (\text{A.8})$$

Combining everything into one equation for the bending stiffness results in the following equation:

$$\begin{aligned} EI_x &= E_{\text{plastic}} \cdot (I_{x_{\text{sleeper}}} - I_{x_{\text{sleeper material overlapping with reinforcement}}}) + E_{\text{steel}} \cdot I_{x_{\text{reinforcement}}} \\ &= E_{\text{plastic}} \cdot \left( \frac{bh^3}{12} - 4 \left( \frac{\pi}{4} r^4 + \pi r^2 \cdot y_{\text{reinforcement}}^2 \right) \right) + E_{\text{steel}} \cdot 4 \left( \frac{\pi}{4} r^4 + \pi r^2 \cdot y_{\text{reinforcement}}^2 \right) \end{aligned} \quad (\text{A.9})$$

For both sleeper types this becomes:

$$\begin{aligned} EI_{x_{201}} &= E_{\text{plastic}} \cdot \left( \frac{250 \cdot 150^3}{12} - 4 \left( \frac{\pi}{4} \frac{16^4}{2} + \pi \frac{16^2}{2} \cdot \left( \frac{112}{2} \right)^2 \right) \right) + E_{\text{steel}} \cdot 4 \left( \frac{\pi}{4} \frac{16^4}{2} + \pi \frac{16^2}{2} \cdot \left( \frac{112}{2} \right)^2 \right) \\ &= E_{\text{plastic}} \cdot (69.50 \cdot 10^6) + E_{\text{steel}} \cdot (0.82 \cdot 10^6) \end{aligned} \quad (\text{A.10})$$

$$\begin{aligned} EI_{x_{202}} &= E_{\text{plastic}} \cdot \left( \frac{250 \cdot 150^3}{12} - 4 \left( \frac{\pi}{4} \frac{25^4}{2} + \pi \frac{25^2}{2} \cdot \left( \frac{96}{2} \right)^2 \right) \right) + E_{\text{steel}} \cdot 4 \left( \frac{\pi}{4} \frac{25^4}{2} + \pi \frac{25^2}{2} \cdot \left( \frac{96}{2} \right)^2 \right) \\ &= E_{\text{plastic}} \cdot (68.80 \cdot 10^6) + E_{\text{steel}} \cdot (1.52 \cdot 10^6) \end{aligned} \quad (\text{A.11})$$

As the Young modulus for steel is constant (see 2.3.1) this value can be substituted in equations A.10 and A.11. With a value  $E_{\text{steel}} = 210000 \text{ MPa}$  this becomes:

$$EI_{x_{201}} = E_{\text{plastic}_{\text{PE}}} \cdot (67.78 \cdot 10^6) + 5.32 \cdot 10^{11} \text{ [Nmm}^2\text{]} \quad (\text{A.12})$$

$$EI_{x_{202}} = E_{\text{plastic}_{\text{HDPE}}} \cdot (65.71 \cdot 10^6) + 9.66 \cdot 10^{11} \text{ [Nmm}^2\text{]} \quad (\text{A.13})$$

With a range of probable plastic stiffnesses the total stiffness is calculated and gathered in tables A.2 and A.3. The smeared Youngs modulus that divides the total  $EI$  by  $I$  again so the steel contribution is smeared over the whole cross section. As both tables show, this smeared stiffness does not change significantly. In short the expected stiffness of the 201 type is approximately  $8000 \text{ N/mm}^2$  and approximately  $14700 \text{ N/mm}^2$  for the 202 type.

Table A.2: Sleeper bending stiffness in the vertical direction for several plastic material Youngs moduli. Stiffnesses are calculated with equation A.12. The smeared stiffness  $E_{\text{smeared}}$  is calculated by dividing the  $EI_{201}$  with  $I_{zz} = 70.3 \cdot 10^6$  (value from equation 2.21). Bold values represent the expected minimum and maximum Young modulus.

$E_p$ [N/mm <sup>2</sup> ]	$EI_{201}$ [Nmm <sup>2</sup> ]	$E_{\text{smeared}}$ [N/mm <sup>2</sup> ]	Steel contribution [%]
0	$5.32 \cdot 10^{11}$	7566	100.0%
100	$5.39 \cdot 10^{11}$	7663	98.7%
150	$5.42 \cdot 10^{11}$	7711	98.1%
200	$5.46 \cdot 10^{11}$	7759	97.5%
250	$5.49 \cdot 10^{11}$	7807	96.9%
300	$5.52 \cdot 10^{11}$	7855	96.3%
350	$5.56 \cdot 10^{11}$	7904	95.7%
<b>400</b>	$5.59 \cdot 10^{11}$	7952	95.2%
450	$5.63 \cdot 10^{11}$	8000	94.6%
500	$5.66 \cdot 10^{11}$	8048	94.0%
550	$5.69 \cdot 10^{11}$	8096	93.5%
600	$5.73 \cdot 10^{11}$	8145	92.9%
<b>650</b>	$5.76 \cdot 10^{11}$	8193	92.4%
700	$5.79 \cdot 10^{11}$	8241	91.8%
750	$5.83 \cdot 10^{11}$	8289	91.3%
800	$5.86 \cdot 10^{11}$	8337	90.8%

Table A.3: Sleeper bending stiffness in the vertical direction for several plastic material Youngs moduli. Stiffnesses are calculated with equation A.13. The smeared stiffness  $E_{\text{smeared}}$  is calculated by dividing the  $EI_{202}$  with  $I_{zz} = 70.3 \cdot 10^6$  (from equation 2.21). Bold values represent the expected minimum and maximum Young modulus.

$E_p$ [N/mm <sup>2</sup> ]	$EI_{202}$ [Nmm <sup>2</sup> ]	$E_{\text{smeared}}$ [N/mm <sup>2</sup> ]	Steel contribution [%]
0	$9.66 \cdot 10^{11}$	13739	100.0%
300	$9.86 \cdot 10^{11}$	14019	98.0%
600	$10.1 \cdot 10^{11}$	14300	96.1%
650	$10.1 \cdot 10^{11}$	14346	95.8%
700	$10.1 \cdot 10^{11}$	14393	95.5%
750	$10.2 \cdot 10^{11}$	14440	95.1%
800	$10.2 \cdot 10^{11}$	14487	94.8%
850	$10.2 \cdot 10^{11}$	14533	94.5%
900	$10.3 \cdot 10^{11}$	14580	94.2%
<b>950</b>	$10.3 \cdot 10^{11}$	14627	93.9%
1000	$10.3 \cdot 10^{11}$	14674	93.6%
1050	$10.4 \cdot 10^{11}$	14720	93.3%
<b>1100</b>	$10.4 \cdot 10^{11}$	14767	93.0%
1150	$10.4 \cdot 10^{11}$	14814	92.7%
1200	$10.4 \cdot 10^{11}$	14861	92.5%
1250	$10.5 \cdot 10^{11}$	14907	92.2%

# B

## BOEF CALCULATIONS

This appendix describes the method that is used to solve the BOEF differential equation with Matlab. The code is not that extraordinary, but is included to create a clear picture about the calculations. The basic calculation is not that hard to solve. A big problem arises when it is tried to incorporate non-constant foundation stiffnesses. Matlab is not able to solve these equations within affordable time. Therefore the only calculations made have a constant sleeper foundations stiffness.

The model does incorporate a distributed load instead of point loads at the rails. It is assumed that the rail and baseplate combination does distribute the loading over the whole area of the base plate. Resulting in a distributed load centred around the rail. The load is 'applied' by making use of the Heaviside step function, to create a 'continuous' function for  $q$ .

With the use of the Figure B.1a shows a graphical representation of the loading. In the end the distributed load is only present at the base plate, so the magnitude of the force is  $q = Q/w_{\text{base plate}}$ . The used wheel load  $Q$  that is used for this analysis is 30% of  $Q_{\text{DAF}}$ , 209 kN thus  $Q = 62.7$  kN.

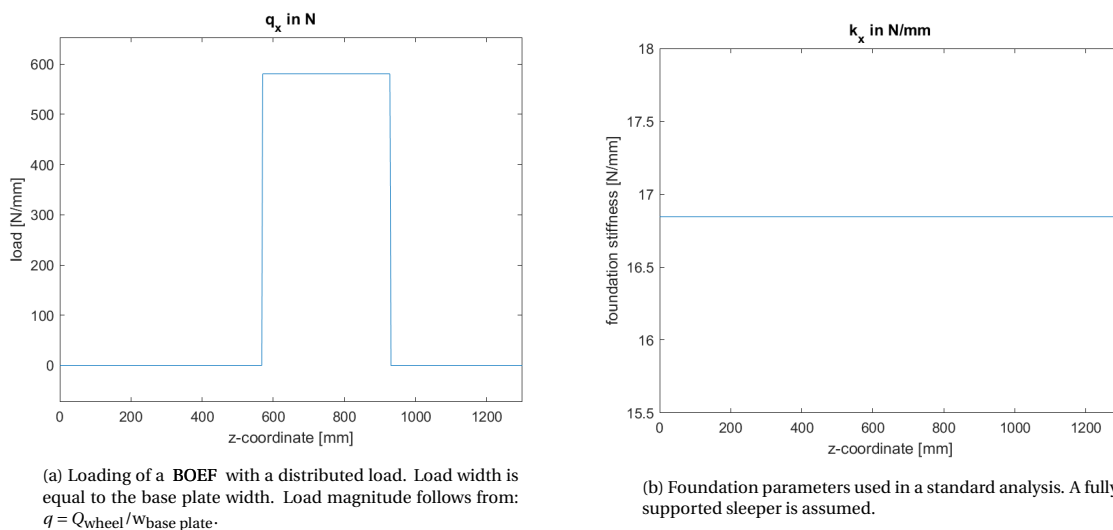


Figure B.1: Standard parameters as used as input in the BOEF differential equations. Half of a sleeper is shown as all analysis use symmetry.

### B.1 SENSITIVITY ANALYSIS

To get a grasp of which parameters have the biggest influence on the sleepers, some parameters are changed to view the different in deformation graphs. The sleeper foundation stiffness  $k_d$  is changed and the sleeper bending stiffness  $EI$  is changed as well. The used ranges is based on lower and upper limits that are possi-

ble in the track. Starting with the foundation stiffness, the lower limit is set on a foundation modulus  $C$  of  $0.02 \text{ N/mm}^3$  which is given by Esveld [1] as lower limit. As upper limit a value ten times as large is given at  $0.2 \text{ N/mm}^3$ . With the formula:

$$k_d = C_{\text{ballast-sleeper}} \cdot A_{\text{ballast-sleeper}} \quad (\text{B.1})$$

Where:

$$A_{\text{ballast-sleeper}} = 2600 \cdot 250 = 650\,000 \text{ mm}^2 \text{ (Area of sleeper in contact with ballast)}$$

As the BOEF analytic model only includes half of the sleeper, so the final stiffness used is also half of the mentioned  $k_d$  values. The other variable that is changed is the Young modulus. The relative range that is used is the same between the lower and highest sleeper stiffness. The default value is set equal to the found value of  $12995 \text{ MPa}$ . The other values have roughly the same relative difference as the foundation stiffness thus ranging from  $2599$  to  $23\,100 \text{ MPa}$ .

The results from the sensitivity analysis are shown in figure B.2. The results show clearly that the BOEF is more sensitive to changes in the foundation stiffness than in the Young modulus. This means that the choice for a correct foundation stiffness is more important than the Young's modulus.

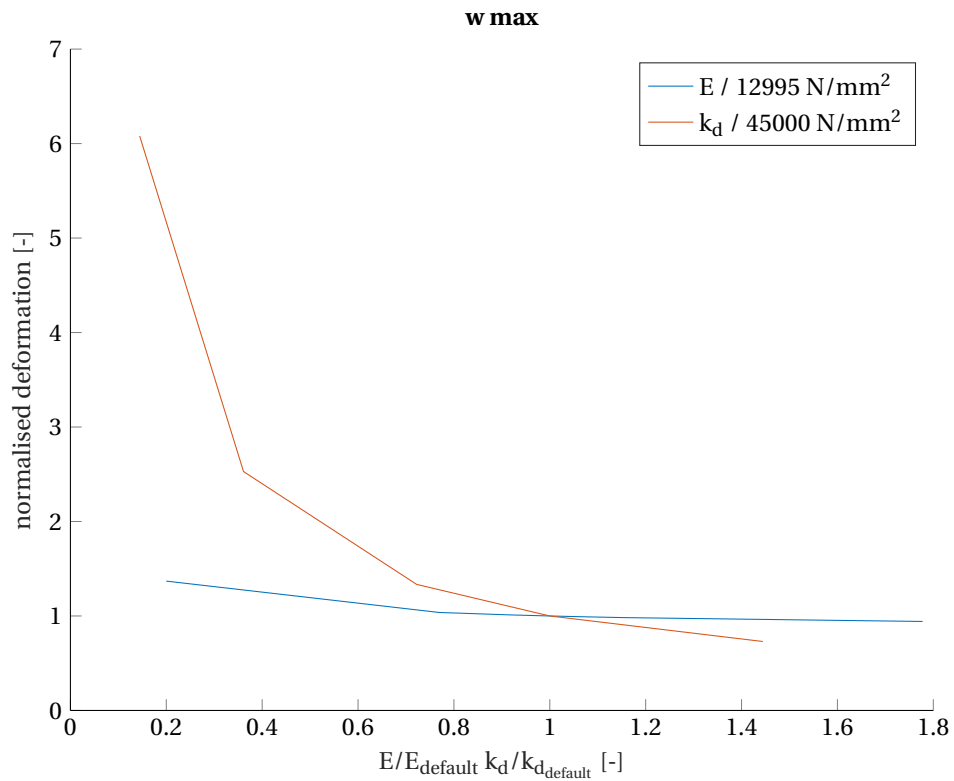


Figure B.2: Sensitivity of BOEF for changing foundation and sleeper stiffness. Shown foundation stiffness is per half sleeper.

## B.2 MATLAB CODE

Below the full code is shown, without the plot creation process, which is just plotting the resulting variable array's.

```

1 %% Variables
2 syms w1(x)
3 syms phi1(x)
4 syms kappal(x)
5 syms V1(x)
6 syms M1(x)
7 syms k_temp
8
9 %%dimensions
10 L = 2600;
11 spoorwijdte = 1500;
12 L_RH = 360;
13
14 %%properties
15 breedte = 250; % mm
16 hoogte = 150; % mm
17 I = 1/12*breedte*hoogte^3; % mm^4
18 E = 12995; % Mpa == N/mm^2 Lojda
19 EI = E*I;
20
21 %%loads
22 sleeperLoadPercentage = 0.3;
23 Q = sleeperLoadPercentage * (209000 / 2);
24 Q = 30000;
25 q = Q / L_RH;
26 k_d = 21900; %N/mm; %eq:DeterminationOfHalfDiscreteSpring
27 k_x = k_d / (L/2);
28
29
30 %% Location specific parameters:
31 force_middle_point = spoorwijdte/2; %symmetrical
32 force_length = L_RH;
33 % Gehele lengte
34
35 q_x = q * (...
36     (heaviside(x-(force_middle_point - force_length/2)) - heaviside(x-(
37         force_middle_point + force_length/2))) ... %Left section
38 );
39
40 %% Differential equation
41
42 odel = EI*diff(w1,4) + k_temp*w1 == q_x;
43
44 phi1(x) = -diff(w1,x);
45 kappal(x) = diff(phi1,x);
46 M1(x) = EI * kappal;
47 V1(x) = diff(M1,x);
48
49 odes = [odel];
50
51 %% Boundary conditions
52 eq1 = phi1(0) == 0;      eq2 = V1(0) == 0;    % symmetry @ x = 0
53 eq3 = V1(L/2) == 0;     eq4 = M1(L/2) == 0; % free end

```

```

52
53 Const = [eq1, eq2, eq3, eq4];
54
55 %% Solve
56 toc(startTime)
57
58 solution(x) = dsolve([odes, Const]);
59 solution(x) = subs(solution, k_temp, k_x);
60
61 w1 = simplify(vpa(real(solution), 10), 20)
62
63 fn = fieldnames(solution);
64 for k_=1:numel(fn) %simplify the found constants
65     C.(fn{k_}) = simplify(solution.(fn{k_}));
66 end
67
68 %reinitiate all the other functions:
69 phil(x) = -diff(w1, x);
70 kappal(x) = diff(phil, x);
71 M1(x) = EI * kappal;
72 V1(x) = diff(M1, x);
73
74 %Vertaal de functies naar een array.
75 left_boundary = force_middle_point - force_length/2;
76 right_boundary = force_middle_point + force_length/2;
77 epsilon = 0.00000001; % to counteract the undefined values on the edges of the
    loading.
78
79 w1_array = [vpa(w1(0:left_boundary-epsilon)) vpa(w1(left_boundary+epsilon:
    right_boundary-epsilon)) vpa(w1(right_boundary+epsilon:L/2))];
80 M1_array = [vpa(M1(0:left_boundary-epsilon)) vpa(M1(left_boundary+epsilon:
    right_boundary-epsilon)) vpa(M1(right_boundary+epsilon:L/2))];
81 V1_array = [vpa(V1(0:left_boundary-epsilon)) vpa(V1(left_boundary+epsilon:
    right_boundary-epsilon)) vpa(V1(right_boundary+epsilon:L/2))];
82 Phil_array = [vpa(phil(0:left_boundary-epsilon)) vpa(phil(left_boundary+epsilon:
    right_boundary-epsilon)) vpa(phil(right_boundary+epsilon:L/2))];

```

# C

## RAIL PROFILE

The regarded rail type is the standard rail: 54E1 also known as UIC54, this rail profile is a standard Vignole rail. In figure C.1 the parameters of the rail profile are shown. Next to the visualisation of the profile, the modelling technique and assumptions for the FEA are also explained.

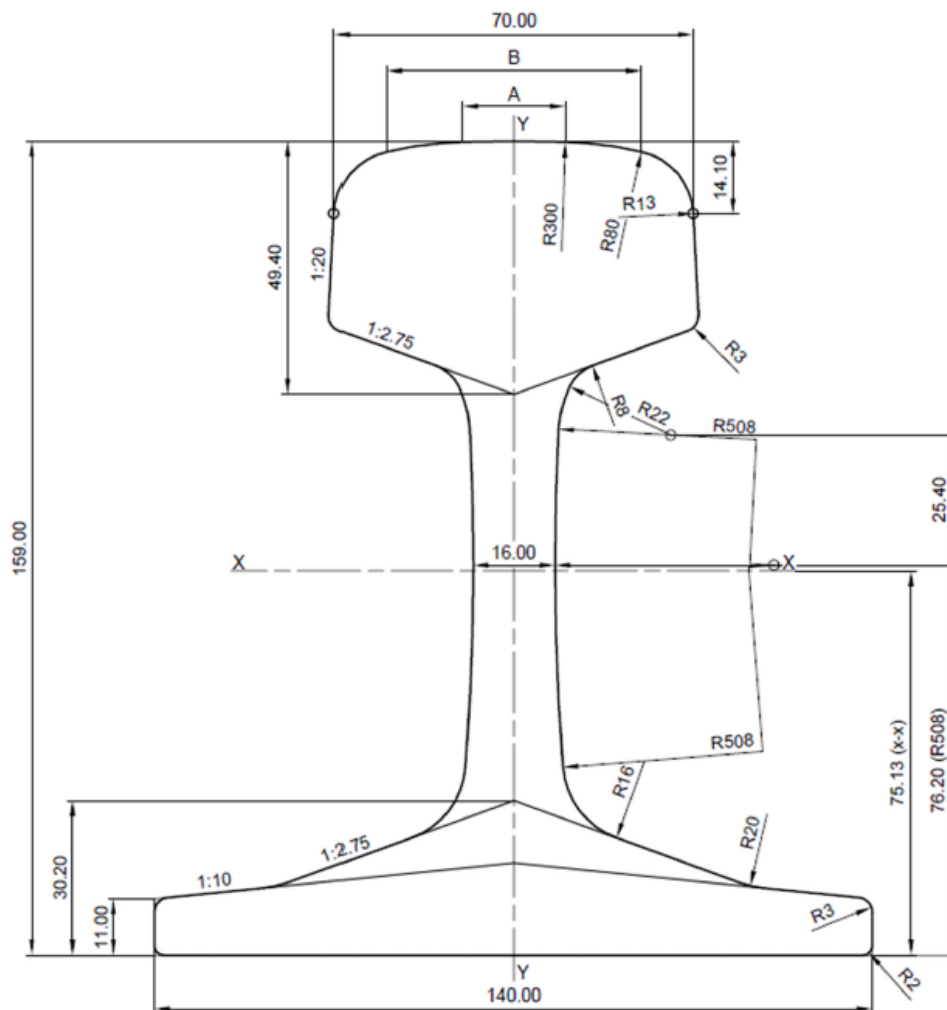


Figure C.1: Cross sectional properties of the 54E1 rail profile [52].

## C.1 FINITE ELEMENT INTERPRETATION

To make the construction in the finite element software easier, some changes to the original rail geometry are made to simplify the modelling.

The simplifications made to the rail profile are mainly to reduce the amount of curves in the cross section. As the rail is not the main subject of this research, the element size can be relatively large. Although larger elements make it hard to follow small curves at the rail edges.

The sides of the railhead are therefore modelled as being fully vertical, instead of the 1 to 20 angle that they are on. This is also done for the web, it is modelled as having a continuous thickness of 16 mm. So without any curvature instead of the 300 mm radius curvature which is present in the real profile. Also the radius of the contact area on the top of the railhead is removed and made fully horizontal. To summarize the differences originated due to the modelling:

- No rounded edges
- Vertical web
- Vertical rail head
- Horizontal contact area

The differences in cross sectional properties are shown in table C.1. All differences are regarded as being minor enough to not influence the final results greatly.

Table C.1: Cross section properties for a 54E1 rail profile and the modelled 54E1 representation. Rail profile values from NEN-EN 13674-1 [52].

	Area [cm <sup>2</sup> ]	I <sub>zz</sub> [cm <sup>4</sup> ]	I <sub>yy</sub> [cm <sup>4</sup> ]
Rail profile	69.77	2337.9	419.2
Model	70.9	2224.2	347.3
Percentage of original	102%	95%	82.8%

## C.2 MESHING

As the final profile contains curves, a mapped mesh requires some additional work. To be able to mesh the whole area with quadrilaterals, some additional lines are added. The rail foot, web and rail head are divided by these additional lines into separate areas. From here the web is easily meshed. The foot and the head require some concatenation of lines. The resulting mesh of the right rail is shown in figure C.2. Some elements are a bit skewed, which could indicate less accurate elements, but as these are in the top of the rail foot it is the best place / less worse location for these elements to exist. The rail foot top should not be a critical location in the considered cases. And in all cases the created elements do not exceed the internal limits that Ansys sets for elongated and skewed elements.

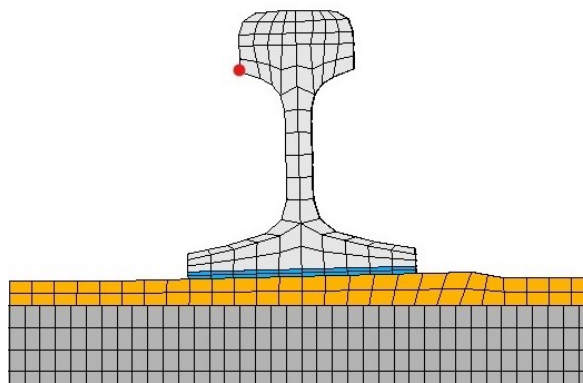


Figure C.2: Overview of the rail profile mesh of the right rail, including the base plate. Red dot indicates the gauge measurement point.

# D

## FINITE ELEMENT MODEL ACCURACY

Two primary models are made with as only difference a different method of modelling the reinforcement. Chapter 4 covers the two modelling methods, an realistic circular model and a schematized model where the reinforcement is octagonal. Summarizing, the octagonal reinforcement is less geometrically accurate, but is easier to divide into smaller elements. The circular reinforcement therefore, when divided into more elements greatly increases the total element count of the sleeper model. To determine the accuracy of both models, the amount of elements per reinforcement bar is changed. More elements usually mean a more accurate model so it is expected that by increasing element count, the sleepers deformations and maximum stresses will converge. In addition to the deformations and stress, a modal analysis will also be performed. With these results the most efficient sleeper models can be found and this is the basis for a full multiple sleeper model.

The resulting models have divisions ranging from 1 division to a maximum of 4, this is the limit to where the models are still solvable by the available computational equipment. The element count is a good indication for the required computational time and required memory. More elements cause the element matrix to be larger and more difficult to invert and thus solve. In combination with the two reinforcement models, the total amount of simulations becomes 8. Table D.1 gives an overview of all the analysis including the element counts of each model. It is easy to see that the element count, and thus computational time, increases significantly with each division step.

Table D.1: Overview of the several static analysis with their basic parameters. Circular and octagonal refer to the used reinforcement modelling method.

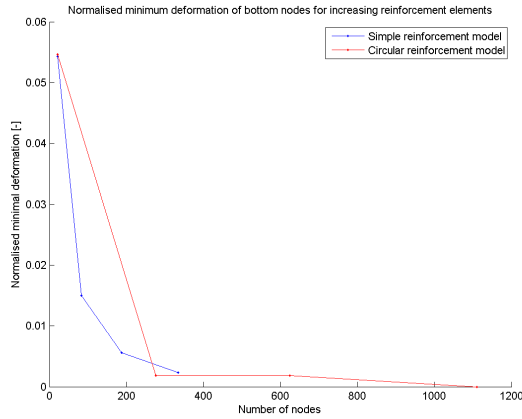
Sleeper type	material	reinforcement elements	Total element count		Sleeper element count	
			octagonal	circular	octagonal	circular
202	HDPE	1 Division	9820	9820	1956	1956
202	HDPE	2 Divisions	40676	170558	30960	156448
202	HDPE	3 Divisions	164937	772023	150642	743478
202	HDPE	4 Divisions	506139	2369507	483144	2313544

### D.1 CONVERGENCE

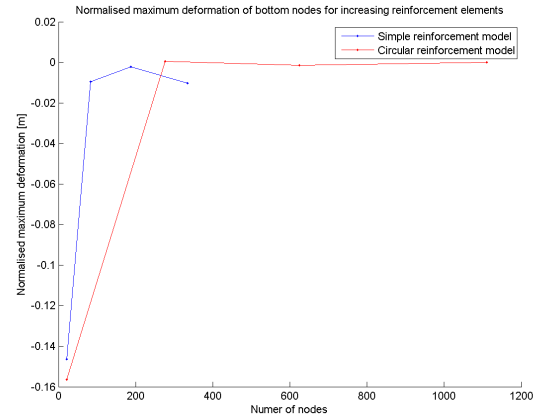
For several cases the maximum and minimum deformations of the model are calculated. The results are shown in figure D.1a and D.1b for increasing node count (the node count is used as substitute for the element count). As can be seen, the deformations converge. It is also clear that the circular reinforcement is more accurate compared to the octagonal mesh. At least the circular reinforcement quickly converges, where the octagonal reinforcement needs more elements to get to the same value.

The models frequency modes are also compared to each other. As the mass of the models does not significantly change the results are not expected to differ a lot from each other. As figure D.3 shows, the correspond-

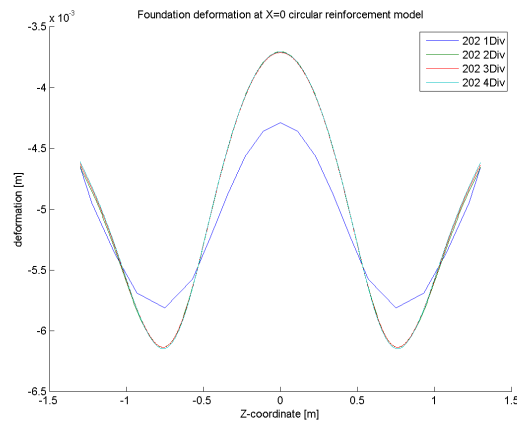
ing frequencies correspond quite nicely except for one sleeper type. The 1 division model is the odd one out. The explanation is simple, as the observed modes are the bending modes, the lengthwise distribution of elements has a large influence on the result. For example a beam consisting of a single element does not have a bending mode at all, as it is not capable of bending. The conclusion is that the single division model has not enough elements along its length to describe the bending modes in an accurate fashion. The large difference in elements is clearly visible in the model.



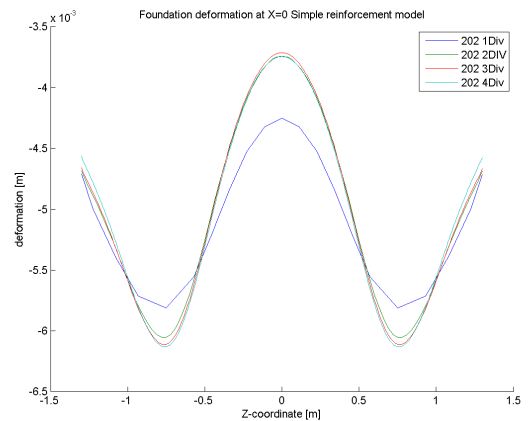
(a) Overview of the minimal displacement in the sleeper.



(b) Overview of the maximum displacement in the sleeper.



(a) Overview of the foundation nodes displacement in the sleeper for a octag-



(b) Overview of the foundation nodes displacement in the sleeper for a circular reinforcement.

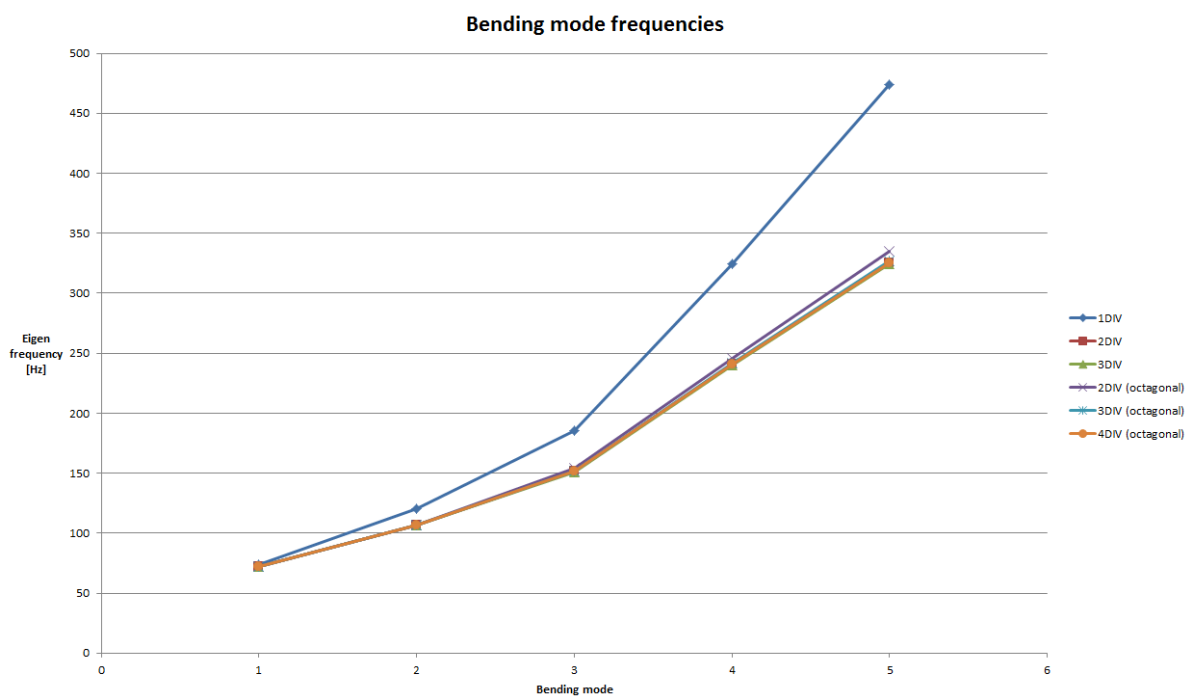


Figure D.3: Overview of the modal frequencies of the first bending mode for each analysis.



# E

## BAD FOUNDATION, INFLUENCE OF PARAMETERS

The standard constraints of a railway track are naturally favourable, with tamped ballast and a high foundation stiffness below the rail seat. This appendix describes the method used to create a deteriorated foundation. Two parameters  $A$  and  $C$  are used to create several possible foundation constraints, ranging from stiff centre loading to stiff supported edges.

### E.1 SIMULATING A BAD FOUNDATION

If sleepers are correctly tamped, the ballast stiffness is the highest directly in the tamped area. Under normal conditions this is directly done below the rail seats. This support condition does not cause rotation of the base plate under normal operating conditions, as shown in section 3.4. There are however cases where the ballast support can be disadvantageous and then subsequently active loads can cause rotations. To see what the influence of these 'bad foundations' are, examples of bad foundations have to be examined.

The chosen modelling of the foundation is as follows: two parameters can be tuned to change the foundation properties, being the length of a middle sections and a stiffness multiplier for that section. The first parameter called  $A$ , is a percentage of the sleeper length.  $A$  defines a centre part of the sleeper, symmetric around the middle of the sleeper (E.3). The second parameter called  $C$ , is a multiplier that determines the difference in magnitude between the middle section and the outer parts (E.4). A visual representation is given in figure E.1.

$$L_{\text{sleeper}} = 2 \cdot L_{\text{edge}} + L_{\text{centre}} \quad (\text{E.1})$$

$$L_{\text{edge}} = \frac{1}{2} \cdot L_{\text{sleeper}} \cdot (1 - A) \quad (\text{E.2})$$

$$L_{\text{centre}} = L_{\text{sleeper}} \cdot A \quad (\text{E.3})$$

$$k_{\text{element}_{\text{mid}}} = k_{\text{element}_{\text{edge}}} \cdot C \quad (\text{E.4})$$

Where:

$L_{\text{edge}}$  = length of an outer 'edge' section

$L_{\text{centre}}$  = length of the inner section

$A$  = percentage of sleeper length that determines the size of the (symmetric) center section

$C$  = multiplier of centre section with respect to the outer sections

Aside to the parameters that can be changed, there is the foundation stiffness  $k_d$ . To keep the total foundation stiffness constant, the edge and middle section stiffnesses have to be adjusted. Normally,  $k_d$  is divided by the amount of nodes and that results in an equal stiffness per node, all based on the concept of summation of parallel springs:  $k_{\text{parallel}} = k_1 + k_2 + \dots + k_n$ . In equation E.7 the calculation of  $k_{d_{\text{edge}}}$  and  $k_{d_{\text{mid}}}$  and there respective element stiffnesses are calculated.

$N_{\text{bottom nodes edge}}$  and  $N_{\text{bottom nodes middle}}$  follow from the model and calculated lengths  $L_{\text{edge}}$ ,  $L_{\text{center}}$  and differ per used element size. The way the element stiffness is calculated is procedurally the same as in equation 4.5. Note that the individual  $k_d$ 's are regarded as being springs in parallel which is an approximation of the real situation, where the sleeper and foundation are not infinitely stiff. The resulting expressions that show how  $k_d$  is related to the middle and two outer parts are:

$$k_d = 2 \cdot k_{d_{\text{edge}}} + k_{d_{\text{mid}}} \quad (\text{E.5})$$

$$k_d = 2 \cdot k_{\text{element}_{\text{edge}}} \cdot N_{\text{bottom nodes edge}} + k_{\text{element}_{\text{mid}}} \cdot N_{\text{bottom nodes middle}} \quad (\text{E.6})$$

Substituting E.4 into E.6 results in:

$$\begin{aligned} k_d &= 2 \cdot k_{\text{element}_{\text{edge}}} \cdot N_{\text{bottom nodes edge}} + k_{\text{element}_{\text{edge}}} \cdot C \cdot N_{\text{bottom nodes middle}} \\ &= k_{\text{element}_{\text{edge}}} \cdot (2 \cdot N_{\text{bottom nodes edge}} + C \cdot N_{\text{bottom nodes middle}}) \rightarrow \\ k_{\text{element}_{\text{edge}}} &= \frac{k_d}{2 \cdot N_{\text{bottom nodes edge}} + C \cdot N_{\text{bottom nodes middle}}} \end{aligned} \quad (\text{E.7})$$

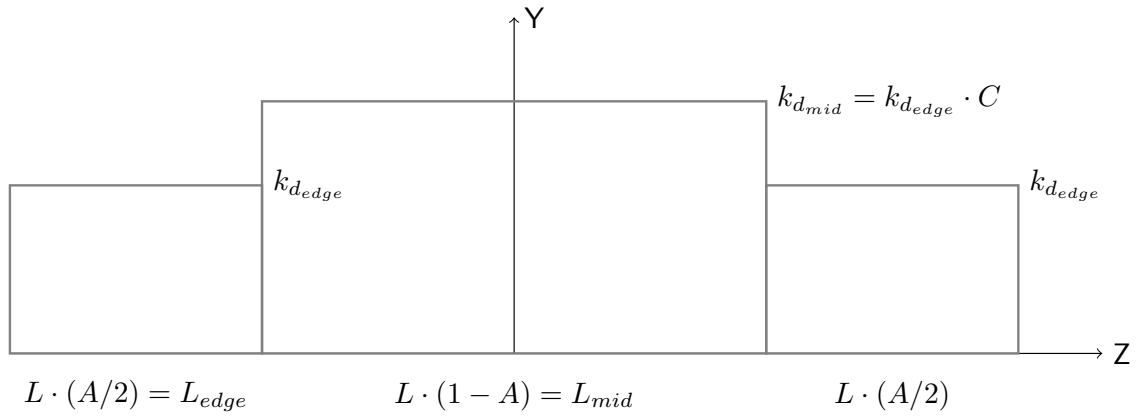


Figure E.1: Modelling of changing foundation parameters.  $k_d = \text{constant}$

### E.1.1 EXPECTATIONS

The behaviour of the chosen modelling results in some effects that are possibly a bit counter-intuitive. Say the starting position is for the value  $A = 0$ , then there is no contribution by the middle sections and only by the side-sections. This means that the foundation is equal to the standard situation with equal stiffness at every location. The other extremity is when  $A$  reaches 1 and the middle section spans the whole sleeper. As the total stiffness should be still equal to  $k_d$ , this also results in the standard situation.

Figure E.2 shows a graphical interpretation of individual element stiffness when changing the value of  $A$ . It shows the changing stiffness at three locations, the start of the base plate (as seen from the middle) the centre and outer edge. The jump represents the change from edge section to middle section.

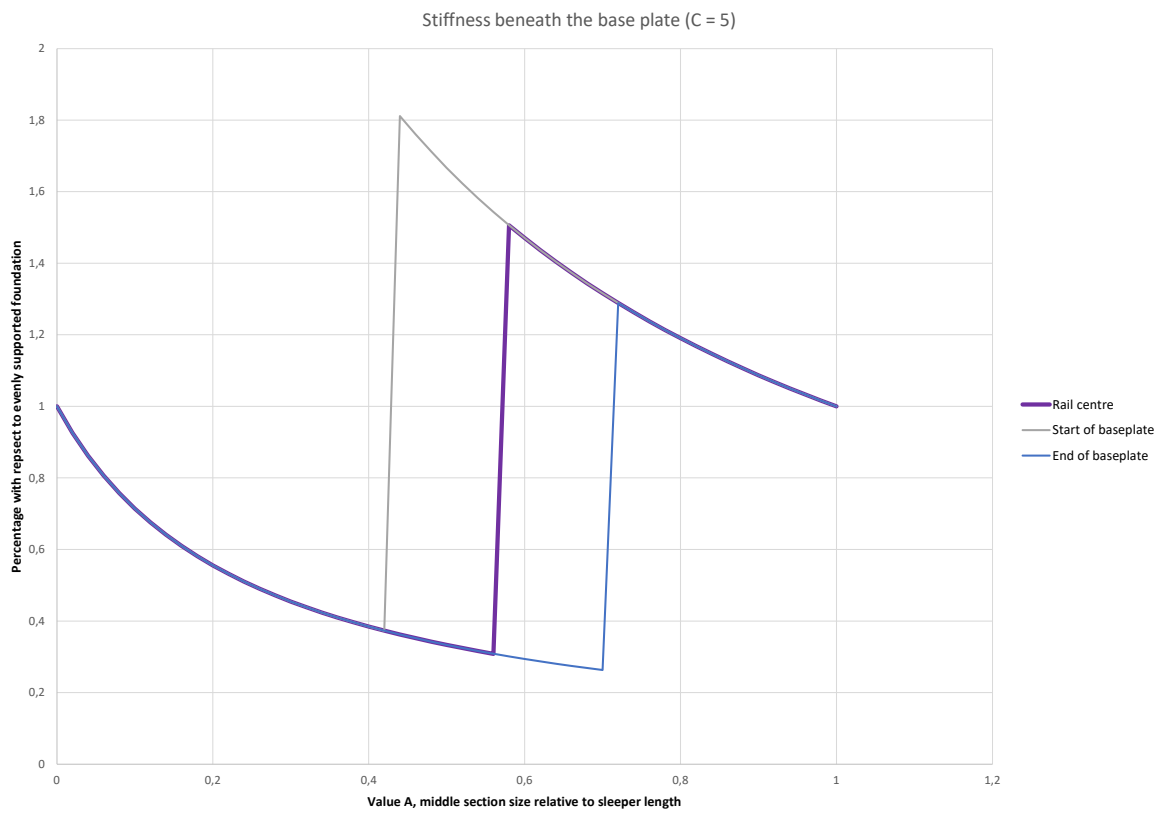


Figure E.2: Relative element stiffness ( $k_{\text{element}}$ ) at three locations beneath the base plate, with respect to a distributed foundation for increasing  $A$ . The  $C$ -value is chosen arbitrarily.



# F

## GAUGE WIDENING

This appendix addresses some common gauge change mechanics. The gauge ( $s$ ) of a railway track is analogue to the track width, it is considered as the distance between both rails. More specific, the gauge is the distance between the rails measured 14 mm below the top of the rail. Many different gauge distances exist in the world, but the most common gauge, and therefore called standard gauge is the 1435 mm track width. In that case the centres of both rails are exactly 1.5 m apart from each other.

A consistent track gauge is essential for a railway under current track speeds. Any change in gauge, be it a decrease or an increase, has a negative effect on the usability. Next to the wheel conicity  $\gamma$  and the wheel radius  $r$ , the track width is a parameter in the self-steering mechanism of the railway system. It works mainly due to the conicity of the wheels that change the radii of both wheels in such a manner that the wheel automatically steers itself to the middle of the track. The self-steering makes that the train swings slightly from left to right while traversing over the rails and can follow curves. This swinging motion from left to right is called the 'hunting motion', it has a wavelength  $\lambda$ . Klingel's formula describes the relation between the gauge and wavelength [1]:

$$\lambda = 2\pi \sqrt{\frac{rs}{2\gamma}} \quad (\text{E.1})$$

Where:

$r$  = wheel radius

$\gamma$  = conicity of the wheels

$s$  = track gauge

From Klingel's formula it is easy to understand that a decrease in gauge ( $s$ ) lowers the wavelength  $\lambda$ . The sideways hunting motion gets more unstable, the lateral accelerations increase and the comfort therefore decreases. Lastly as the wheels are closer to the rail, flange contact occurs, and at this moment the hunting motion becomes unstable. Also the flange-rail contact increases the wear on the wheels and rails. So when a decrease in track width is quite disastrous, is an increase not the opposite? Well, the increase in wavelength is sort of positive and increases the comfort. The main problem is the increased probability that derailment occurs which, if it happens, is more damaging than effects caused by gauge narrowing.

Both effects, gauge widening and narrowing, are unwanted. An extra negative influence is when the gauge is not constant and fluctuates over the length of the track. Any change in track conditions alters the behaviour of the vehicle and induces extra vibrations and forces on the track structure. So keeping a track system as homogeneous as possible is a key part of railway engineering.

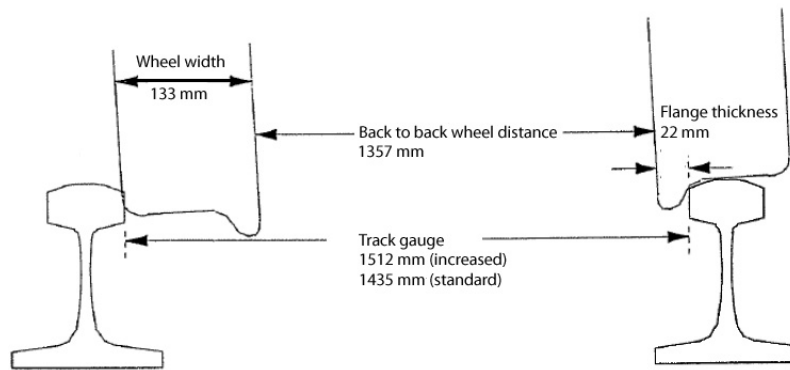


Figure F.1: Track gauge values for a track with increased width, such that a wheel is able to fall in between the rails. Calculation in E.6.

## F.1 PRACTICAL LIMIT

The practical limit which a gauge can widen is easy to understand. The edge case is when both rails are so far apart that one of the wheels is not supported by a rail anymore. In other words, the complete wheel set falls between the rails. In figure F.1 a graphic representation of this situation is given.

To calculate the limit state several vehicle parameters have to be known, this includes: the axle distance, wheel width and flange width. These values are found in the European regulations: 'Technical Specifications for Interoperability', in short TSI 's. This regulation is to homogenise the vehicle parameters used in Europe. The rolling stock ( RST ) section mentions wheel-wheel distances  $> 800$  mm diameter wheels <sup>1</sup> and the standard 1435 mm gauge [53]. Figure F.1 shows the location of each value as well the calculated resulting limit state. The values as used in the TSI are:

$$\text{Back to back wheel distance:} \quad 1357 \leq A_r \leq 1363 \text{ mm} \quad (\text{E.2})$$

$$\text{Front to front distance, } S_r = A_r + S_{d_{\text{left}}} + S_{d_{\text{right}}}: \quad 1410 \leq S_r \leq 1426 \text{ mm} \quad (\text{E.3})$$

$$\text{Flange thickness:} \quad 22 \leq S_d \leq 33 \text{ mm} \quad (\text{E.4})$$

$$\text{Wheel width:} \quad 133 \leq B_r \leq 145 \text{ mm} \quad (\text{E.5})$$

The ultimate limit state for the gauge change is calculated by using the minimal values of these parameters. Resulting in the following limit gauge  $G_{\text{max}}$  and ultimate (minimal) gauge widening value  $\Delta G_{\text{u}}$ :

$$G_{\text{max}} = B_{r_{\text{min}}} + A_{r_{\text{min}}} + S_{d_{\text{min}}} = 133 + 1357 + 22 = 1512 \text{ mm} \quad (\text{E.6})$$

$$\Delta G_{\text{u}} = G_{\text{max}} - G = 1512 - 1435 = 77 \text{ mm} \quad (\text{E.7})$$

## F.2 REGULATIONS ON GAUGE CHANGE

The regulations considering gauge widening can be considered as being the serviceability limit state of the track. Current regulations stated by the European union in NEN-EN 13848-5 [54], have limitations on the allowable gauge in absolute sense and on gauge change over length. In table F.1 the absolute values are shown, the gauge change values are not further looked at. The three categories depend on the type of action that has to be taken. ProRail has its own limits gathered in OHD00022 <sup>2</sup> [55]. The stated limits are of course compliant to the European rules, only the set values by ProRail are more strict and there are only two categories specified. Lastly ProRail uses different speed categories. In table E.2 the Dutch gauge limits are shown.

Considering the first categories that are reached, the European action limit and the ProRail intervention limit, the European limit is  $-6$  mm to  $+26$  mm. ProRail has set these limits to  $-5$  mm to  $+20$  mm. All limits apply to the track gauge, which means that any wear of the railhead, around 14 mm below the railhead influences

<sup>1</sup>The standard wheel size is about 1 m so this value holds for all heavy rail equipment.

<sup>2</sup>OHD stands for "Onderhoudsdocument", translated: maintenance document.

the measured gauge. The latter is not a major influence on straight track, but could be on curves. The reason that the decrease of track gauge has such stricter requirements is due to the fact that a smaller track leads to a less stable hunting motion. The value that is used further in this research, is the Prorail intervention limit of +20 mm.

Table F1: European gauge widening limits. Nominal track gauge to mean track gauge over 100 m (NEN-EN 13848-5 [54]).

speed (km/h)	action limit (mm)		intervention limit (mm)		immediate action limit (mm)	
	minimum	maximum	minimum	maximum	minimum	maximum
$V \leq 80$	-7	25	-9	30	-11	35
$80 < V \leq 120$	-7	25	-9	30	-11	35
$102 < V \leq 160$	-6	25	-8	30	-10	35

Table F2: Gauge widening limits set by ProRail. Incidental local gauge widening limits (ProRail [55]).

speed (km/h)	intervention limit (mm)		safety limit (mm)	
	minimum	maximum	minimum	maximum
$V \leq 40$	-6	26	-9	35
$40 < V \leq 160$	-5	20	-8	30

### F.3 GAUGE WIDENING SOURCES

César Bastos [56] provides a summary on some gauge widening sources and their expected effect. The list is not said to be an exhaustive list off every component, but provides a good starting point. Table E3 shows the table as published, it is based on American regulations and concrete sleepers, however the sources are not expected to be very different.

It is not difficult to imagine several contributions that add up to the previously established ProRail limit of 20 mm. From the five possible options in table E3, two are sleeper related, two are rail related and the remaining (Sleeper rail seat deterioration tolerance) is a combination between fastening deterioration and sleeper deterioration. Those sleeper and non-sleeper related sources are discussed separately in the next sections and the rail seat deterioration appears in both sections.

Table F3: Estimate of track gauge increase (for concrete sleepers) due to various track infrastructure conditions. From César Bastos [56].

Track infrastructure condition	Estimated maximum track gauge increase in mm.
Concrete sleeper manufacturing tolerance	1.59
Sleeper rail seat deterioration tolerance	28.70
Rail manufacturing tolerance	3.18
Rail Wear tolerance	15.24
Maximum tolerable rail lateral movement allowed by fastening systems	12.7

#### F.3.1 NON SLEEPER-RELATED SOURCES

Three contributions to gauge widening are discussed:

- The rail manufacturing tolerance
- The rail wear tolerance
- The fastening system (part of sleeper rail seat deterioration tolerance from table E3)

The rail manufacturing tolerance allowed by ProRail is equal to the NEN-EN 13674-1 [52]. The mentioned limits are not directly relatable to gauge widening, but are in the order of magnitude of 0.5 mm and two contribution factors with some link to gauge widening can be distinguished: railhead width and rail asymmetry.

Those are not going to be discussed in further detail, but the stated 3.18 mm is therefore regarded a high value in comparison with the European regulations.

The second influencing factor on the measured track gauge is the wear of the rail head. This value is large with respect to the other contributions. In OHD00001 the limits on vertical wear of the railhead are specified. Those limits are 10 to 16 mm depending on the track speed [57]. The higher the track speed, the less wear is allowed. High railhead wear is mainly of importance in curves where there is regular flange contact and on these locations special engineered rail profiles can be used to limit or distribute the wear over the profile [1].

Another source of gauge widening is the horizontal displacement of the fastening system. This could be between the base plate and rail or between the base plate and the sleeper. The Eurocode specifies that the maximum static influence of any fastening system on the track gauge should be within 1 mm [58, 59]. Chen and Andrawes [60] have done research on the deflections inside the fastening system for a concrete sleeper track. The measured deflections of the rail web are in the order of 1.5 mm.

Contribution to gauge widening by non sleeper-related sources is included in any gauge measurement as the absolute displacement of the rail is measured. This makes above contributions less important to this specific research than any sleeper related gauge widening. As a result the influence of the wear values and fastening system are considered static values and not comprehensively discussed.

### F.3.2 SLEEPER-RELATED SOURCES

The sleeper itself has some properties that influence the maintaining of gauge. One has to do with the base plate connection. A less stiff material such as plastic makes it harder to fixate the baseplate without any room for deformation. Research has been done on the holding of spikes Lampo et al. [61] and Lotfy et al. [62] showed that there are no issues for systems with pre drilled holes. Lotfy and Issa [63] evaluates the horizontal railhead displacement due to repeated loading of an HDPE sleeper. The resulting maximum horizontal displacement of the railhead is about 25.4 mm, this is quite significant compared to the previously mentioned limit values of 26 mm. The increase in deflection due to the repeated loading however is in the order of 4 mm after 3 million cycles. Thus the main displacement is elastic and due to the magnitude of the loading itself and not due to the load periodicity. This means that the static deformation is the main parameter to consider.

Temperature can also influence the gauge. As an example, reinforced concrete sleepers could shrink due to drying of the concrete and make the gauge to narrow. As van Belkom [28] mentions, plastic on itself has a high thermal expansion which needs to be constraint by applying reinforcement of some kind. ProRail addresses this issue in their specification for plastic sleepers and issues a maximum increase of track gauge of 1 mm which roughly corresponds to a thermal expansion coefficient less than  $2.3 \cdot 10^{-5} / K$  [55].

The other deformations due to loads are of main interest in this research. Some research has been done for concrete sleepers, but there is not much research done on plastic sleepers. Some focus on the deformation of the rail to examine rail roll for example [60] and some focus on the lateral strength of the track frame thus mainly the lateral resistance of the track / sleepers [64, 65].

Bastos et al. [66] assessed concrete sleepers with different foundation parameters. The maximal found gauge widening value is 2.62 mm. This value occurs in case of centre supported concrete sleepers and when loaded by a 89 kN load per rail seat, which is about 50% of a freight car axle load. This researched showed that the centre supported sleepers experience a lot more gauge widening than when the sleeper was supported directly below the rail seat (as is the standard). Therefore also the foundation parameters are changed to investigate their influence on the gauge.

## F.4 GAUGE WIDENING LIMITS

To be able to chose a limit state to what the FEM model has to comply, the factors mentioned in F.3.2 are subtracted from the limit values, to get a value for the limit gauge widening. Note that the list with influencing factors is not limited to the ones mentioned here.

$$\begin{aligned}
 \Delta G_{\text{wear}} &= 16 \text{ mm} \\
 \Delta G_{\text{thermal expansion}} &= 1 \text{ mm} \\
 \Delta G_{\text{fastening}} &= 1 \text{ mm} \\
 \Delta G_{\text{sleeper factors}} &= \Delta G_{\text{wear}} + \Delta G_{\text{thermal expansion}} + \Delta G_{\text{fastening}} = 16 + 1 + 1 = 18 \text{ mm}
 \end{aligned}
 \tag{E.8}$$

The different possible limit states are combined in table F.4.

Table F.4: Limit state overview.

Type of limit state	Gauge widening limit in mm.
Maintenance (mls)	20
Serviceability (sls)	26
Ultimate (uls)	77

combined with F.8 this results in the following maximum sleeper deformations that are possible without exceeding the limit state values.

$$\Delta G_{S_{mls}} = 20 - 18 = 2 \text{ mm} \quad (\text{F.9})$$

$$\Delta G_{S_{sls}} = 26 - 18 = 8 \text{ mm} \quad (\text{F.10})$$

$$\Delta G_{S_{uls}} = 77 - 18 = 59 \text{ mm} \quad (\text{F.11})$$

As the ultimate limit state is a lot larger than the usability limit state, it is not expected that sleeper deformations are in that deformation range. And if it does, the sleeper certainly does fit the brief. Therefore a reasonable value is expected to be the serviceability limit state and the value of 8 mm is the threshold value used.

## F.5 FINITE ELEMENT RESULTS

As shown in section 3.4 the expected gauge change due to vertical loading is small due to the direct support below both rails. The simulation with degraded foundation support could however result in an increase of gauge. The multi-sleeper model is used for this method to remove the influence of the boundary conditions. This also spreads the loading over the sleepers so the reduced loading conditions do not have to be used, as in the single sleeper models. Only two multiple sleeper models are considered, a model with 201 PE sleepers and a model with 202 HDPE sleepers. Both consist of 19 sleepers and with a centre to centre spacing of 600 mm, this means that the whole system spans from  $-6 \text{ m}$  to  $6 \text{ m}$ . The results are shown in figure F.2 and show that the maximum widening is less than 2.5 mm. This is lower than the maintenance limit state and it is expected that many of the deformation is temporary. It can be concluded that the limit of 8 mm is not exceeded, even for ultimate loads. The next question becomes how many of the deformations are plastic or creep related and how do they increase over time.

An other case that has been examined is the behaviour when the foundations are not perfect. A stiffer middle section provides a negative effect on the gauge. The foundation parameters are changed in the following manner to model bad supports: the middle part is decreased in size until an extreme lowest value of  $A = 0.1$  (10% of  $L$ ). And the foundation multiplier  $C$  is increased from 1.2 to 6. The middle part of this bad foundation is therefore always stiffer than the outside edges. Something that is not obligatory, but is just done to limit the cases. In figure F.5 the results are shown. The maximum gauge change follows from the node displacements of the model and that is shown for varying foundation stiffnesses and lengths. The absolute maximum gauge change that is recorded is about 6 mm. This happens when the multiplication factor  $C$  is the largest, which is to be expected and when the parameter  $A$  is 0.5. The decreasing gauge change value when increasing the supported foundation size, can be explained by the fact that the total  $k_d$  of the whole sleeper is kept the same. This can be illustrated by looking at the limit cases. If  $A = 0$  the situation is equal to a basic configuration where there are no differences with respect to the standard simulations. The other edge case where  $A = 1$  is equal to this same configuration as the 'stiffer' part has the same dimensions of a whole sleeper, but the  $k_d$  is also the same as in the standard case. In cases where the total foundation stiffness is changed the results are different when increasing the (un)supported area.

One load case is considered, which is load case 4, a somewhat less realistic scenario where the full load on a single sleeper is 100 % of the axle load, 110 kN (equation 3.1). The calculated values from the FEA, including the previously mentioned maximum of 6 mm are combined in table F.5. The table shows that even for very uneven foundations, the displacements are reasonable and still are below the determined maximum of 8 mm (see F.4). The linear behaviour of the model is clearly visible in the deformations between the load cases, where the displacements are doubled when loaded by twice the amount of force in the second load case.

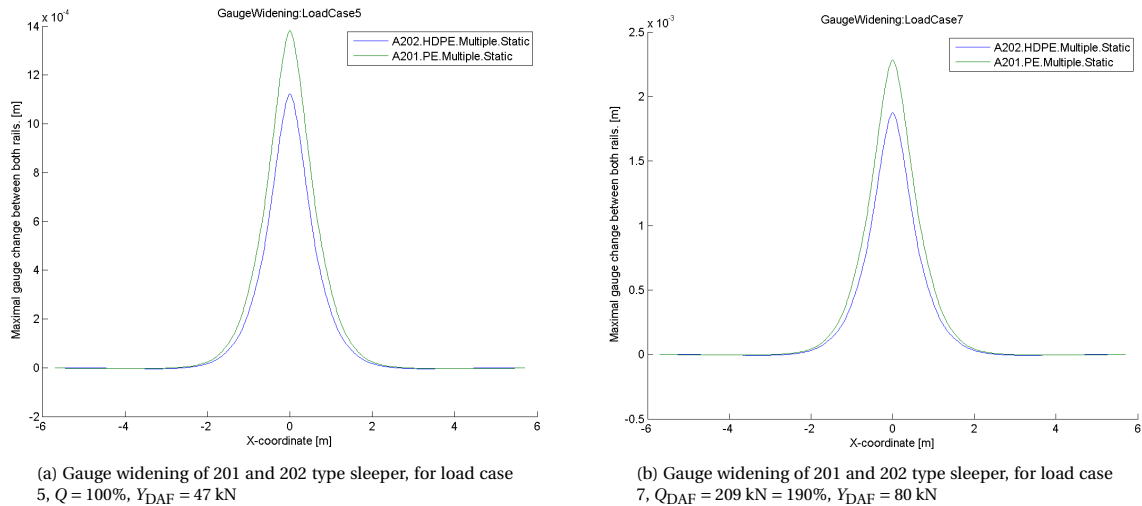


Figure E2: Gauge widening of 201 and 202 type sleeper, for two load cases.

Table E5: Maximum gauge change for load case 3 and 4, when the middle half of the sleeper is supported by a stiffer foundation ( $A = 0.5$ ).

Center multiplier	Load case 3	Load case 4
$C = 1$ (standard foundation)	-0.107	-0.213 mm
$C = 2$	0.683	1.351 mm
$C = 4$	1.634	3.238 mm
$C = 5$	1.971	3.905 mm
$C = 7.5$	2.595	5.142 mm
$C = 10$	3.002	6.003 mm

Table E6: Sorted gauge widening values for two load cases on a single sleeper model. All values are in mm.

Gauge widening [mm]	LoadCase5 ( $Q = 100\%$ , $Y = 47$ kN)	LoadCase7 ( $Q = 190\%$ , $Y = 47$ kN)	Difference
202 HDPE	1.123	1.382	0,259
201 PE	1.875	2.285	0.410

## F.6 CONCLUSION

The conclusion of the FEM simulations is that a under specific (degraded) foundation circumstances the gauge is increased significantly. With fully supported sleeper the order of gauge widening is around 2.5 mm under high vertical and lateral loads. If the foundation is further degraded until it is only centre supported, the gauge increase to 6.0 mm under only vertical loading, but for the same exceptional vertical loading. So the stiffer centre does increase the gauge quite significantly, but still within the set and safe margins. This means that a deteriorated track is expected to still hold the gauge pretty decent. One important point to notice is that material creep is not taken into account. And it is also advised to have good measuring methods available, so bad sections can be tracked and repaired within reasonable time instead of letting the foundation deteriorate further to become more and more dangerous. In the end, the behaviour of the sleepers with regard to gauge change, is relatively easy to measure in situ with a measurement train. This allows for frequent testing under working conditions and therefore provide valuable and accurate data.

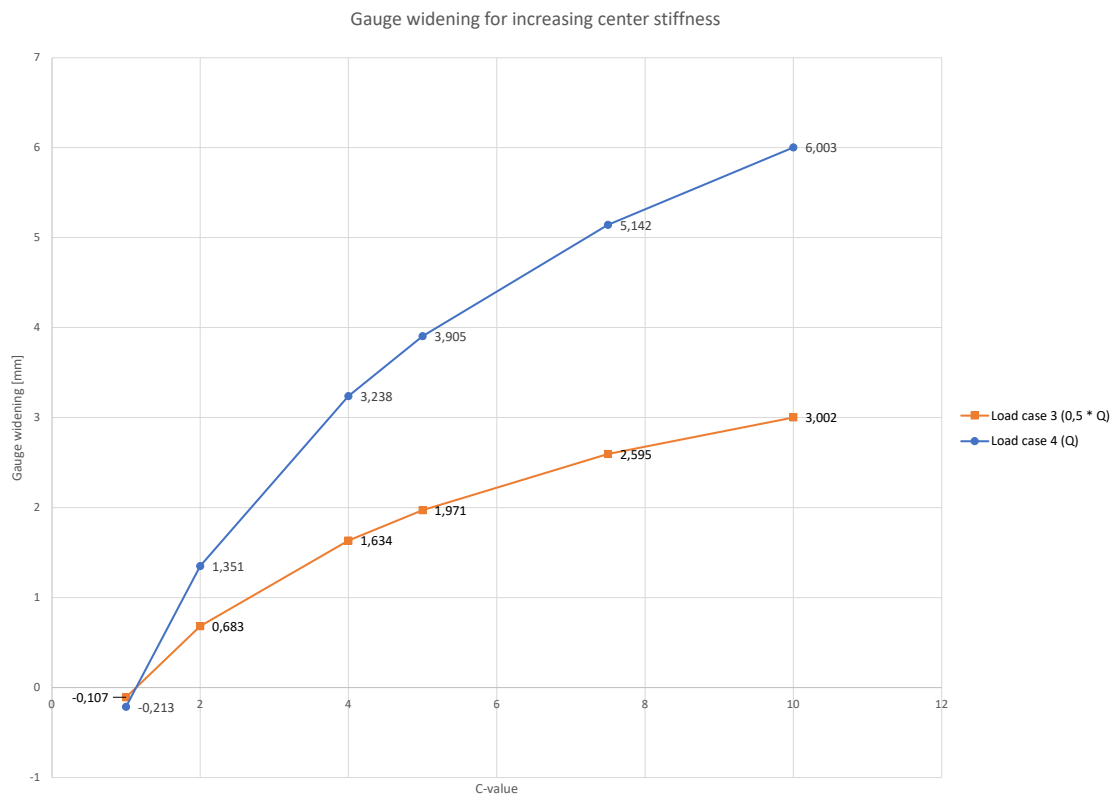


Figure E3: Gauge widening for increased C-values. A = 0.5

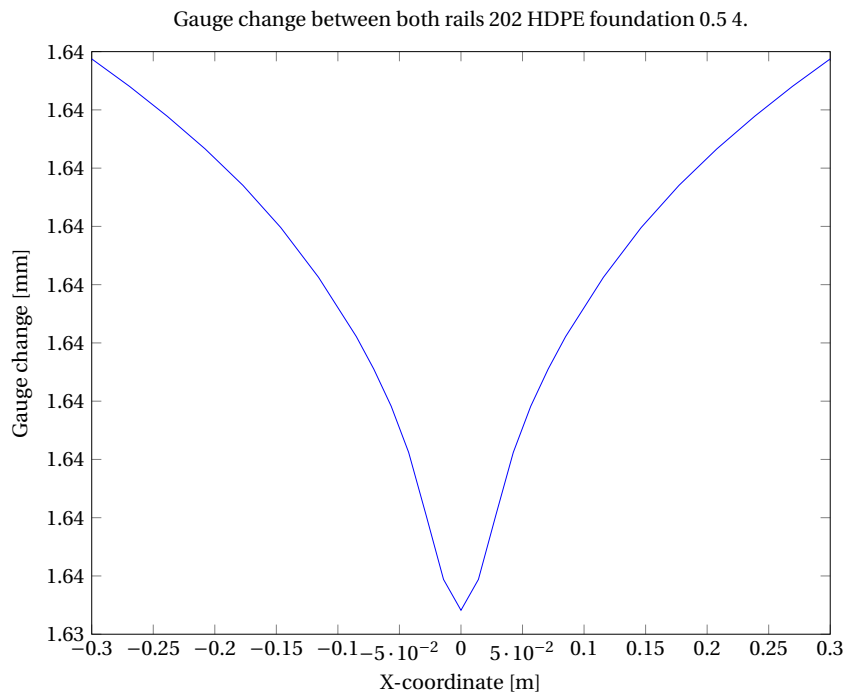


Figure E4: Gauge widening with bad foundation for load case 3. A = 0.5, C = 4.

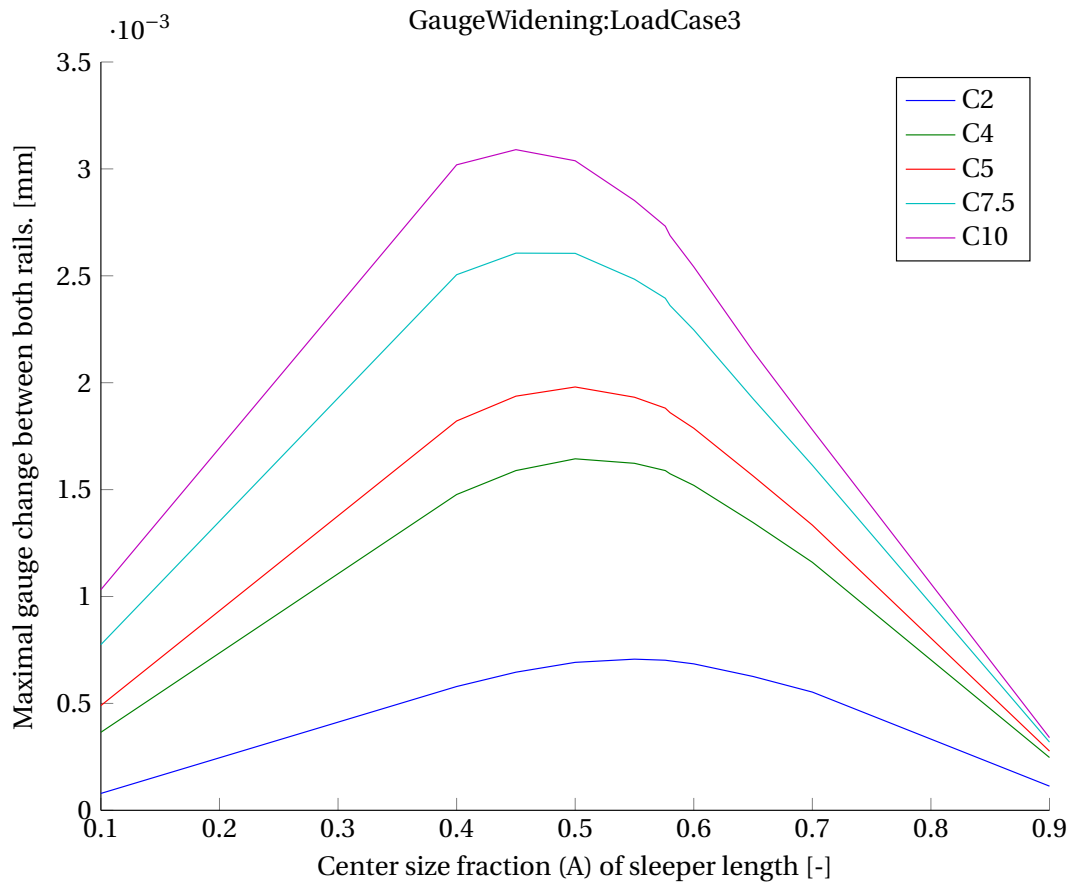


Figure E5: Gauge widening with bad foundations for different stiffer centres.

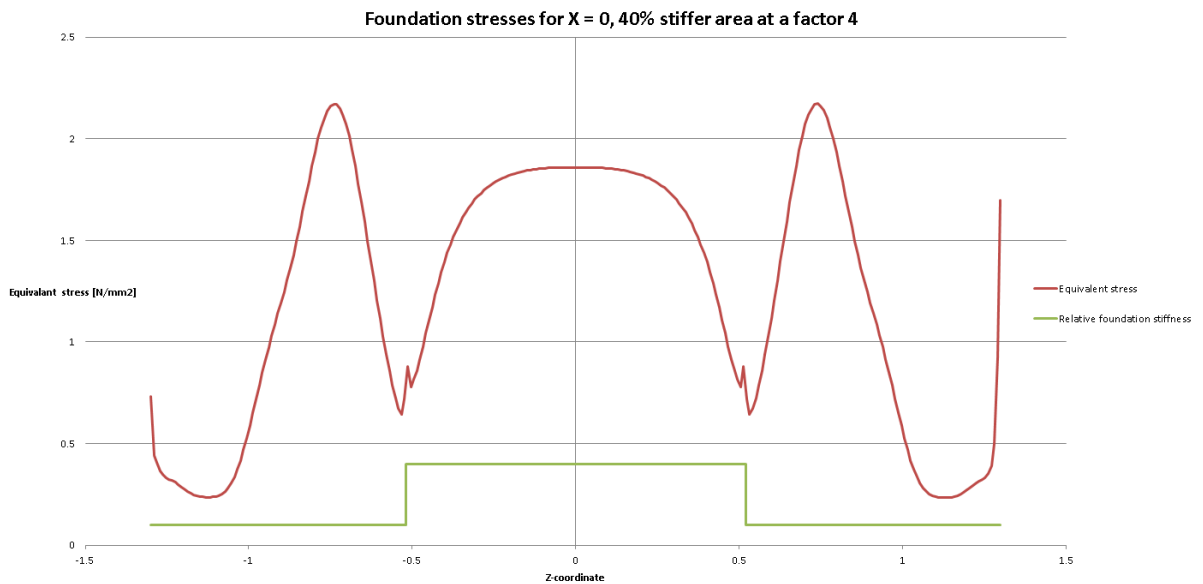


Figure E6: Example of foundation stresses where the middle 40% (1040 mm) is supported by a 4 times stiffer foundation.

## BIBLIOGRAPHY

- [1] C. Esveld. *Modern Railway Track*. MRT-Productions, second edition, 2001. ISBN 9789080032439.
- [2] Sakdirat Kaewunruen and Alex M. Remennikov. Dynamic flexural influence on a railway concrete sleeper in track system due to a single wheel impact. *Engineering Failure Analysis*, 16(3):705–712, 2009.
- [3] I. Lotfy, M. Farhat, M. A Issa, and M. Al-Obaidi. Flexural behavior of high-density polyethylene railroad cross-ties. *Proc IMechE Part F: Journal Rail and Rapid Transit*, 230(3):813–824, 2016. doi: 10.1177/0954409714565655.
- [4] Pizhong Qiao, Julio F Davalos, and Michael G Zipfel. Modeling and optimal design of composite-reinforced wood railroad cross-tie. *Composite structures*, 41(1):87–96, 1998.
- [5] A. Manalo, T. Aravinthan, W. Karunasena, and A. Ticoalu. A review of alternative materials for replacing existing timber sleepers. *Composite Structures*, 92(3):603–611, 2010.
- [6] Amir Ghorbani and Seçkin Erden. Polymeric composite railway sleepers. *Uluslar ArasibRayli Sistemler Muhendisligi Sempozyumu (ISERSE'13)*, pages 9–11, 2013.
- [7] Clifford E Bonnett. *Practical Railway Engineering; chapter Track*. Imperial College Press, 2005.
- [8] ProRail. OVS00056-5.1-V010 - Baan en Bovenbouw Spoor in ballast. Design manual, ProRail, 2017.
- [9] Gerard Van Erp and Malcolm Mckay. Recent australian developments in fibre composite railway sleepers. *Electronic Journal of Structural Engineering*, 13(1):62–6, 2013.
- [10] Wahid Ferdous, Allan Manalo, Gerard Van Erp, Thiru Aravinthan, Sakdirat Kaewunruen, and Alex Remennikov. Composite railway sleepers—recent developments, challenges and future prospects. *Composite Structures*, 134:158–168, 2015. doi: <https://doi.org/10.1016/j.compstruct.2015.08.058>.
- [11] ProRail. SPC00009-V002 - Hardhouten dwarsliggers, wisselliggers en brughouten. Product specification, ProRail, 2006.
- [12] Thomas Nosker, Richard Renfree, Jennifer Lynch, Mark Lutz, Barry Gillespie, Richard Lampo, and Kenneth E Van Ness. A performance-based approach to the development of a recycled plastic/composite cross-tie. Technical report, SOCIETY OF PLASTICS ENGINEERS INC, 1998.
- [13] J.T.K. Quik, E. Dekker, and M.H.M.M. Montforts. Safety and sustainability analysis of railway sleeper alternatives: Application of the safe and sustainable material loops framework. 2020. URL <https://www.rivm.nl/bibliotheek/rapporten/2020-0126.pdf>.
- [14] EN 13145:2001+A1:2011. Railway applications - track - wood sleepers and bearers. Legal rule or regulation, CEN, 2011.
- [15] 13230-6:2020 E. Railway applications - track - concrete sleepers and bearers - part 6: Design. Legal rule or regulation, CEN, 2020.
- [16] P. Koch. Frequentie en trillingseigenschappen plastic dwarsligger. Bsc thesis, Delft University of Technology, 2018.
- [17] M.A.J.P. van Dam. Kunststof dwarsliggers in spoorconstructies – Buiggedrag en Klemmingssysteem. Bsc thesis, Delft University of Technology, 2018.
- [18] Vít Lojda, Aran van Belkom, and Hana Krejčíříková. Investigation of the elastic modulus of polymer sleepers under a quasistatic and cyclic loading. *Civil and Environmental Engineering*, 2019. doi: <https://doi.org/10.2478/cee-2019-0016>. URL <https://content.sciendo.com/downloadpdf/journals/cee/15/2/article-p125.pdf>.

- [19] Neil F Doyle. Railway track design: a review of current practice. Technical report, Bureau of transport economics Canberra, 1980.
- [20] Thomas Nelson Erke Wang and Rainer Rauch. Back to elements-tetrahedra vs. hexahedra. In *Proceedings of the 2004 international ANSYS conference*, 2004.
- [21] L. J. H. van der Drift. 3- en 4-puntsbuigproef van een kunststof dwarsligger. Bsc thesis, Delft University of Technology, 2020. URL <http://resolver.tudelft.nl/uuid:f6c52405-a7cf-434e-8852-291864bedc45>.
- [22] Lankhorst Engineered Products. Composite railway sleepers advantages, 2020. URL <https://www.lankhorstrail.com/en/composite-railway-sleepers>.
- [23] M. van Gompel. Kunststof dwarsligger wint terrein in europa, 2016. URL <https://www.spoorpro.nl/spoorbouw/2016/05/10/kunststof-dwarsligger-wint-terrein-in-europa/>.
- [24] Dr. M.H. Kolstein. *Fibre-reinforced polymer (FRP) composites in structural applications*. Faculty of Civil Engineering and Geosciences, 2008.
- [25] Pavel Oblak, Joamin Gonzalez-Gutierrez, Barbara Zupančič, Alexandra Aulova, and Igor Emri. Processability and mechanical properties of extensively recycled high density polyethylene. *Polymer Degradation and stability*, 114:133–145, 2015.
- [26] Lankhorst Engineered Products BV. KLP Hybrid Polymer Switch & Crossing Sleeper. Product brochure, Lankhorst, 2014.
- [27] NEN-ISO 12856-1:2014(E). Plastics - plastic railway sleepers for railway applications (railroad ties) - part 1: Material characteristics. Legal rule or regulation, CEN, 2014.
- [28] A. van Belkom. Recycled plastic railway sleepers - analysis and comparison of sleeper parameters and the influence on track stiffness and performance. Report, Lankhorst Engineered Products, 2015.
- [29] Aran van Belkom. A simplified method for calculating load distribution and rail deflections in track, incorporating the influence of sleeper stiffness. *Advances in Structural Engineering*, 23(11):2358–2372, 2020. doi: 10.1177/1369433220911144. URL <https://doi.org/10.1177/1369433220911144>.
- [30] M. Oregui, Z. Li, and R. Dollevoet. An investigation into the modeling of railway fastening. *International Journal of Mechanical Sciences*, 92:1–11, 2015.
- [31] J.E. Garnham and C.L. Davis. 5 - rail materials. In R. Lewis and U. Olofsson, editors, *Wheel–Rail Interface Handbook*, pages 125 – 171. Woodhead Publishing, 2009. ISBN 978-1-84569-412-8. doi: <https://doi.org/10.1533/9781845696788.1.125>. URL <http://www.sciencedirect.com/science/article/pii/B9781845694128500057>.
- [32] EN 10080:2005 (E). Steel for the reinforcement of concrete - weldable reinforcing steel - general. Legal rule or regulation, CEN, 2005.
- [33] European union agency for railways. Eurocode 3: Design of steel structures - part 1-1: General rules and rules for buildings. Legal rule or regulation, CEN, 2014.
- [34] Trackelast. Trackelast datasheet fc9 rail pad, 2016. URL <http://www.trackelast.com/datasheets/Trackelast-DS-FC9-Rai>
- [35] Prof.dr. J.M.J.M. Bijen, prof.dr.ir. Ch.F Hendriks, dr.ir. A.L.A. Fraaij, and dr.ir. M. de Rooij. *Duurzame Bouwmaterialen*. Faculty of Civil Engineering and Geosciences, 2007.
- [36] J. Smid and A van Belkom. KLP-PE compound (LN 508.651 and 652). Internal product specification, Lankhorst, 2012.
- [37] J. Smid and A van Belkom. Material properties klp-hs (ln 508.679). Internal product specification, Lankhorst, 2016.
- [38] Zdenka Prochazkova. Push-out test of steel reinforcement from recycled plastic beams. Internal product specification, Lankhorst, 2013.

- [39] Zdenka Prochazkova, Alexios E Tamparopoulos, and Alfred Strauss. Push-out test of steel reinforcement from recycled plastic beams. *BETON-UND STAHLBETONBAU*, pages 169–173, 2013.
- [40] P.P.G.R.R.A. Gradin, Paul G. Howgate, Ragnar Seldén, and R. Brown. Dynamic - mechanical properties. *Pergamon Press plc, Comprehensive Polymer Science: the Synthesis, Characterization, Reactions & Applications of Polymers.*, 2:533–569, 1989.
- [41] W. Brostow. *Mechanical Properties*, chapter 24. Springer, New York, NY, 2007. doi: {[https://doi-org.tudelft.idm.oclc.org/10.1007/978-0-387-69002-5\\_24](https://doi-org.tudelft.idm.oclc.org/10.1007/978-0-387-69002-5_24)}.
- [42] Sheldon Imaoka. Analyzing viscoelastic materials. *ANSYS Advantage*, 2(4), 2008.
- [43] NEN-EN 15528. Railtoepassingen - baanvakcategoriën - aansluiting tussen belastbaarheid van voertuigen en baanvak. Legal rule or regulation, CEN, 2015.
- [44] ProRail. Netverklaring 2018, 3.3.2.2 aslast en tonmetergewicht, 2016.
- [45] Holmes, D.P. Mechanics of Materials: Bending – Shear Stress, -. URL <https://www.bu.edu/moss/mechanics-of-materials-bending-shear-stress/>.
- [46] Jaroslav Štigler. Optimal mapped mesh on the circle. In *ESSS South American ANSYS Users Conference, Florianópolis, Brazil*, pages 10–13, 2009.
- [47] Carsten Steger. On the calculation of arbitrary moments of polygons. *Munich Univ., Munich, Germany, Tech. Rep. FGBV-96-05*, 1996.
- [48] Inc. ANSYS. Combin14 - spring-damper. Technical report, ANSYS, Inc., 2016. URL [https://www.mm.bme.hu/~gyebro/files/ans\\_help\\_v182/ans\\_elem/Hlp\\_E\\_COMBIN14.html](https://www.mm.bme.hu/~gyebro/files/ans_help_v182/ans_elem/Hlp_E_COMBIN14.html).
- [49] Javad Sadeghi. *Investigation of characteristics and modelling of railway track system*. Thesis, university of Wollongong, 1997.
- [50] A. van Belkom. Design manual - railway sleepers. Report, Lankhorst Engineered Products, 2015.
- [51] D Hoffmann and S Freudenstein. Test on Lankhorst KLP hybrid plastic sleepers type 101 and 201 according to requirements of the Eisenbahnbundesamt (EBA). Report, Technical Universtiy Of Munich, 2016.
- [52] NEN-EN 13674-1. Railway applications - track - rail - part 1: Vignole railway rails 46 kg/m and above. Legal rule or regulation, CEN, 2017.
- [53] European union agency for railways. Concerning a technical specification for interoperability relating to the 'rolling stock — locomotives and passenger rolling stock' subsystem of the rail system in the european union. Legal rule or regulation, European Commission, 2014.
- [54] NEN-EN 13848-5. Railway applications - track - track geometry quality - part 5: Geometric quality levels - plain line, switches and crossings. Legal rule or regulation, CEN, 2017.
- [55] ProRail. OHD00022-2-V004 - Instandhoudingsspecificaties voor de spoorgeometrie. Maintenance document OHD00022-2-V004, ProRail, 2009.
- [56] Josué César Bastos. *Analysis of the performance and failure of railroad concrete crossties with various track support conditions*. Thesis, University of Illinois, 2016.
- [57] ProRail. OHD00001-V003 - Spoorstaven. Maintenance document, ProRail, 2012.
- [58] NEN-EN 13481-2. Railway applications - track - performance requirements for fastening systems - part 2: Fastening systems for concrete sleepers. Legal rule or regulation, CEN, 2017.
- [59] NEN-EN 13481-3. Railway applications - track - performance requirements for fastening systems - part 3: Fastening systems for wood sleepers. Legal rule or regulation, CEN, 2012.

- [60] Zhe Chen and Bassem Andrawes. A mechanistic model of lateral rail head deflection based on fastening system parameters. *Proceedings of the Institution of Mechanical Engineers, Part F: Journal of Rail and Rapid Transit*, 231(9):999–1014, 2017.
- [61] Richard Lampo, Thomas Nosker, and Henry Sullivan. Development, testing, and applications of recycled-plastic composite cross ties. *US Army Engineer R&D Centre*, 2003.
- [62] I. Lotfy, M. Farhat, and M. A Issa. Effect of pre-drilling, loading rate and temperature variation on the behavior of railroad spikes used for high-density-polyethylene crossties. *Proc IMechE Part F: Journal Rail and Rapid Transit*, 231(1):44–56, 2017. doi: 0.1177/0954409715620755.
- [63] I. Lotfy and M. A Issa. Evaluation of the longitudinal restraint, uplift resistance, and long-term performance of high-density polyethylene crosstie rail support system using static and cyclic loading. *Proc IMechE Part F: Journal Rail and Rapid Transit*, 231(8):835–849, 2017. doi: 10.1177/0954409716647094.
- [64] Andrew Kish, David Y Jeong, Denise Dzwonczyk, et al. Experimental investigation of gauge widening and rail restraint characteristics. Technical report, United States. Federal Railroad Administration, 1984.
- [65] Xinggao Shu and Nicholas Wilson. Simulation of dynamic gauge widening and rail roll: effects on derailment and rolling contact fatigue. *Vehicle System Dynamics*, 46(1):981–994, 2008. doi: 10.1080/00423110802037214.
- [66] Josué C Bastos, Marcus S Dersch, J Riley Edwards, and Bassem O Andrawes. Determination of the influences of deteriorated track conditions on gauge widening in concrete sleeper track. In *11th World Congress on Railway Research*, 2016.